Role of Histone Modifications and Chromatin Interacting Non-Coding RNAs in Regulating Cardiac Gene Transcription

Prabhu Mathiyalagan, BSc., MSc.

Submitted in total fulfillment of the requirement of the degree of Doctor of Philosophy

2013

BakerIDI Heart and Diabetes Institute
and
Faculty of Medicine, Nursing and Health Sciences
Monash University,
Australia

Copyright Notices

Notice 1

Notice 2

DECLARATAION

This is to certify that

(i) The thesis comprises only my original work towards the PhD except where indicated in the Preface

(ii) Due acknowledgement has been made in the text to all other material used

(iii) The thesis is less than 100,000 words in length, exclusive of tables, maps, bibliographies and appendices.

_____

Prabhu Mathiyalagan

BakerIDI Heart and Diabetes Institute

Melbourne, Victoria, Australia

ACKNOWLEDGEMENTS

Firstly, I would like to sincerely thank my principal supervisor Prof. Assam El-Osta for giving me the oppurtunity to pursue this project at the Human Epigenetics laboratory, BakerIDI. I feel fortunate to have had Prof. El-Osta, who has a strong international reputation in the field of epigenetics as my PhD supervisor and I'm thankful to his commitment and mentorship throughout the project.

I would also like to thank my co-supervisors Prof. Xiao-Jun Du and Dr. Jun Okabe for their kind advice and for involving in discussions regarding experimental approaches required for the successful completion of the project.

I also thank Dr. Izhak Haviv, Dr. Richard Tothill, Dr. Luciano Pirola and Dr. Nancy Amin for their kind support as well as for providing insights to chromatin immunoprecipitation techniques especially at the very beginning of my PhD candidature.

My thanks also go to Lisa Chang and Jenny Ooi, thanks to both of you for great support as well as for active discussions involving experimental optimization as well as project directions.

I would like to thank the past and present members of the epigenetics in human health and disease laboratory for their friendship, for sharing their technical and scientific expertise including effective feedback on my project. It was fun working in this laboratory and I have enjoyed all the company.

I also thank Sam Keating, for his contribution particularly toward the end of the project for discussions involving manuscript publications.

I acknowledge the support of the faculty of medicine, nursing and health sciences, Monash University throughout my phd candidature and also for the Monash graduate scholarship.

Life as an international student is never easy and I thank my parents for their continued love and support throughout my stay away from home. Without both of you, it is impossible for me to have this PhD project completed successfully. Thank you Mum and Dad for your love as well as discussions on some of the aspects of this project. I dedicate this thesis to both of you.

PREFACE

Some of the work presented in this thesis was contributed by other people. I am very grateful and sincerely thankful for the time they took to contribute this work to my thesis.

Dr. Xiao-Jun Du and his team for developing mouse models of TAC and administration of trichostatin A, *in vivo*. Also for preparing the Echocardiographic parameters and LV mass in TAC exposed TSA hearts specifically for this project. (Table 1, Page 87)

PEER-REVIEWED PUBLICATIONS

The work associated with this thesis has been / is being published in the following articles.

Research articles

1. Mathiyalagan, P., Chang, L., Du, X.J., and El-Osta, A. (2010). CARDIAC VENTRICULAR CHAMBERS ARE EPIGENETICALLY DISTINGUISHABLE. *Cell Cycle 9*, 612-617. (Pages 59-64)

2. Mathiyalagan, P., Okabe, J., Chang, L., Su, Y., Du, X.J., and El-Osta, A. (2013). THE PRIMARY MICRORNA-208B INTERACTS WITH POLYCOMB-GROUP PROTEIN, EZH2, TO REGULATE GENE EXPRESSION IN THE HEART. *Nucleic Acids Research*. 2013 Oct 16 [Epub ahead of print] (Pages 84-101)

Review articles

Mathiyalagan, P., Keating ST., Du, X.J., and El-Osta, A. (2013). INTERPLAY OF CHROMATIN MODIFICATIONS AND LONG NON-CODING RNAS IN THE HEART. *Epigenetics*. 2013 Oct 10 [Epub ahead of print] (Pages 4-33)

Manuscript under peer-review

Mathiyalagan, P., Keating ST., Du, X.J., and El-Osta, A. CHROMATIN REMODELING AND POST-TRANSLATIONAL HISTONE MODIFICATIONS REGULATE CARDIAC GENE EXPRESSION. (Pages 34-57)

Manuscript in preparation

ANTISENSE NON-CODING RNA AND H3K27ME3 MODIFICATION DISTINGUISH SEXUALLY DIMORPHIC CARDIAC MYOSIN HEAVY CHAIN GENE EXPRESSION. (Pages 66-83)

CONFERENCE PROCEEDINGS

1. Epigenetics Australian Scientific Conference, 1-4 Dec 2009, Melbourne, VIC, Australia.
Title of the presentation (Poster): "*Cardiac Ventricular Chambers are Epigenetically Distinguishable*."

2. Heart Foundation Conference, 16-18 May 2013, Adelaide, South Australia, Australia.
Title of the presentation (Oral): "*The Primary Transcript of MicroRNA-208b Modulates Gene Expression in Cardiac Hypertrophy by Chromatin Interaction*."

3. American Heart Association, Scientific Sessions, 16-20 Nov 2013, Dallas, Texas, USA.
To be presented on Monday, November 18, 2013, 9:00 am.
Title of the presentation (Oral): "*The Primary Transcript of MicroRNA-208b Modulates Gene Expression in Cardiac Hypertrophy by Chromatin Interaction*."

AWARDS AND HONORS

1) Monash Graduate Scholarship (MGS) award for PhD

2) Landes highlights (2010): Cell Cycle paper: I 'heart' Epigenetics, *Epigenetics* 5:2, 88.

3) BakerIDI Bright Sparks Travel Award recipient, 2013.

TABLE OF CONTENTS

ABBREVIATIONS

Ab	Antibody
ACE	Angiotensin-converting-enzyme
ANP	Atrial natriuretic peptide
ANRIL	Antisense non-coding RNA in the INK4 locus
AS	Antisense
ASXL2	Additional Sex Combs Like 2
ATPase	Adenosinetriphosphatase
bdP	Bi-directional promoter
BNP	B-type natriuretic peptide
Brdu	Bromodeoxyuridine
BRG1	Brahma-related gene 1
cDNA	Complementary deoxyribonucleic acid
CHD	Coronary heart disease
ChIP	Chromatin immunoprecipitation
Ct	Cycle threshold
DHS	DNase hypersensitive site
DMEM	Dulbecco's Modified Eagle Medium
DMSO	Dimethyl sulfoxide
LVDd	Left ventricular end-diastolic dimension
DNA	Deoxyribonucleic acid
eCSC	Endogenous cardiac stem cells
EDTA	Ethylenediaminetetraacetic acid
EZH2	Enhancer of zeste homolog 2
FCS	Fetal calf serum
H3K27	Histone H3 lysine residue 27
H3K36	Histone H3 lysine residue 36
H3K4	Histone H3 lysine residue 4
H3K9	Histone H3 lysine residue 9
HAT	Histone acetyltransferase
HDAC	Histone deacetylase
HDACi	Histone deacetylase inhibition

HDM	Histone demethylase
HMT	Histone methyltransferase
IgG	Immunoglobulin G
Kb	Kilobase
KD	Knockdown
lncRNA	Long non-coding RNA
LV	Left ventricle
LVDs	Left ventricular end-systolic dimension
MEF2	Myocyte enhancer factor 2
mg	Milligram
MHC	Myosin heavy chain
miR	MicroRNA
ml	Milliliter
mM	Millimolar
MNase	Micrococcal Nuclease
mRNA	Messenger RNA
ncRNA	Non-coding RNA
ng	Nanogram
NVCM	Neonatal ventricular cardiomyocytes
PARP	Poly ADP ribose polymerase
PBS	Phosphate buffered saline
PcG	Polycomb-group
Pri-miR	Primary microRNA
qRT-PCR	Quantitative realtime polymerase chain reaction
RNA	Ribonucleic acid
RV	Right ventricle
Sca1+	Stem cell antigen-1 positive
SDS	Sodium dodecyl sulfate
SEM	Standard error of the mean
SERCA2a	Sarcoplasmic reticulum Ca(2+) ATPase 2a
SET	Su(var)3-9 and 'Enhancer of zeste'
shRNA	Short-hairpin RNA

SIRT	Sirtuin
snoRNA	Small nucleolar RNA
SW	Swiss Webster
SWI/SNF	SWItch/Sucrose NonFermentable
TAC	Transverse aortic constriction
Tris-HCL	tris(hydroxymethyl)aminomethane-hydrochloride
TSA	Trichostatin A
α-MHC	Alpha-myosin heavy chain
β-MHC	Beta-myosin heavy chain
μg	Microgram
μl	Microliter

ABSTRACT

Cardiac hypertrophy is associated with pathological remodeling of the ventricles of the heart. Hypertrophy-induced changes in gene expression pattern results in re-establishment of fetal gene program in the adult heart. Enhanced expression of fetal and growth-factor genes as well as decreased expression of adult-specific genes are characteristic of genetic reprogramming during cardiomyocyte hypertrophy. Signaling pathways mediating the hypertrophic growth of cardiomyocytes suggest regulation at multiple molecular levels. Indeed, master regulators such as cardiac transcription factors and stress-induced changes to circulating hormone levels are thought to mediate these gene expression changes within the myocardium.

Recent studies from cancer, neurological and developmental diseases comprehensively describe a new level of gene regulation referred as epigenetics. The two best-studied examples of epigenetic modifications are the addition or removal of methyl group to the nucleotide bases that make up the genetic material of an individual, as well as addition or removal of methyl and/or acetyl group to amino acid residues contained within histone proteins that package DNA into nucleosomes. Unlike genetic mutations, neither the chemical modification to DNA nor to the histone proteins alters the order of nucleotide sequence. However, such modifications are clearly associated with transcriptional competency of nearby genes. Hyper- and hypo- methylation of DNA at genes required for cell cycle regulation have been observed in diseases like cancer. Clearly, such modifications to DNA are identified to regulate the expression of genes implicated in oncogenesis.

Emerging studies raise a compelling argument for epigenetic mechanisms especially co-regulatory proteins that mediate methylation and acetylation of histones as key mediators of hypertrophy induced gene expression in the heart. Epigenetic enzymes such as the DNA methyltransferases (DNMT), histone acetyltransferases (HAT) and histone deacetylases (HDAC), in complex with chromatin remodeling proteins such as BRG1 and PARP, mediate stress induced pathological signaling within the myocardium. Over the last decade, understanding the function and pharmacological modulation of HDAC enzymes has been the focus in cardiac research. HDACs serve

to remove acetyl group from amino acid residues harboured within histone and non-histone proteins. Therapeutic inhibition of HDAC enzymes especially class I HDACs shows promising improvements in pre-clinical and clinical studies of heart failure. In pre-clinical models of cardiac hypertrophy, HDAC inhibition has been shown to block and even reverse the pathological remodeling of the ventricles caused by pressure-overload. These observations are attributed to distinct enzymes, HATs and HDACs that mediate the addition and removal of acetyl groups, respectively to histone proteins. The expression as well as activity of these enzymes is altered during cardiac hypertrophy leading to aberrant histone acetylation ultimately affecting gene expression. Together HDACs, HATs and Brg1, serve to remodel chromatin and regulate hypertrophy-associated gene expression program including the prototypical cardiac myosin heavy chain isoform shift during pathogenesis.

Complex interactions of co-regulatory proteins that serve to remodel chromatin and gene function require a multitude of interactions in a co-ordinated manner. Recent identification of functional RNAs such as the short and long non-coding RNAs (ncRNAs) underscore the molecular complexity that drives specific interactions between genes and co-regulatory proteins. The complementary RNA to *β-MHC* gene, referred as *antisense* (*AS*) *β-MHC* was recently proposed to regulate the prototypical *MHC*-isoform shift in pressure-overload exposed ventricles. The precise functions of the transcript other than regulating *β-MHC* expression remain unknown. In addition to *AS β-MHC*, a collection of long ncRNAs has been proposed to regulate pathological gene expression in the heart, yet the mechanism of action remains uncharacterized. Non-coding RNAs offer valid candidates of therapeutic targets to manipulate global expression of target genes. Indeed, miRNA-208b and miRNA-208a are both encoded by cardiac *MHC* genes, whose expressions are closely associated with cardiac hypertrophy. Therapeutic inhibition of miRNA-208 family has proven beneficial in pre-clinical models of pathological hypertrophy. Studying the complex interactions of these distinct molecular species that function in a co-ordinated fashion has furthered our understanding of the complexity driven by pathological changes associated with the ventricular remodeling.

The work presented in this thesis provides novel insights into gene regulatory mechanisms mediated by long ncRNAs (lncRNAs) working in conjunction with post-translational chemical modifications of histones in the pathological mouse heart.

CHAPTER ONE

LITERATURE REVIEW

1.1 Interplay of chromatin modifications and long non-coding RNAs in the heart

Short title: LncRNAs regulate cardiac gene expression

Authors: Prabhu Mathiyalagan[1], Samuel T. Keating[1], Xiao-Jun Du[2] and Assam El-Osta[1,3,4,5*]

[1]Epigenetics in Human Health and Disease Laboratory, Baker IDI Heart and Diabetes Institute, The Alfred Medical Research and Education Precinct, Melbourne Victoria 3004, Australia

[2]Experimental Cardiology Laboratory, Baker IDI Heart and Diabetes Institute, 75 Commercial Road, The Alfred Medical Research and Education Precinct, Melbourne, Victoria 3004 Australia.

[3]Epigenomics Profiling Facility, Baker IDI Heart and Diabetes Institute, The Alfred Medical Research and Education Precinct, Melbourne, Victoria 3004, Australia

[4]Department of Pathology, The University of Melbourne, Victoria 3010, Australia

[5]Faculty of Medicine, Monash University, Victoria 3800, Australia

*Correspondence:

Prof. Assam El-Osta

[redacted] (**Email**); [redacted] (**Telephone**);

613 8532 1100 (**Fax**)

Keywords: Cardiac Hypertrophy, Gene regulation, long non-coding RNA, chromatin, histone modifications

1.1.1 Abstract

Precisely regulated patterns of gene expression are dependent on the binding of transcription factors with co-regulatory determinants referred to as co-activators and co-repressors. These regulatory components function with the core transcriptional machinery to serve in critical activities to alter chromatin modification and regulate gene expression. Cardio-vascular development requires cell-type specific patterns of gene expression to achieve selective developmental programs. With clear implications for the epigenetic control of gene expression signatures, the ENCODE (ENCyclopedia Of DNA Elements) Project Consortium determined that about 90% of the human genome is transcribed while only 1-2% of transcripts encode proteins. Emerging evidence suggests that non-coding RNA (ncRNA) serves as a signal for decoding epigenetic mechanisms and provides a potential molecular basis for cell type-specific and promoter-specific patterns of gene expression. A novel role for the histone methyltransferase enzyme Ezh2 has been uncovered in the regulation of gene expression patterns, which has been implicated, in cardiac hypertrophy and the focus of this article.

1.1.2 Introduction

The mammalian heart is the first functional organ to develop within the vertebrate embryo. The chambers of the heart undergo structural changes during development mediated by specific cellular cues such as hormone stimulation. These stage-specific developmental transitions in the cardiac lineage are precisely regulated by spatial and temporal events on chromatin to regulate gene expression patterns.[1] For example, genes specifically expressed at later stages in cardiac development, such as cardiomyocyte maturation and terminal differentiation are often mono-methylated on histone H3 lysine 4 (H3K4me1), whereas activation at later stages is specified by H3K4me3 modification.[1] Stage-specific chromatin signatures are established by combinatorial readout of histone modifications. For example, both methylation and acetylation of histone proteins at distinct lysine positions can establish chromatin "signature" and serve as binding sites for co-regulatory complexes.[2] Gene activation in pluripotent stem cells is associated with H3K4me1 of gene promoters, which are activated at later stages in the cardiac lineage, which is in contrast to genes repressed at this stage and specified by high levels of H3K27me3 at gene sequences. Genes that code for the adult isoform cardiac contractile protein α-*myosin heavy chain* (α-*MHC*) as well as the transcription factor *Nkx2.5* are activated only at later stages of cardiac differentiation. The activation of these genes shows high levels of H3K27me3 deposition at pluripotent stage, which are gradually erased and replaced by H3K4me3 modification.[3]

Cardiomyocytes respond by adaptive mechanisms to changing environmental stimuli such as increased workload. These physiological changes are marked by an increase in cardiomyocyte size and ventricular mass, which is referred to as cardiac hypertrophy. Chronic exercise training or pregnancy can increase heart muscle mass and contractile ability, often referred to as physiological hypertrophy.[4] Similarly pathophysiological surroundings such as acute and chronic myocardial stress including hypertension, valvular disease and myocardial infarction can dramatically increase the size of the ventricular chamber.[4, 5] This is referred to as pathological cardiac hypertrophy and like physiological hypertrophy, stimulates a phase of neurohumoral and biomechanical signals within the myocardium. While it is

considered that physiological hypertrophy is generally advantageous as well as reversible, pathological hypertrophy causes irreversible remodeling leading to deformation of the ventricles and reduced heart contractility.[6]

The discovery of specific activator and repressor complexes important in cardiac development has revealed several mechanistic insights into myocardial function, cardiac development as well as heart disease. Ventricular hypertrophy is associated with re-activation of fetal genes that include *Anp*, *Bnp* and *β-MHC* as well as the suppression of *Serca2a* and *α-MHC* genes in the adult heart.[6] The recruitment of ATPase-dependent chromatin remodeling complexes that belong to the SWI/SNF family[7] have been shown to contextually associate with either histone acetyltransferases (HATs) or histone deacetylases (HDACs) and regulate cardiac gene expression.[8] Indeed, the recruitment and binding of p300 HAT enzyme on gene promoters is closely associated with the establishment of chamber-specific gene expression patterns under physiological states and implicated in the treatment of heart failure.[9] In addition, recent studies have expanded the complexity of regulatory determinants that participate in cardiac gene expression, for example histone modifying proteins such as Ezh2 and Asxl2 specify *MHC* gene expression in postnatal cardiac homeostasis.[10, 11] The results of these experimental data support a diverse network of signaling pathways that underlie both physiological and pathological cardiac gene regulation.

Mechanisms that regulate gene expression are under the direct control of specific classes of transcription factors and core machinery that serve to alter chromatin structure and function. However the precise actions of transcription factors in cardiac disease as well as the enzymatic activities of chromatin remodeling determinants including histone and non-histone modifying enzymes are poorly characterized. The complexity of these transcriptional regulators presents a major conceptual problem and one that is addressed in this review on non-coding RNAs (ncRNA). The potential molecular mechanism we discuss is one targeting many classes of histone reading and writing enzymes that functionally serve to alter gene structure and expression. Recent experimental observations show that chromatin remodeling and histone

modification confer important transcriptional programs as a result of development and cardiac disease.[12-15] The complex interplay of transcriptional co-regulators interacting with long non-coding RNAs (lncRNA) serve to localize key DNA-binding proteins directing specific post-translational modifications regulating gene expression has been recently described and the focus of our discussion.[16-18]

1.1.3 Physiological roles of lncRNAs in the heart

Recent advances in nucleic acid sequencing technologies have revealed that nearly 90% of the genome is transcribed in one tissue type or another, with estimates of approximately 70-98% constitute ncRNA.[19-21] These transcripts are broadly classified in two groups according to nucleotide length; the short ncRNAs (<200 nt) such as microRNA (miRNA) and lncRNAs (>200 nt) such as the natural antisense transcripts (NATs) (**Table 1**). Interestingly, ncRNAs are thought to interact with chromatin and regulate gene transcription. When in 1993 two studies published back-to-back in *Cell* describing short non-coding RNAs in *C.elegans*, the importance of these findings was probably under-appreciated.[22, 23] How ncRNAs recognize and interact with target sequences to regulate gene expression still remains poorly characterized. Although short ncRNAs are strongly conserved but of unknown function, the seminal discoveries by the groups led by Ambros and Ruvkun have revealed a regulatory complexity mediated by ncRNAs. The field has expanded tremendously with a better understanding of the significance of these ncRNA molecules in biology and disease. Recent studies now show that during development, ncRNAs are expressed in a dynamic fashion and regulated by specific cellular and environmental cues.[16, 17]

The importance of short ncRNAs in heart development was elegantly demonstrated by cardiac-specific deletion of miRNA-processing enzyme, Dicer.[24] The miRNAs *miR-1* and *miR-133* are abundant in the heart and are associated with cardiovascular development and myeloid differentiation.[25-27] Recently, functional paradigms for several lncRNAs have been described such as the participation in embryonic differentiation and cell-lineage development as well as transcriptional control.[16, 17, 28, 29] While the lncRNAs can serve as spliceosome and ribosome components in eukaryotic RNA metabolism, recent experimental observations

suggest a role for lncRNAs in organizing chromatin conformation and shaping the genome. For example, chromatin interacting lncRNAs were recently identified as key determinants of gene imprinting (such as *Xist* and *Kcnq1ot1* as well as *Air*) whereas the recruitment of PRC2 components are implicated in gene suppression events that involve *Hotair* and *Tug1*.[30-32] Recently, knockdown of lncRNAs expressed in embryonic stem cells has revealed more than one hundred functional lncRNAs associated with the maintenance of pluripotency.[33] In addition, several lncRNAs have been implicated in normal heart physiology. For example, *Braveheart* (*Bvht*) and *Fendrr* are thought to have critical roles in cardiac lineage specification during early developmental stages of the mouse embryo.[16, 17] The silencing of *Bvht* in mES cells results in the loss of cardiomyocyte beating in embryoid bodies (EB) at day 11 of differentiation.[16] Furthermore, tissue-specific *Fendrr* is a regulator of heart and body wall development in the mouse.[17] While these results are not fully understood, it is hypothesized that *Bvht* and *Fendrr* control gene expression by interacting with the regulatory cofactors, PRC2 and TrxG/MLL complexes. These studies highlight the importance of long ncRNA transcripts defining chromatin structure and gene expression necessary for heart development. Recent studies have also identified putative roles for lncRNAs in cancer (such as the over expression of *Malat1* and *Hotair*), anemia (under expression of *LincRNA-EPS*), Alzheimer's (over expression of *Bace1-AS*) and Huntington's disease (under expression of *Htt-AS*).[34-37] In addition to the general involvement of DNA-binding motifs that function in the recruitment of transcription factors, new roles for lncRNAs in mediating chromatin-protein interactions have recently been described.[20, 38] Long ncRNAs have putative sequence motifs and structural domains implicated in protein association and binding to specific gene sequences. Indeed, several chromatin-interacting proteins have recently been described to have ncRNA-binding domains such as the polycomb-group (PcG) proteins, which are involved in the suppression of gene expression and chromatin modification.[39, 40]

1.1.4 Non-coding RNAs connect EZH2 with chromatin

The expression of lncRNAs including NATs to several genes in heart tissues have recently been shown to regulate gene transcription and protein translation.[14, 15] The antisense (AS) transcripts which are expressed from cardiac genes such as *Nppa* (*AS-Nppa*) and *β-MHC* (*AS β-MHC*) are examples of gene regulatory lncRNAs in the myocardium. The Ezh2 lysine methyltransferase has a binding domain thought to mediate interaction with lncRNAs.[39] For instance, phosphorylation of threonine (T365) within the Ezh2 ncRNA-binding domain is associated with binding to the lncRNAs, *Hotair* and *Xist*.[30] Well characterised in cancer and considered a potential regulator of malignant transformation, the specific interactions of ncRNAs with histone modifying determinants such as Ezh2 remain poorly described in the heart.[41] In general, several lysine methyltransferase enzymes have a conserved SET-domain region, which is thought to be critical to chromatin association as well as catalytic activity. A number of methyl-writing SET-domain family members such as G9a, Set7, Smyd3, Set2, Set1 and Ezh2 can bind to single-stranded DNA and RNA.[42-45] In addition, several MLL family proteins that contain the SET-domain are known to interact with ncRNA either directly or indirectly.[46, 47] The methyl-erasing enzyme, LSD1, is thought to bind directly with the 3' end of *Hotair* and regulate *HoxD* gene expression.[48]

Recent data published by several groups suggest putative regulatory roles for antisense transcripts in mediating Ezh interactions with chromatin in the heart (**Table 2**).[10, 49] The expression of genes encoding contractile proteins and transcription factors implicated in heart disease are altered in Ezh2-knockout mouse models.[10] Deep sequencing of chromatin immunoprecipitated from the mouse heart using antibodies that recognize Ezh2 show direct interaction with genes implicated in cardiac disease (**Table 2**).[49] Interestingly, Ezh2 appears to bind novel bi-directional promoters (bdP) that regulate the expression of sense and antisense RNA. For example, altered expression of tumour suppressor genes (*Cdkn2b*, *Cdkn2a*, and *Arf*) within the chromosome 9p21 region encoding the *Ink4/Arf* locus was observed in hearts of Ezh2-null mice.[10, 49] Expression of the overlapping *Anril* antisense transcript is thought to regulate these genes by Ezh2-mediated PcG silencing.[50] However, it

remains to be determined whether *Anril* expression in cardiomyocytes directly regulates the interaction of Ezh2 with chromatin at the 9p21 region. In favour of a role in cardiac homeostasis, individuals homozygous for risk SNP allele at the 9p21 region show altered *Anril* expression and increased susceptibility to atherogenic plaque development, coronary heart disease (CHD) and diabetes.[51, 52] While Cdkn2a expression levels were reduced in 9p21 knockout hearts, there was no evidence for cardiac hypertrophy or cardiovascular pathology.[53] Other studies also report *Anril* interactions with PcG proteins such as Cbx7 and Suz12 to regulate *Cdkn2b* and *Cdkn2a* gene expression.[54, 55] Over-expression of *Anril* in cultured cells significantly altered the expression of a large number of genes proposing *trans* mechanism of gene regulation.[55] Ontology analysis has identified numerous genes involved in the regulation of nucleus and chromatin architecture.[55] These observations imply a role for Ezh2 in mediating chromatin interactions of *Anril* transcript.

Cardiac hypertrophy and failure are associated with changes in the expression of α- and β-*MHC* mRNAs and this shift in myosin-isoform distribution serves important roles in cardiac muscle fiber shortening.[56] The silencing of α-*MHC* in failing human hearts has led renewed interest to restore expression of this gene in hypertrophic tissue.[56] The *MHC* genes are clustered on chromosome 14 in humans and mice (chr 15 in rat) and the α- and β- *MHC* genes are separated by an intergenic sequence of ~4.5kb in length (**Figure 1**).[57] The β-*MHC* gene is upstream of α-*MHC* and both transcribe mature mRNA approximately 7kb in length.[57] The complexity of *MHC* gene regulation presents interesting conceptual and experimental challenges with the identification of transcripts on the opposite DNA strand. This complementary sequence to the canonical mRNA represents the antisense or non-coding RNA.[58] The intergenic region of *MHC* is thought to contain a bdP that transcribes both strands of DNA producing antisense (*AS*) β-*MHC* and α-*MHC* transcripts in opposite directions.[58] Transcription of the *AS* β-*MHC* progresses in the direction of the β-*MHC* gene and it is considered to regulate the expression of *MHC* genes in response to pressure overload and diabetes.[58, 59]

The regulation of *MHC* isoforms requires the coordinated actions of a core machinery that include DNA transcription factors, chromatin remodeling, and expression of antisense RNA transcripts. Furthermore, the complex regulation of the *MHC* genes includes both transcriptional and post-transcriptional mechanisms.[12, 58] Recent experiments in Ezh2 mutant mice reveal changes to *MHC* gene expression characteristic of the hypertrophic heart, suggesting a direct role for this enzyme in *MHC* isoform regulation.[10] In addition to H3K27me3 modification mediated by Ezh2, regulatory features of the bdP involve binding of histone-modifying enzymes such as Hdac9, Asxl2, and chromatin remodeling enzymes such as Brg1 and Parp1 (**Figure 1**).[11, 60] Moreover, either the presence or absence of DNase hypersensitive sites is associated with *MHC* gene expression at various developmental stages of the heart which is indicative of chromatin remodeling.[61] Whilst it is presently unclear how chromatin-modifying enzymes regulate *MHC* transcription, the expression of the *AS β-MHC* transcript may participate in recruitment of enzymes such as Ezh2 to the bdP to regulate *MHC* isoform expression in healthy and diseased hearts.

1.1.5 Novel ncRNAs in the heart

The growing list of lncRNAs expressed in the myocardium involved in the healthy heart and cardiac disease are summarised in **Table 3**. RNA sequencing has revealed specific transcriptome profiles for coding and non-coding transcripts that distinguish the stages of hypertrophy and heart failure in the myocardium.[62] Recent transcriptome studies have identified more than 1300 previously unannotated exons with altered expression levels in animal models of hypertrophy and heart failure.[62] Among these, approximately 682 exons displayed differential expression between hypertrophic and heart failure models. The majority (81%) of unannotated RNAs expressed in heart failure models were low protein coding or non-coding RNAs. For example, the expression of *H19* lncRNA was higher in animals with heart failure when compared to those animals with cardiac hypertrophy. The function of *H19* in the myocardium as well as its association with heart disease remains poorly characterized. Transcriptome profiling of human heart explants has shown the expression of four previously uncharacterized novel ncRNAs marked by specific histone modifications.[63] The results from these studies suggest that a large number

of novel transcripts expressed in failing myocardium are either not expressed or not detected because of transcript abundance. Serial analysis of gene expression (SAGE) across many tissue types from humans has identified cardiac-specific expression of a novel lncRNA, *NCRNA00116*.[64] The function of this transcript in heart development and disease as well as several proposed antisense transcripts are poorly understood.[65]

1.1.6 Methodologies for the analysis of complex interactions between lncRNA and chromatin

Recent methodological developments in transcript analysis have seen a tremendous amount of information generated from massive parallel sequencing using innovative approaches in search of functions for lncRNAs. While historically difficult to ascribe function to the large number of non-coding RNAs, these transcripts are readily identified by RNA sequencing approaches. A number of lncRNAs contain chromatin binding domains and sequences implicated to bind to regulatory proteins as well as sequences required for gene expression.[38, 40] In the next section, we discuss some of the methodological developments that have enabled the characterization lncRNAs and their interactions with chromatin.

1.1.7 Methods used in the detection and characterization of lncRNAs

Important protein-coding genes including those implicated in heart disease have antisense transcription and ncRNA expression.[66, 67] Conventionally in first-strand synthesis, complementary DNA (cDNA) is generated at low temperatures (37^{o}C) using random/oligo-dT primers that are non-specific to gene sequences as well as lacking strand-specific (5' to 3' orientation) information. To distinguish the sense from the antisense transcript, strand-specific oligonucleotides are used to anneal either mRNA (sense) or ncRNA (antisense) at high temperatures (50-60^{o}C) followed by first-strand cDNA synthesis and quantification. For example, strand-specific primers to cardiac *MHC* and *troponin* genes have been used to quantitatively measure sense (mRNA) and antisense (ncRNA) expression in the heart.[68, 69] Recently, several novel procedures have been developed to quantify strand-specific expression of the transcriptome (**Table 4**).[70, 71]

Almost 90% of the human transcriptome is alternatively spliced in terminally differentiated cells such as cardiomyocytes and neurons.[72] This permits the generation of large numbers of RNA (splice variants) and protein isoforms from a limited number of genes.[73] For example, distinct alternative splicing of the cardiac steroid receptor activator (Sra) transcript can generate Sra protein-coding transcript as well as non-coding regulatory Sra transcript.[74] In another case, a novel splice variant to the *Hotair* transcript lacking a previously determined Ezh2 interacting domain has been reported.[75] These splicing variations of lncRNA transcripts is thought to be a critical determinant for protein interaction, however their distinct biological roles in the heart as well as disease association remain to be addressed. Consistent with this idea, splice variants in the heart are known to exist for *Anril* and regulate circularization of this transcript where one variant interacts with Ezh2 and the other is masked for Ezh2 binding domain.[76] However, the precise mechanism of alternative splicing mediated ncRNA binding to Ezh2 remains poorly understood. The identification of splice variants to ncRNA transcripts is key to understand and predict ncRNA-binding proteins interactions. Several strategies such as exon-scanning and rapid amplification of cDNA ends (RACE) have successfully identified splice variants to cardiac *troponin I*- and *Nppa*- antisense transcripts (**Table 4**).[65, 77] Other examples include *Kcnq1ot1* and *Hottip* were determined by RACE.[47, 78]

Deep sequencing of RNA (RNA-Seq) approaches generate millions of reads that often fail to accurately identify gene structure as well as result in missing genomic regions transcribed at low levels, as well as non-polyadenylated ncRNAs.[79] Transcript profiling can be studied using tiling arrays or targeted RNA CaptureSeq (RNA capture sequencing).[75, 80] For example, Mercer *et al*[75] used tiling arrays that contained sequences corresponding to unannotated regions, whose rare and transient expression are thought to be below the detection limits of conventional RNA-Seq. Surprisingly, the study reported complex ncRNA transcription and widespread expression of rare transcripts.[75] In addition to previously characterized transcript variants such as *Tp53* (p53), at least three novel isoforms that lacked sequences required for intra-p53 interactions as well as p53 transactivation domain

were identified. Similarly, an alternative splice junction to *Hotair* transcript was characterized and thought to interfere with PcG binding.[75] Taken together, these data suggest that post-transcriptional splicing can regulate ncRNA interactions with DNA-binding transcription factor complexes.

Recent experimental observations suggest dynamic regulation of ncRNA stability in response to environmental cues. Pulse labeling of endogenous RNA followed by deep sequencing (BRIC-Seq) has identified novel and highly stable lncRNAs such as the *AK091718* transcript, whose expression is linked with cell growth.[29] BRIC-Seq, a method to study RNA decay also revealed short half-lives ($t_{1/2}$ < 4h) for regulatory lncRNAs such as the cardiac *Anril* transcript, *Hotair*, *Tug1* and *Gas5*. That study highlighted hundreds of short-lived regulatory RNAs designated as Short-Lived non-coding Transcripts (SLiTs) that are implicated in nuclear function.[29] An alternative method of studying RNA stability is transcriptional inhibition by Actinomycin D (ActD).[81] Mouse neuroblastoma cells exposed to ActD over a 32hr period identified over 800 lncRNAs and 12,000 mRNAs that were classified as either highly stable (half-life > 16h) or of low stability (half-life < 2h).[82] The regulatory RNA, *Neat1* was identified as one of the least stable ncRNAs and is thought to be dynamically regulated. Similarly, global run-on sequencing (GRO-Seq) and native elongating transcript sequencing (NET-Seq) techniques can be used to study immediate and transient changes to nascent RNA transcripts in response to extracellular stimuli.[83, 84] Indeed, a study using these methodologies identified the immediate transcriptional response to estrogen signaling that lncRNAs are dynamically regulated.[83] The low stability of regulatory RNAs does not suggest that the lncRNAs are non-functional rather this implies that these RNAs act immediately after transcription via chromatin interaction.

1.1.8 Long ncRNA-chromatin interaction assays

Long ncRNAs that stably interact with chromatin at specific genomic sites can be detected by fluorescent *in situ* hybridization (FISH) of the target RNA using antisense RNA probes.[85] FISH has traditionally been the method of choice to study chromatin interactions of lncRNAs.[86, 87] More recently, FISH was employed to determine the

chromatin localization of lncRNA *Kcnq1ot1* of maternal and paternal alleles in the developing heart.[88] Locus-specific lncRNA interactions can be examined using formaldehyde fixation and chromatin immunoprecipitation methods (RNA-ChIP) that use antibodies that recognize RNA-binding proteins such as Ezh2 and G9a.[78] Alternatively, native RNA-ChIP using MNase digestion can also be used to study chromatin associated RNAs.[89] In contrast to formaldehyde crosslinking, the immunoprecipitation of native chromatin allows direct mapping of mono-nucleosomes.[90]

Long ncRNAs can interact in a locus-specific manner through complementary sequence recognition independent of protein interactions.[91] The use of biotinylated RNA tiling probes complementary to target lncRNA was recently employed to immunoprecipitate associated DNA sequences and proteins. Examples include ChIRP (chromatin isolation by RNA purification) and CHART (chromatin hybridization analysis of RNA targets) have identified novel genome-wide interacting sites for lncRNAs such as *Hotair* and *Rox2*.[92, 93] The advent of high-throughput sequencing has enabled the direct detection of RNA isolated by cross-linking immunoprecipitation (HITS-CLIP) and photoactivatable ribonulceoside enhanced crosslinking and immunoprecipitation (PAR-CLIP) which utilize UV-radiation to crosslink adjacent proteins to RNA.[94, 95] These methodologies were recently used to identify the interaction of Ezh2 with several ncRNAs including the cardiac *ANRIL* transcript.[96]

1.1.9 Structural analysis of lncRNAs

Besides sequence-based chromatin recognition, RNA folding can also influence ncRNA interaction with chromatin.[97] Genes such as *Dystrophin*, *Cytochrome P-450*, *MLL* and *ETS-1* code for circular transcripts.[98-101] The hypertrophy responsive *NCX1* gene is known to produce circular poly(A-) transcripts in the human heart.[102] Although for many years the biological significance of circular RNA was unclear, recent evidence now suggests that they may be targeted by miRNAs and act as miRNA sponges to regulate genome-wide post-transcriptional control.[103, 104] Accordingly, circular antisense RNAs are targeted by RISC components for gene

regulation.[105] The mechanism of circularization of RNA is generally a result of non-canonical post-transcriptional exon scrambling (PTES). Non-canonical PTES appears to be a predominant event in human liver and heart tissues.[106] Because of their low abundance, the majority of circular transcripts are largely undetectable by conventional RNA-sequencing. To investigate the circular component of the transcriptome, protocols employ RNaseR, an enzyme that degrades linear but not circular transcripts.[101] Next generation sequencing identified PTES mediated circular RNA transcripts to hundreds of human genes, the majority of which were not polyadenylated.[101] Recently, circular and linear forms of cardiac antisense RNA, *Anril* have been reported.[76] The expression of the endogenous circular *Anril* transcript might be associated with atherosclerotic vascular disease. In addition to structural regulation of RNA by PTES, thousands of human mRNA and ncRNA transcripts are extensively methylated[107] and these RNA modifications are thought to alter Argonaute binding as well as transcript folding.[108] Moreover, recent identification of specific ncRNA structures such as the TINCR boxes regulate the interaction of these transcripts with proteins.[97] Long ncRNAs such as *TINCR* contain several intrinsic structures that determine protein partners for interaction. A novel method has been employed that couples RNA structure analysis with genome-wide sequencing, referred to as FragSeq (fragmentation sequencing). The protocol incorporates the Nuclease P1 enzyme, which cleaves single-stranded nucleic acids thereby preserving the intra- and inter-molecular RNA interactions.[109] The development of these methodologies have enabled genome-wide analysis of RNA structure.[110]

1.1.10 Conclusions and future considerations

Recent experimental observations are building a compelling case for the participation of lncRNA in regulating cardiac gene expression. This is probably best exemplified at the bdP of the *MHC* genes and includes the interaction of Ezh2 with the *antisense β-MHC* transcript to regulate *MHC* isoform expression (**Figure 1**). Several technological developments have been critical to understand the role of ncRNAs in the heart. Indeed, the advent of massive parallel sequencing has brought improved understanding of the regulatory mechanisms underlying cardiac pathology and developmental growth as well as integrating functional genomics. Although the

relevance of the non-coding genome to cardiac disease has mainly been studied in the context of the widespread disruption of expression, recent evidence now indicates that ncRNAs are also critical determinants of gene regulation. Taken together with their emerging role with chromatin and modification, the non-coding genome should provide new strategies and specific targets to prevent, restore or reverse the effects of pathological hypertrophy in the failing heart.

Acknowledgements

The authors acknowledge grant and fellowship support from the National Health and Medical Research Council (NHMRC) and the National Heart Foundation of Australia (NHF). P.M. was awarded a Monash Graduate Scholarship and A.E-O. and X-J. D. are NHMRC Senior Research Fellows. Supported in part by the Victorian Government's Operational Infrastructure Support program.

Disclosures

None

1.1.11 References

1. Wamstad JA, Alexander JM, Truty RM, Shrikumar A, Li F, Eilertson KE, et al. Dynamic and coordinated epigenetic regulation of developmental transitions in the cardiac lineage. Cell 2012; 151:206-20.
2. Strahl BD, Allis CD. The language of covalent histone modifications. Nature 2000; 403:41-5.
3. Paige SL, Thomas S, Stoick-Cooper CL, Wang H, Maves L, Sandstrom R, et al. A temporal chromatin signature in human embryonic stem cells identifies regulators of cardiac development. Cell 2012; 151:221-32.
4. Bernardo BC, Weeks KL, Pretorius L, McMullen JR. Molecular distinction between physiological and pathological cardiac hypertrophy: experimental findings and therapeutic strategies. Pharmacol Ther 2010; 128:191-227.
5. Kehat I, Molkentin JD. Molecular pathways underlying cardiac remodeling during pathophysiological stimulation. Circulation 2010; 122:2727-35.
6. Frey N, Olson EN. Cardiac hypertrophy: the good, the bad, and the ugly. Annu Rev Physiol 2003; 65:45-79.
7. Chang L, Kiriazis H, Gao XM, Du XJ, El-Osta A. Cardiac genes show contextual SWI/SNF interactions with distinguishable gene activities. Epigenetics 2011; 6:760-8.
8. Backs J, Olson EN. Control of cardiac growth by histone acetylation/deacetylation. Circ Res 2006; 98:15-24.
9. Mathiyalagan P, Chang L, Du XJ, El-Osta A. Cardiac ventricular chambers are epigenetically distinguishable. Cell Cycle 2010; 9:612-7.
10. Delgado-Olguin P, Huang Y, Li X, Christodoulou D, Seidman CE, Seidman JG, et al. Epigenetic repression of cardiac progenitor gene expression by Ezh2 is required for postnatal cardiac homeostasis. Nat Genet 2012; 44:343-7.
11. Lai HL, Grachoff M, McGinley AL, Khan FF, Warren CM, Chowdhury SA, et al. Maintenance of adult cardiac function requires the chromatin factor Asxl2. J Mol Cell Cardiol 2012; 53:734-41.
12. Han P, Hang CT, Yang J, Chang CP. Chromatin remodeling in cardiovascular development and physiology. Circ Res 2011; 108:378-96.
13. Takeuchi JK, Lou X, Alexander JM, Sugizaki H, Delgado-Olguin P, Holloway AK, et al. Chromatin remodelling complex dosage modulates transcription factor function in heart development. Nature communications 2011; 2:187.
14. Schonrock N, Harvey RP, Mattick JS. Long noncoding RNAs in cardiac development and pathophysiology. Circ Res 2012; 111:1349-62.
15. Luther HP. Role of endogenous antisense RNA in cardiac gene regulation. J Mol Med (Berl) 2005; 83:26-32.
16. Klattenhoff CA, Scheuermann JC, Surface LE, Bradley RK, Fields PA, Steinhauser ML, et al. Braveheart, a long noncoding RNA required for cardiovascular lineage commitment. Cell 2013; 152:570-83.
17. Grote P, Wittler L, Hendrix D, Koch F, Wahrisch S, Beisaw A, et al. The tissue-specific lncRNA Fendrr is an essential regulator of heart and body wall development in the mouse. Dev Cell 2013; 24:206-14.
18. Mattick JS. RNA as the substrate for epigenome-environment interactions: RNA guidance of epigenetic processes and the expansion of RNA editing in animals underpins development, phenotypic plasticity, learning, and cognition. Bioessays 2010; 32:548-52.

19. Mercer TR, Dinger ME, Mattick JS. Long non-coding RNAs: insights into functions. Nat Rev Genet 2009; 10:155-9.
20. Mercer TR, Mattick JS. Structure and function of long noncoding RNAs in epigenetic regulation. Nat Struct Mol Biol 2013; 20:300-7.
21. Clark MB, Amaral PP, Schlesinger FJ, Dinger ME, Taft RJ, Rinn JL, et al. The reality of pervasive transcription. PLoS Biol 2011; 9:e1000625; discussion e1102.
22. Lee RC, Feinbaum RL, Ambros V. The C. elegans heterochronic gene lin-4 encodes small RNAs with antisense complementarity to lin-14. Cell 1993; 75:843-54.
23. Wightman B, Ha I, Ruvkun G. Posttranscriptional regulation of the heterochronic gene lin-14 by lin-4 mediates temporal pattern formation in C. elegans. Cell 1993; 75:855-62.
24. Chen JF, Murchison EP, Tang R, Callis TE, Tatsuguchi M, Deng Z, et al. Targeted deletion of Dicer in the heart leads to dilated cardiomyopathy and heart failure. Proc Natl Acad Sci U S A 2008; 105:2111-6.
25. Schlesinger J, Schueler M, Grunert M, Fischer JJ, Zhang Q, Krueger T, et al. The cardiac transcription network modulated by Gata4, Mef2a, Nkx2.5, Srf, histone modifications, and microRNAs. PLoS Genet 2011; 7:e1001313.
26. Zhao Y, Ransom JF, Li A, Vedantham V, von Drehle M, Muth AN, et al. Dysregulation of cardiogenesis, cardiac conduction, and cell cycle in mice lacking miRNA-1-2. Cell 2007; 129:303-17.
27. van Rooij E, Sutherland LB, Qi X, Richardson JA, Hill J, Olson EN. Control of stress-dependent cardiac growth and gene expression by a microRNA. Science 2007; 316:575-9.
28. Dinger ME, Amaral PP, Mercer TR, Pang KC, Bruce SJ, Gardiner BB, et al. Long noncoding RNAs in mouse embryonic stem cell pluripotency and differentiation. Genome Res 2008; 18:1433-45.
29. Tani H, Mizutani R, Salam KA, Tano K, Ijiri K, Wakamatsu A, et al. Genome-wide determination of RNA stability reveals hundreds of short-lived noncoding transcripts in mammals. Genome Res 2012; 22:947-56.
30. Kaneko S, Li G, Son J, Xu CF, Margueron R, Neubert TA, et al. Phosphorylation of the PRC2 component Ezh2 is cell cycle-regulated and up-regulates its binding to ncRNA. Genes Dev 2010; 24:2615-20.
31. Han Y, Liu Y, Gui Y, Cai Z. Long intergenic non-coding RNA TUG1 is overexpressed in urothelial carcinoma of the bladder. J Surg Oncol 2013; 107:555-9.
32. Khalil AM, Guttman M, Huarte M, Garber M, Raj A, Rivea Morales D, et al. Many human large intergenic noncoding RNAs associate with chromatin-modifying complexes and affect gene expression. Proc Natl Acad Sci U S A 2009; 106:11667-72.
33. Guttman M, Donaghey J, Carey BW, Garber M, Grenier JK, Munson G, et al. lincRNAs act in the circuitry controlling pluripotency and differentiation. Nature 2011; 477:295-300.
34. Schmidt LH, Spieker T, Koschmieder S, Schaffers S, Humberg J, Jungen D, et al. The long noncoding MALAT-1 RNA indicates a poor prognosis in non-small cell lung cancer and induces migration and tumor growth. Journal of thoracic oncology : official publication of the International Association for the Study of Lung Cancer 2011; 6:1984-92.
35. Hu W, Yuan B, Flygare J, Lodish HF. Long noncoding RNA-mediated anti-apoptotic activity in murine erythroid terminal differentiation. Genes Dev 2011; 25:2573-8.

36. Faghihi MA, Modarresi F, Khalil AM, Wood DE, Sahagan BG, Morgan TE, et al. Expression of a noncoding RNA is elevated in Alzheimer's disease and drives rapid feed-forward regulation of beta-secretase. Nat Med 2008; 14:723-30.
37. Chung DW, Rudnicki DD, Yu L, Margolis RL. A natural antisense transcript at the Huntington's disease repeat locus regulates HTT expression. Hum Mol Genet 2011; 20:3467-77.
38. Rinn JL, Chang HY. Genome regulation by long noncoding RNAs. Annu Rev Biochem 2012; 81:145-66.
39. Margueron R, Reinberg D. The Polycomb complex PRC2 and its mark in life. Nature 2011; 469:343-9.
40. Kanhere A, Jenner RG. Noncoding RNA localisation mechanisms in chromatin regulation. Silence 2012; 3:2.
41. Benetatos L, Voulgaris E, Vartholomatos G, Hatzimichael E. Non-coding RNAs and EZH2 interactions in cancer: Long and short tales from the transcriptome. Int J Cancer 2013; 133:267-74.
42. Nagano T, Mitchell JA, Sanz LA, Pauler FM, Ferguson-Smith AC, Feil R, et al. The Air noncoding RNA epigenetically silences transcription by targeting G9a to chromatin. Science 2008; 322:1717-20.
43. Pagans S, Kauder SE, Kaehlcke K, Sakane N, Schroeder S, Dormeyer W, et al. The Cellular lysine methyltransferase Set7/9-KMT7 binds HIV-1 TAR RNA, monomethylates the viral transactivator Tat, and enhances HIV transcription. Cell Host Microbe 2010; 7:234-44.
44. Krajewski WA, Nakamura T, Mazo A, Canaani E. A motif within SET-domain proteins binds single-stranded nucleic acids and transcribed and supercoiled DNAs and can interfere with assembly of nucleosomes. Mol Cell Biol 2005; 25:1891-9.
45. Xu S, Wu J, Sun B, Zhong C, Ding J. Structural and biochemical studies of human lysine methyltransferase Smyd3 reveal the important functional roles of its post-SET and TPR domains and the regulation of its activity by DNA binding. Nucleic Acids Res 2011; 39:4438-49.
46. Ruthenburg AJ, Allis CD, Wysocka J. Methylation of lysine 4 on histone H3: intricacy of writing and reading a single epigenetic mark. Mol Cell 2007; 25:15-30.
47. Wang KC, Yang YW, Liu B, Sanyal A, Corces-Zimmerman R, Chen Y, et al. A long noncoding RNA maintains active chromatin to coordinate homeotic gene expression. Nature 2011; 472:120-4.
48. Tsai MC, Manor O, Wan Y, Mosammaparast N, Wang JK, Lan F, et al. Long noncoding RNA as modular scaffold of histone modification complexes. Science 2010; 329:689-93.
49. He A, Ma Q, Cao J, von Gise A, Zhou P, Xie H, et al. Polycomb repressive complex 2 regulates normal development of the mouse heart. Circ Res 2012; 110:406-15.
50. Kotake Y, Nakagawa T, Kitagawa K, Suzuki S, Liu N, Kitagawa M, et al. Long non-coding RNA ANRIL is required for the PRC2 recruitment to and silencing of p15(INK4B) tumor suppressor gene. Oncogene 2011; 30:1956-62.
51. Broadbent HM, Peden JF, Lorkowski S, Goel A, Ongen H, Green F, et al. Susceptibility to coronary artery disease and diabetes is encoded by distinct, tightly linked SNPs in the ANRIL locus on chromosome 9p. Hum Mol Genet 2008; 17:806-14.
52. McPherson R, Pertsemlidis A, Kavaslar N, Stewart A, Roberts R, Cox DR, et al. A common allele on chromosome 9 associated with coronary heart disease. Science 2007; 316:1488-91.

53. Visel A, Zhu Y, May D, Afzal V, Gong E, Attanasio C, et al. Targeted deletion of the 9p21 non-coding coronary artery disease risk interval in mice. Nature 2010; 464:409-12.
54. Yap KL, Li S, Munoz-Cabello AM, Raguz S, Zeng L, Mujtaba S, et al. Molecular interplay of the noncoding RNA ANRIL and methylated histone H3 lysine 27 by polycomb CBX7 in transcriptional silencing of INK4a. Mol Cell 2010; 38:662-74.
55. Sato K, Nakagawa H, Tajima A, Yoshida K, Inoue I. ANRIL is implicated in the regulation of nucleus and potential transcriptional target of E2F1. Oncol Rep 2010; 24:701-7.
56. Krenz M, Robbins J. Impact of beta-myosin heavy chain expression on cardiac function during stress. J Am Coll Cardiol 2004; 44:2390-7.
57. Mahdavi V, Chambers AP, Nadal-Ginard B. Cardiac alpha- and beta-myosin heavy chain genes are organized in tandem. Proc Natl Acad Sci U S A 1984; 81:2626-30.
58. Haddad F, Qin AX, Bodell PW, Zhang LY, Guo H, Giger JM, et al. Regulation of antisense RNA expression during cardiac MHC gene switching in response to pressure overload. Am J Physiol Heart Circ Physiol 2006; 290:H2351-61.
59. Haddad F, Jiang W, Bodell PW, Qin AX, Baldwin KM. Cardiac myosin heavy chain gene regulation by thyroid hormone involves altered histone modifications. Am J Physiol Heart Circ Physiol 2010; 299:H1968-80.
60. Hang CT, Yang J, Han P, Cheng HL, Shang C, Ashley E, et al. Chromatin regulation by Brg1 underlies heart muscle development and disease. Nature 2010; 466:62-7.
61. Huang WY, Liew CC. A conserved GATA motif in a tissue-specific DNase I hypersensitive site of the cardiac alpha-myosin heavy chain gene. Biochem J 1997; 325 (Pt 1):47-51.
62. Lee JH, Gao C, Peng G, Greer C, Ren S, Wang Y, et al. Analysis of transcriptome complexity through RNA sequencing in normal and failing murine hearts. Circ Res 2011; 109:1332-41.
63. Movassagh M, Choy MK, Knowles DA, Cordeddu L, Haider S, Down T, et al. Distinct epigenomic features in end-stage failing human hearts. Circulation 2011; 124:2411-22.
64. Gibb EA, Vucic EA, Enfield KS, Stewart GL, Lonergan KM, Kennett JY, et al. Human cancer long non-coding RNA transcriptomes. PLoS One 2011; 6:e25915.
65. Annilo T, Kepp K, Laan M. Natural antisense transcript of natriuretic peptide precursor A (NPPA): structural organization and modulation of NPPA expression. BMC Mol Biol 2009; 10:81.
66. Katayama S, Tomaru Y, Kasukawa T, Waki K, Nakanishi M, Nakamura M, et al. Antisense transcription in the mammalian transcriptome. Science 2005; 309:1564-6.
67. Core LJ, Waterfall JJ, Lis JT. Nascent RNA sequencing reveals widespread pausing and divergent initiation at human promoters. Science 2008; 322:1845-8.
68. Haddad F, Qin AX, Giger JM, Guo H, Baldwin KM. Potential pitfalls in the accuracy of analysis of natural sense-antisense RNA pairs by reverse transcription-PCR. BMC Biotechnol 2007; 7:21.
69. Voigtsberger S, Bartsch H, Baumann G, Luther HP. Cell type-specific expression of endogenous cardiac Troponin I antisense RNA in the neonatal rat heart. Mol Cell Biochem 2009; 324:1-11.
70. He Y, Vogelstein B, Velculescu VE, Papadopoulos N, Kinzler KW. The antisense transcriptomes of human cells. Science 2008; 322:1855-7.

71. Levin JZ, Yassour M, Adiconis X, Nusbaum C, Thompson DA, Friedman N, et al. Comprehensive comparative analysis of strand-specific RNA sequencing methods. Nat Methods 2010; 7:709-15.
72. Wang ET, Sandberg R, Luo S, Khrebtukova I, Zhang L, Mayr C, et al. Alternative isoform regulation in human tissue transcriptomes. Nature 2008; 456:470-6.
73. Mironov AA, Fickett JW, Gelfand MS. Frequent alternative splicing of human genes. Genome Res 1999; 9:1288-93.
74. Chooniedass-Kothari S, Emberley E, Hamedani MK, Troup S, Wang X, Czosnek A, et al. The steroid receptor RNA activator is the first functional RNA encoding a protein. FEBS Lett 2004; 566:43-7.
75. Mercer TR, Gerhardt DJ, Dinger ME, Crawford J, Trapnell C, Jeddeloh JA, et al. Targeted RNA sequencing reveals the deep complexity of the human transcriptome. Nat Biotechnol 2012; 30:99-104.
76. Burd CE, Jeck WR, Liu Y, Sanoff HK, Wang Z, Sharpless NE. Expression of linear and novel circular forms of an INK4/ARF-associated non-coding RNA correlates with atherosclerosis risk. PLoS Genet 2010; 6:e1001233.
77. Bartsch H, Voigtsberger S, Baumann G, Morano I, Luther HP. Detection of a novel sense-antisense RNA-hybrid structure by RACE experiments on endogenous troponin I antisense RNA. RNA 2004; 10:1215-24.
78. Pandey RR, Mondal T, Mohammad F, Enroth S, Redrup L, Komorowski J, et al. Kcnq1ot1 antisense noncoding RNA mediates lineage-specific transcriptional silencing through chromatin-level regulation. Mol Cell 2008; 32:232-46.
79. van der Brug M, Nalls MA, Cookson MR. Deep sequencing of coding and non-coding RNA in the CNS. Brain Res 2010; 1338:146-54.
80. Kampa D, Cheng J, Kapranov P, Yamanaka M, Brubaker S, Cawley S, et al. Novel RNAs identified from an in-depth analysis of the transcriptome of human chromosomes 21 and 22. Genome Res 2004; 14:331-42.
81. Hurwitz J, Furth JJ, Anders M, Evans A. The role of deoxyribonucleic acid in ribonucleic acid synthesis. II. The influence of deoxyribonucleic acid on the reaction. J Biol Chem 1962; 237:3752-9.
82. Clark MB, Johnston RL, Inostroza-Ponta M, Fox AH, Fortini E, Moscato P, et al. Genome-wide analysis of long noncoding RNA stability. Genome Res 2012; 22:885-98.
83. Hah N, Danko CG, Core L, Waterfall JJ, Siepel A, Lis JT, et al. A rapid, extensive, and transient transcriptional response to estrogen signaling in breast cancer cells. Cell 2011; 145:622-34.
84. Churchman LS, Weissman JS. Nascent transcript sequencing visualizes transcription at nucleotide resolution. Nature 2011; 469:368-73.
85. Levsky JM, Singer RH. Fluorescence in situ hybridization: past, present and future. J Cell Sci 2003; 116:2833-8.
86. Chureau C, Chantalat S, Romito A, Galvani A, Duret L, Avner P, et al. Ftx is a non-coding RNA which affects Xist expression and chromatin structure within the X-inactivation center region. Hum Mol Genet 2011; 20:705-18.
87. Tripathi V, Ellis JD, Shen Z, Song DY, Pan Q, Watt AT, et al. The nuclear-retained noncoding RNA MALAT1 regulates alternative splicing by modulating SR splicing factor phosphorylation. Mol Cell 2010; 39:925-38.
88. Korostowski L, Sedlak N, Engel N. The Kcnq1ot1 long non-coding RNA affects chromatin conformation and expression of Kcnq1, but does not regulate its imprinting in the developing heart. PLoS Genet 2012; 8:e1002956.

89. Mondal T, Rasmussen M, Pandey GK, Isaksson A, Kanduri C. Characterization of the RNA content of chromatin. Genome Res 2010; 20:899-907.
90. Gregory RI, Randall TE, Johnson CA, Khosla S, Hatada I, O'Neill LP, et al. DNA methylation is linked to deacetylation of histone H3, but not H4, on the imprinted genes Snrpn and U2af1-rs1. Mol Cell Biol 2001; 21:5426-36.
91. Zappulla DC, Cech TR. RNA as a flexible scaffold for proteins: yeast telomerase and beyond. Cold Spring Harb Symp Quant Biol 2006; 71:217-24.
92. Chu C, Qu K, Zhong FL, Artandi SE, Chang HY. Genomic maps of long noncoding RNA occupancy reveal principles of RNA-chromatin interactions. Mol Cell 2011; 44:667-78.
93. Simon MD, Wang CI, Kharchenko PV, West JA, Chapman BA, Alekseyenko AA, et al. The genomic binding sites of a noncoding RNA. Proc Natl Acad Sci U S A 2011; 108:20497-502.
94. Ule J, Jensen KB, Ruggiu M, Mele A, Ule A, Darnell RB. CLIP identifies Nova-regulated RNA networks in the brain. Science 2003; 302:1212-5.
95. Hafner M, Landthaler M, Burger L, Khorshid M, Hausser J, Berninger P, et al. Transcriptome-wide identification of RNA-binding protein and microRNA target sites by PAR-CLIP. Cell 2010; 141:129-41.
96. Guil S, Soler M, Portela A, Carrere J, Fonalleras E, Gomez A, et al. Intronic RNAs mediate EZH2 regulation of epigenetic targets. Nat Struct Mol Biol 2012; 19:664-70.
97. Kretz M, Siprashvili Z, Chu C, Webster DE, Zehnder A, Qu K, et al. Control of somatic tissue differentiation by the long non-coding RNA TINCR. Nature 2013; 493:231-5.
98. Hsu MT, Coca-Prados M. Electron microscopic evidence for the circular form of RNA in the cytoplasm of eukaryotic cells. Nature 1979; 280:339-40.
99. Surono A, Takeshima Y, Wibawa T, Ikezawa M, Nonaka I, Matsuo M. Circular dystrophin RNAs consisting of exons that were skipped by alternative splicing. Hum Mol Genet 1999; 8:493-500.
100. Zaphiropoulos PG. Exon skipping and circular RNA formation in transcripts of the human cytochrome P-450 2C18 gene in epidermis and of the rat androgen binding protein gene in testis. Mol Cell Biol 1997; 17:2985-93.
101. Salzman J, Gawad C, Wang PL, Lacayo N, Brown PO. Circular RNAs are the predominant transcript isoform from hundreds of human genes in diverse cell types. PLoS One 2012; 7:e30733.
102. Li XF, Lytton J. A circularized sodium-calcium exchanger exon 2 transcript. J Biol Chem 1999; 274:8153-60.
103. Hansen TB, Jensen TI, Clausen BH, Bramsen JB, Finsen B, Damgaard CK, et al. Natural RNA circles function as efficient microRNA sponges. Nature 2013.
104. Memczak S, Jens M, Elefsinioti A, Torti F, Krueger J, Rybak A, et al. Circular RNAs are a large class of animal RNAs with regulatory potency. Nature 2013.
105. Hansen TB, Wiklund ED, Bramsen JB, Villadsen SB, Statham AL, Clark SJ, et al. miRNA-dependent gene silencing involving Ago2-mediated cleavage of a circular antisense RNA. EMBO J 2011; 30:4414-22.
106. Al-Balool HH, Weber D, Liu Y, Wade M, Guleria K, Nam PL, et al. Post-transcriptional exon shuffling events in humans can be evolutionarily conserved and abundant. Genome Res 2011; 21:1788-99.
107. Squires JE, Patel HR, Nousch M, Sibbritt T, Humphreys DT, Parker BJ, et al. Widespread occurrence of 5-methylcytosine in human coding and non-coding RNA. Nucleic Acids Res 2012; 40:5023-33.

108. Motorin Y, Helm M. RNA nucleotide methylation. Wiley interdisciplinary reviews RNA 2011; 2:611-31.
109. Underwood JG, Uzilov AV, Katzman S, Onodera CS, Mainzer JE, Mathews DH, et al. FragSeq: transcriptome-wide RNA structure probing using high-throughput sequencing. Nat Methods 2010; 7:995-1001.
110. Westhof E, Romby P. The RNA structurome: high-throughput probing. Nat Methods 2010; 7:965-7.
111. Benhamed M, Herbig U, Ye T, Dejean A, Bischof O. Senescence is an endogenous trigger for microRNA-directed transcriptional gene silencing in human cells. Nat Cell Biol 2012; 14:266-75.
112. Morris KV, Chan SW, Jacobsen SE, Looney DJ. Small interfering RNA-induced transcriptional gene silencing in human cells. Science 2004; 305:1289-92.
113. Huang XA, Yin H, Sweeney S, Raha D, Snyder M, Lin H. A major epigenetic programming mechanism guided by piRNAs. Dev Cell 2013; 24:502-16.
114. Schubert T, Pusch MC, Diermeier S, Benes V, Kremmer E, Imhof A, et al. Df31 protein and snoRNAs maintain accessible higher-order structures of chromatin. Mol Cell 2012; 48:434-44.
115. Han J, Kim D, Morris KV. Promoter-associated RNA is required for RNA-directed transcriptional gene silencing in human cells. Proc Natl Acad Sci U S A 2007; 104:12422-7.
116. Melo CA, Drost J, Wijchers PJ, van de Werken H, de Wit E, Oude Vrielink JA, et al. eRNAs are required for p53-dependent enhancer activity and gene transcription. Mol Cell 2013; 49:524-35.
117. Johnsson P, Ackley A, Vidarsdottir L, Lui WO, Corcoran M, Grander D, et al. A pseudogene long-noncoding-RNA network regulates PTEN transcription and translation in human cells. Nat Struct Mol Biol 2013; 20:440-6.
118. Hawkins PG, Morris KV. Transcriptional regulation of Oct4 by a long non-coding RNA antisense to Oct4-pseudogene 5. Transcription 2010; 1:165-75.
119. Bond AM, Vangompel MJ, Sametsky EA, Clark MF, Savage JC, Disterhoft JF, et al. Balanced gene regulation by an embryonic brain ncRNA is critical for adult hippocampal GABA circuitry. Nature neuroscience 2009; 12:1020-7.
120. Horard B, Gilson E. Telomeric RNA enters the game. Nat Cell Biol 2008; 10:113-5.
121. Haeger P, Cuevas R, Forray MI, Rojas R, Daza C, Rivadeneira J, et al. Natural expression of immature Ucn antisense RNA in the rat brain. Evidence favoring bidirectional transcription of the Ucn gene locus. Brain Res Mol Brain Res 2005; 139:115-28.
122. Ishii N, Ozaki K, Sato H, Mizuno H, Saito S, Takahashi A, et al. Identification of a novel non-coding RNA, MIAT, that confers risk of myocardial infarction. J Hum Genet 2006; 51:1087-99.
123. Roeszler KN, Itman C, Sinclair AH, Smith CA. The long non-coding RNA, MHM, plays a role in chicken embryonic development, including gonadogenesis. Dev Biol 2012; 366:317-26.
124. Tran VG, Court F, Duputie A, Antoine E, Aptel N, Milligan L, et al. H19 antisense RNA can up-regulate Igf2 transcription by activation of a novel promoter in mouse myoblasts. PLoS One 2012; 7:e37923.
125. Khalil AM, Faghihi MA, Modarresi F, Brothers SP, Wahlestedt C. A novel RNA transcript with antiapoptotic function is silenced in fragile X syndrome. PLoS One 2008; 3:e1486.

126. Sleutels F, Zwart R, Barlow DP. The non-coding Air RNA is required for silencing autosomal imprinted genes. Nature 2002; 415:810-3.
127. Ritter O, Luther HP, Haase H, Baltas LG, Baumann G, Schulte HD, et al. Expression of atrial myosin light chains but not alpha-myosin heavy chains is correlated in vivo with increased ventricular function in patients with hypertrophic obstructive cardiomyopathy. J Mol Med (Berl) 1999; 77:677-85.
128. Potts JD, Vincent EB, Runyan RB, Weeks DL. Sense and antisense TGF beta 3 mRNA levels correlate with cardiac valve induction. Dev Dyn 1992; 193:340-5.
129. Robb GB, Carson AR, Tai SC, Fish JE, Singh S, Yamada T, et al. Post-transcriptional regulation of endothelial nitric-oxide synthase by an overlapping antisense mRNA transcript. J Biol Chem 2004; 279:37982-96.
130. Friedrichs F, Zugck C, Rauch GJ, Ivandic B, Weichenhan D, Muller-Bardorff M, et al. HBEGF, SRA1, and IK: Three cosegregating genes as determinants of cardiomyopathy. Genome Res 2009; 19:395-403.
131. Rodriguez-Campos A, Azorin F. RNA is an integral component of chromatin that contributes to its structural organization. PLoS One 2007; 2:e1182.

1.1.12 Figure 1

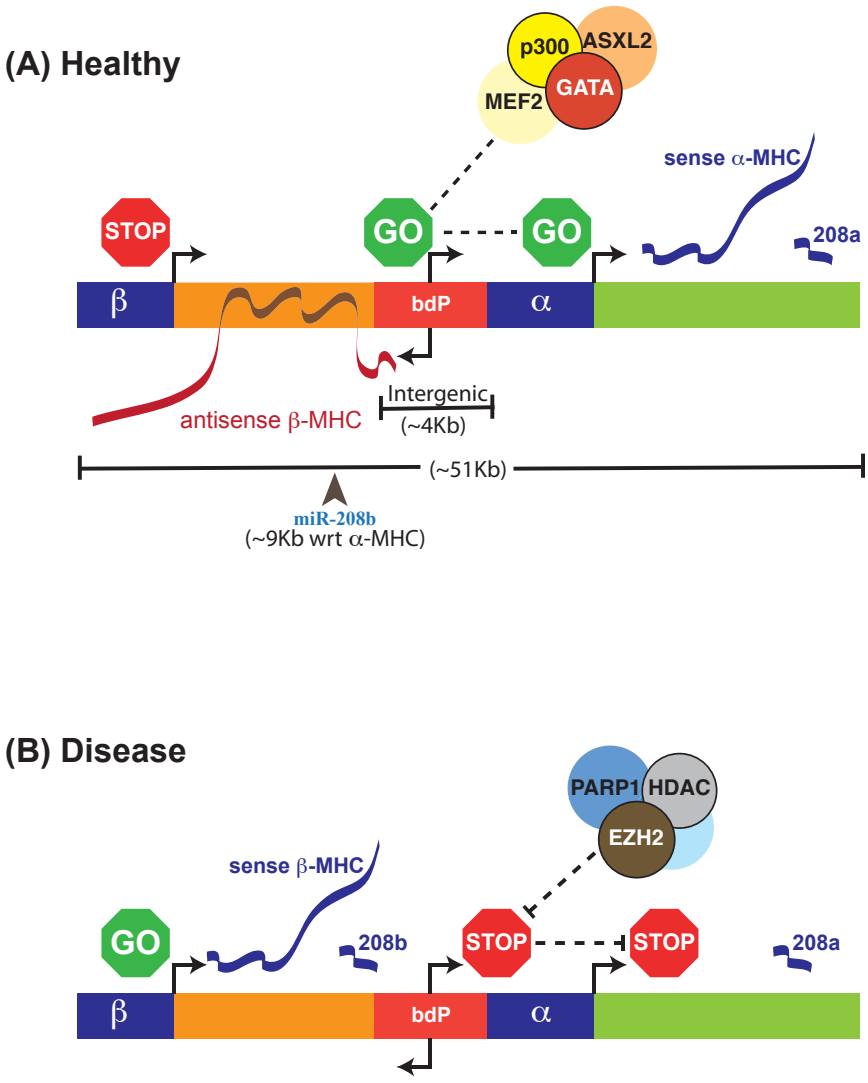

1.1.13 Figure Legends

Figure 1. Complex interactions of epigenetic factors at the cardiac MHC genes regulate the expression of myosin ncRNAs. The expression of cardiac α- and β-*MHC* genes is dynamic and antithetically regulated in (A) healthy and (B) diseased heart. The bi-directional promoter (bdP) within the α- and β-*MHC* intergenic region comprises binding sequences for GATA, CTF1/NF1, RAR, T3R, MEF-2 transcription factors. Both the α- and β-*MHC* genes encode microRNAs, *miRNA-208a* and *miRNA-208b* whose expressions and functions are associated with heart health and disease. Besides these myosin ncRNA expressions, the bdP is known to produce lncRNA, *AS* β-*MHC* that serve to regulate β-*MHC* sense (mRNA) transcription by chromatin interaction. Recent experiments link epigenetic proteins such as BRG1, HDACs and Ezh2 to direct association at the intergenic bdP and suppression of *AS* β-*MHC* and α-*MHC* genes leaving sense transcription and expression of β-*MHC* gene in diseased heart.

1.1.14 Table 1. Classification of functional ncRNAs. Transcriptional gene silencing functions of short (grey background) and long ncRNAs by chromatin interaction.

ncRNA class	Chromatin interaction
MicroRNA (miRNA)	Yes[111]
Small interfering RNA (siRNA)	Yes[112]
Piwi-interacting RNA (piRNA)	Yes[113]
Small nuclearRNA (snRNA)	Yes[89]
Small nucleolarRNA (snoRNA)	Yes[114]
Natural antisense transcript (NAT)	Yes[78]
Large intergenic ncRNA (lincRNA)	Yes[32]
Promoter associated RNA (paRNA)	Yes[115]
Circular RNA (circRNA)	Yes[76]
Enhancer RNA (eRNA)	Yes[116]
Pseudogene RNA (trans-NAT)	Yes[117, 118]
Transcribed ultraconserved regions (T-UCRs)	Yes[119]
Short-lived RNA transcripts (SLiTs)	Yes[29]
Telomeric repeat-containing RNA (TERRA)	Yes[120]
Transfer RNA (tRNA)	Not reported
Ribosomal RNA (rRNA)	Not reported

1.1.15 Table 2. Chromatin immunoprecipitaion in mouse left ventricle shows specific interaction of Ezh2 at genes with bi-directional transcription. Listed are genes as enriched by ChIP using antibodies that recognize Ezh2 and H3K27me3 modification.[49] Genes on sense and antisense strands are distinguished by an underline. Significant proportion of the genes enriched by Ezh2-ChIP in the mouse heart show specific binding of Ezh2 at key cardiac genes with antisense RNA expression. Several cardiac genes with antisense RNA expression including the cardiac regulatory lncRNA genes *Anril*, *Miat* and *Nppa-AS* appear to be bound by Ezh2. Genes encoding non-cardiomyocyte expression programs such as the *Pax6*, which expresses opposite strand transcript is also repressed by direct binding of Ezh2 in the heart. Increased expression of Myosin light chain (*Myl4*) and *Tgfβ-3* genes was observed in Ezh2 deficient mice,[10, 49] both of which are known to express regulatory antisense transcripts however show no direct association of Ezh2 at these promoters.[49]

1) Ink4a, Ink4b, Ak148321/ANRIL	16) Irx5, 4933436c20Rik
2) Pax6, Pax6ost1	17) Fbxo44, Fbxo2
3) Nppa, Nppa-as1	18) Otx2, Otx2os1
4) Miat, 1700028D13Rik	19) H2-K2, AA388235
5) α-MHC, β-MHC, AS β-MHC	20) Pcnxl2, Bc021891
6) Foxd2, 9130206I24Rik	21) Dlx6, Dlx6as-1
7) Hoxc11, Hoxc12, Hotair	22) Tbx2, 2610027K06Rik
8) Gata3, 4930412O13Rik	23) Myl4 (ALC-1), Myl4-AS
9) Dio3, Dio3os	24) cTn1 (Tnnt3), cTn1-AS
10) Ucn, Ucn-as	25) Tgfβ3, Tgfβ3-AS
11) Islr2, 1600029o15Rik	
12) Dll4, Gm14207	
13) Pou3f3, 2610017I09Rik	
14) 2610100L16Rik, Gm10724	
15) Hoxa4, Hoxa5, Hoxa6, Hoxa7, 2700086A05Rik	

Long ncRNA	Cardiac function	Disease association	Expression in disease (↑/↓)	Methods of identification	Mechanism of regulation	Splice variants
Anril	Regulation of INK4/ARF locus, genes involved in nuclear and chromatin architecture[53]	Cardiac hypertrophy, Atherosclerosis	↑	RNA-ChIP, RACE-PCR, circRNA assays	Chromatin interaction	Reported
cTnI-AS	Regulation of cTnI mRNA[69]	Unknown	Unknown	RACE	RNA duplex formation	None reported
Nppa-AS1	Regulation of NPPA mRNA[65]	Unknown	Unknown	RACE	RNA duplex formation	Reported
AS-Ucn	Regulation of sense transcription/translation[121]	Unknown	Unknown	RNase Protection Assay	Overlapping sense transcription	None reported
Miat or Gomafu	Splicing, Retinal cell fate specification[122]	Myocardial Infarction	↑	Northern blot, RACE	Chromatin interaction / *Nanog* TF binding	Reported
Fendrr	Cardiac mesoderm formation[17]	Unknown	Unknown	RACE, RNA-ChIP, ISH	Chromatin interaction	None reported
Mhm	Cardiomyocyte Proliferation[123]	Cardiac hypertrophy, arrhythmia	Unknown	Northern blot, *In Situ* hybridization	Chromatin interaction	Reported
H19	Imprinting and *Igf2* regulation[62]	Hypertrophy & Heart failure	↑	RNA-ChIP, Strand-specific PCR	Chromatin interaction	Reported
91H (AS-H19)	Regulation of *Igf2*[124]	Unknown	Unknown	Strand-specific PCR	Unknown	None reported
Kcnq1ot1	Embryonic heart formation, Regulation of Cdkn1c, KvLQT1 genes[88]	Unknown	Unknown	RACE, FISH, RNA-ChIP	Chromatin interaction	Reported
Fmr1-AS1 or Fmr4	Cell proliferation[125]	Proposed	Unknown	RACE, Northern blot	Chromatin interaction proposed	Reported
Air	Embryonic heart formation, Imprinting of *Igf2r* in adult hearts[126]	Unknown	Unknown	RNA-ChIP, FISH	Chromatin interaction	Reported
Mlc-Alc-1 antisense	Regulation of MLC-1 mRNA[127]	ToF, HOCM	↑	Strand-specific PCR	Unknown	None reported
AS-Tgfβ3	Hear chamber formation[128]	Unknown	Unknown	RNase protection assay	RISC-mediated silencing proposed	None reported
sONE (AS-eNOS)	eNOS synthesis[129]	Unknown	Unknown	Strand-specific PCR, *In Situ* hybridization	Unknown	None reported
Sra	Myogenesis, SRA proteins synthesis[130]	DCM	↓	Strand-specific PCR, Splice variant assays, RNA-ChIP	Chromatin interaction	Reported
AS β-MHC	*β-MHC* gene transcription[58]	Cardiac hypertrophy	↓	Strand-specific PCR	Chromatin interaction	None reported
Braveheart	Cardiovascular lineage commitment[16]	Unknown	Unknown	RACE, native RNA-IP	Chromatin interaction	Reported

1.1.16 Table 3. Long ncRNA expression in the heart

ANRIL, Antisense non-coding RNA in the INK4 locus; **cTnI**, Cardiac troponin I; **NPPA-AS1**, natriuretic peptide precursor A-antisense transcript 1; **AS-UCN**, Urocortin antisense; **MIAT**, Myocardial Infarction associated transcript; **MHM**, Male HyperMethylated; **MLC-ALC-1**, myosin light chain-atrial light chain-1;**AS-TGFβ3**, Transforming growth factor β-3 antisense RNA; **SRA**, steroid receptor RNA activator; **ToF**, tetrology of fallot; **HOCM**, Hypertrophic obstructive cardiomyopathy; **DCM**, dilated cardiomyopathy. **RACE**, Rapid amplification of cDNA ends; **FISH**, Fluorescent In Situ Hybridization.

1.1.17 Table 4. Methodologies for detection, characterization and structural analysis of lncRNA. ncRNA-chromatin interactions assays are highlighted with grey background.

Method	Advantage
Strand-specific qRT-PCR	Sense and antisense RNA quantification[68, 69]
ASSAGE	Reveals transcript direction[70]
RNA ligation using distinct adaptors	Reveals transcript direction[71]
NET-Seq	Transcriptional pausing[84]
GRO-Seq	Immediate, transient changes to transcriptome[83]
Exon-scanning	Splice variant detection[65, 77]
RACE	Splice variant detection, Obtain full-length transcript sequence[47, 78]
RNA CaptureSeq	Detection of transcripts of low abundance, Novel splice variant detection[75]
BRIC-Seq	Transcript stability, RNA decay[29]
SAGE (SuperSAGE)	Novel, tissue-specific lncRNA detection[64]
PolyA$^-$ RNA-Seq	Identification of bimorphic transcripts and circular RNAs[101]
RNA bisulfite conversion	RNA methylation, RNA folding, footprint sequences[70]
PTES identification	Splice variants, circular RNA prediction[106]
FragSeq	Intra- and inter- RNA base pairing[109]
RNaseR assay	Circular transcriptome studies[101, 104]
Native chromatin preparation	Purifies CARs, PolyA$^-$ ncRNAs[131]
RNA-FISH	Cellular compartmentalization of transcripts, chromatin interaction[86, 87]
RNA-ChIP	Protein-dependent RNA interaction with chromatin[78]
Native RNA-ChIP	Protein-dependent RNA interaction with chromatin[89]
ChIRP	RNA-dependent chromatin interaction[92]
CHART	RNA-dependent chromatin interaction[93]
HITS-CLIP	Cross-linking of directly interacting RNA-protein complexes[94]
PAR-CLIP	Cross-linking of directly interacting RNA-protein complexes [95]

ASSAGE, Asymmetric strand specific analysis of gene expression; **GRO-Seq**, Global Run-on sequencing; **NET-Seq**, Native elongating transcript sequencing; **RACE**, Rapid amplification of cDNA ends; **BRIC-Seq**, 5'-Bromo-uridine Immunoprecipitation chase-deep sequencing; **SAGE**, Serial analysis of gene expression; **PTES**, Post-transcriptional exon scrambling; **CARs**, Chromatinassociated RNAs; **FISH**, Fluorescent In Situ Hybridization; **ChIP**, Chromatin immunoprecipitation; **ChIRP**, Chromatin Isolation by RNA purification; **CHART**, Capture hybridization analysis of RNA targets; **HITS-CLIP**, High-throughput sequencing of RNA isolated by crosslinking immunoprecipitation; **PAR-CLIP**, Photoactivatable-Ribonucleoside-Enhanced crosslinking and immunoprecipitation.

1.2. Chromatin Remodeling and Post-translational Histone Modifications Regulate Cardiac Gene Expression

Authors: Prabhu Mathiyalagan[1], Samuel T. Keating[1], Xiao-Jun Du[2,4] and Assam El-Osta[1,3,4]*

[1]Epigenetics in Human Health and Disease Laboratory, The Alfred Medical Research and Education Precinct, Melbourne, Victoria 3004, Australia
[2]Experimental Cardiology, Baker IDI Heart and Diabetes Institute, The Alfred Medical Research and Education Precinct, Melbourne, Victoria 3004, Australia
[3]Department of Pathology, The University of Melbourne, Parkville, Victoria, Australia
[4]Central Clinical School, Faculty of Medicine, Monash University, Victoria, Australia

*Correspondence:
Prof. Assam El-Osta
[redacted] (**Email**)
[redacted] (**Telephone**)
613 8532 1100 (**Fax**)

Word Count: < 7500 words

Keywords: Cardiac Hypertrophy, Gene regulation, histone acetylation, histone methylation, HDACi, chromatin remodeling

1.2.1 Abstract

Epigenetic regulation of gene expression is central to cardiovascular physiology and pathology. Recent advances in genome-wide mapping of transcription factors and covalent modification of the chromatin point to an important role for histone acetylation and methylation patterns in determining key developmental programs of cardiac lineage. Recent experimental evidence demonstrate that dynamic regulation of the chromatin landscape is similarly critical for pathological cardiac gene expression in response to stress. At the forefront of such research are the histone deacetylase enzymes (HDACs), whose pharmacological inhibition is currently topical and promising for treatment of heart failure. HDACs interact with a complex co-regulatory network of transcription factors, chromatin remodeling complexes, and specific histone modifiers to regulate gene expression in the heart. A prominent example is the Ezh2 histone methyltransferase (HMT), which was recently proposed to have a significant role in cardiac physiology in adults and cardiac lineage specification during embryo development. This review comprehensively explores the regulatory impact of histone modifications in cardiac development, health and disease. With a focus on transcriptional control in rodent models of heart disease we discuss recent experimental findings emphasizing specific components of diverse regulatory complexes that mediate chromatin modification in the myocardium. Following recent implication of numerous HMTs and HDACs in heart disease, there is a growing potential for epigenetic drugs to manipulate pathological gene expression.

1.2.2 Introduction

The mechanical force required for heart function is achieved by complex contractions of cardiac muscle fibers within the myocardium (heart muscle). As predominant constituents of heart muscle, cardiomyocytes are the primary determinants of cardiac contractility. During normal development the heart achieves anatomical specialization by separation to four individual chambers, the left and right atria and the left and right ventricles. Chamber specification is tightly coordinated by temporal and spatial expression of cardiac transcription factors such as Tbx5, Gata-4, Mef-2, Csk/Nkx2-5 and Hand, which collectively determine specific gene expression patterns.[1-4] Precise regulation of myocardial transcription is critical for homeostatic control in adults because cardiomyocytes reach terminal differentiation and lose their ability to divide shortly after birth.[5] Consequently epigenetic regulation of gene expression is thought to be critical and changes to the chromatin template such as post-translational histone modifications are associated with pathological ventricular remodeling after myocardial infarction.[6] For example, cardiac-specific deletion of Ezh2 and Ptip, key factors required for histone methylation impaired heart function in mouse models.[6, 7] Expression of hypertrophy marker genes such as the *β-MHC* and *Anp* was elevated in Ezh2 knockout mice, while Ptip knockout mouse hearts exhibited conduction defect. Indeed, *de novo* mutations in genes encoding histone methyltransferase enzymes (HMT) required for H3K4 and H3K27 methylation such as MLL2, Suv420H1, Kdm5s and Kdm5b were identified with high incidence in severe congenital heart disease patients.[8] Together, these recent data identify novel epigenetic regulators in the heart and support strong participation for chromatin modifications in regulating physiological and pathological cardiac gene expression.

Throughout one's lifetime, the heart is subject to a variety of physiological demands such as exercise or pregnancy. In addition, pathological surroundings such as pressure overload (aortic valve stenosis, hypertension), myocardial infarction, myocarditis and idiopathic dilated cardiomyopathy induce cardiac adaptations.[9, 10] Cardiovascular disease typically stimulates enlargement of cardiomyocytes and consequent thickening of the myocardium, referred to as cardiac hypertrophy. While both physiological and pathological mechanisms result in increased cardiomyocyte

size by hypertrophic growth, pathological cardiac hypertrophy is regarded as a maladaptive response leading to irreversible remodeling of the ventricular chambers and eventually heart failure. Accordingly, pharmacological inhibition of hypertrophic cardiomyocyte growth has proven promising for heart failure patients.[11] At the level of gene expression, cardiac hypertrophy is characterized by re-establishment of the fetal gene program required for cardiomyocyte growth.[12] Generally, the phase of hypertrophy is followed by the induction of pro-fibrotic and pro-inflammatory pathways leading to the formation of interstitial fibrosis within the myocardium with increased risk of cardiac morbidity and mortality.[13, 14]

Pharmacological inhibition of outside-in signaling pathways involving G-protein coupled receptors (GPCRs) such as β-adrenergic receptors, ion-channels such as L-type Ca^{2+} and Na^{+}/H^{+} exchangers, as well as cytoplasmic protein kinases such as CAMKII are known to attenuate cardiac hypertrophy and heart failure.[15, 16] However, these drugs are often ineffective and can inhibit pathways that are either redundant in cardiomyocytes or mediating compensatory changes. Recent studies have identified several enzymes that chemically modify histone proteins and non-histone proteins (eg. transcription factors) as key regulators of pathological gene expression in cardiac hypertrophy.[17, 18] In addition to ATPase-dependent chromatin remodelers such as Brahma-related gene 1 (Brg1) and Parp,[19] histone protein tails are targeted by enzymes for chemical modifications such as acetylation and methylation in cardiac hypertrophy and heart failure.[20-22] The functional bridge between chromatin modifiers and signaling mediators is established through transcription factors that either suppress or promote gene expression.[23] Factors such as Mef2 and Gata4 are thought to physically associate with enzymes that modify histones for activation of gene targets.[24,25] These data support diverse regulation of gene transcription by complex interactions involving transcription factors, co-regulatory determinants, chromatin remodelers, as well as histone modifying enzymes in the myocardium. Thorough understanding of these complex interactions at the chromatin template is likely to improve identifying therapeutic targets for the treatment of cardiac hypertrophy and heart failure.

1.2.3 Chromatin remodeling of the hypertrophic heart

Chromatin architecture in higher eukaryotes is fundamental to nuclear functions of gene expression, DNA repair, recombination and replication.[26-28] Consisting of a family of ATPase-dependent chromatin remodeling complexes, SWI/SNF regulate transcription in the heart in concert with co-activator and co-repressor complexes.[29] As essential components of the SWI/SNF complex, Brahma (Brm) and Brg1 are considered critical chromatin remodeling machinery for vertebrate heart formation. A recent study,[29] revealed dosage-sensitive interdependence between BRG1 and cardiac transcription factors such as Gata4, Nkx2-5 and Tbx5. Specifically, Brg1 haploinsufficiency in mice reduced Tbx5 / Gata4 binding to target gene promoters and vice versa. The study precisely demonstrated that the relative allelic balance between Brg1 and cardiac transcription factors is essential for promoter binding and gene regulation in the heart. Recently, Brg1 was implicated in the prototypical shift in cardiac myosin heavy chain (*MHC)* isoform expression in a TAC model of pathological hypertrophy.[19] Similarly, the DNA-binding protein Parp1 required for chromatin remodeling in the healthy myocardium was implicated in activation of the pathological β-*MHC* gene in the hypertrophied heart by interaction with Brg1 at the β-*MHC* promoter.[19] Equally, interaction between Brg1 and HDAC enzymes functions to suppress α-*MHC* gene expression in cardiac hypertrophy.[19]

Ventricular hypertrophy is characterized by profound changes in gene expression including the up-regulation of fetal genes such as *Anp*, *Bnp,* β-*MHC*, as well as suppression of genes required for cardiac function and adult heart homeostasis.[12, 30] For example, α-*MHC* and *Serca2a* are maintained at high levels in healthy hearts, whereas hypertrophy reduces expression of these genes. Such gene-suppressive events are regulated by SWI/SNF containing Brm/Brg1-associated histone deacetylase (HDAC) co-repressor complexes.[19, 31] Recruitment of Brm to the proximal promoters of *Anp* and *Bnp* serves to increase transcription, whereas recruitment of Brg1 to α-*MHC* was associated with transcriptional suppression in models of cardiac hypertrophy.[31] How chromatin-remodeling complexes are regulated for binding at specific gene sites in response to hypertrophic stimuli remains unclear. In addition to proposed recruiting functions of transcription factors

and DNA-binding proteins, recent experiments also implicate histone-modifying proteins in such chromatin interactions. For instance, contextual association of chromatin factors with either histone acetyltransferase (HAT) or HDAC enzymes may determine the expression of cardiac genes.[20] In addition to ATPase-dependent chromatin remodeling complexes, recent observations also suggest novel interactions for histone modifying proteins such as Ezh2 and Asxl2 at *MHC* promoters and these proteins are thought to be regulated for binding under disease conditions.[6, 32] These data support a complex network of chromatin associations underlying hypertrophic gene regulation.

1.2.4 Post-translational histone acetylation

Histone tail modifications facilitate nuclear processes that are largely dependent on the accessibility of DNA to transcription factors, as well as co-regulatory and remodelling complexes.[28] The chemistry of chromatin dynamics has been studied in model systems and is best characterized in context of histone acetylation, which has revealed several mechanistic insights into chromatin structure and function. Perhaps the best studied of all histone-modifying enzymes are the HATs and HDACs, which are strongly implicated in gene expression changes associated with pathological cardiac hypertrophy.[18, 20] Histone acetylation neutralizes the positive charge of lysine residues, consequentially weakening the charge-dependent association of histone proteins and DNA to increase the accessibility of the genome to co-regulatory determinants.[28]

With the advent of massive parallel sequencing (Seq) coupled with chromatin immunoprecipitation (ChIP) of global changes to histone modifications, numerous cis-acting regulatory sequences important for cardiomyocytes gene expression have been identified.[33, 34] Creb-binding protein (Cbp) and p300 are HATs required for precise regulation of homeostatic gene expression in the left and right ventricles.[35] Gene sequences enriched for acetylated histones also revealed binding of cardiac transcription factors Srf and Gata4 most likely mediated by p300 acetyltransferase activity at these promoters.[34, 35] Indeed, promoter enrichment for p300 is critical for

gene regulation associated with the development of ventricular chambers.[35] Inactivation of p300 and/or Cbp genes in mice is developmentally lethal at E9 and E11 days respectively and cardiac-specific deletion at later stages of development confers severe abnormalities of the heart.[36] Transgenic expression of p300 induces cardiac hypertrophy in mice, whereas dominant-negative p300 mutants blocked agonist-induced cardiac hypertrophy suggesting p300-HAT activity as a key mediator of cardiac hypertrophy.[37] In accordance with the role of co-regulatory complexes in cell- and promoter-specific regulation of gene expression, P300 interacts with specific cardiac transcription factors such as Gata4, Mef2D, MyoD, and Mef2C to activate gene expression in the heart.[25, 38, 39]

Elevated myocardial stress in the adult heart increases P300 activity resulting in hypertrophy-associated gene activation.[40] Accordingly, disruption of protein fragments responsible for p300 interaction with Gata transcription complexes in primary rat cardiomyocytes attenuated phenylephrine-induced hypertrophy.[41] As a specific inhibitor of p300, curcumin prevents heart failure in rats by inhibiting hypertrophy-induced acetylation and DNA-binding of p300-Gata4 complexes.[42] Indeed, ventricular function was further improved when ACE-inhibitors were administered in combination with curcumin to rodent models of post-myocardial infarction.[43] With clear association of histone modifications to maintenance of the cardiomyocyte gene expression program, defining the regulatory events that contribute to cardiac hypertrophy could lead to better strategies with greater specificity to improve consequences of heart disease.

1.2.5 Histone deacetylation and cardiac gene expression

At the forefront of cardiac chromatin research are HDACs, key mediators of hypertrophy-induced gene expression.[44] Pharmacological inhibition or genetic knockout of HDACs attenuates expression of numerous loci associated with hypertrophy.[18, 45] HDACs are responsible for a series of enzymatic activities that remove acetyl groups from the ε-N-acetyl-L-lysine residue of histone and non-histone proteins. Whereas deacetylation of histone tails is generally linked with gene

suppression, deacetylation of residues harboured by non-histone proteins (e.g. transcription factors) can often serve to activate gene expression.[46] HDACs are broadly classified into four groups according to their function and sequence similarity.[47] The catalytic activity of class I, class II and class IV HDACs are zinc-dependent, while class III HDACs (known as sirtuins) are nicotinamide adenine dinucleotide (NAD^+) dependent.[48] The class I HDACs comprises HDAC-1, -2, -3 and -8, each harbouring a deacetylase domain, localised to the nucleus, and functionally linked with transcriptional suppression.[49] Class II HDACs are further subdivided into class IIa (HDAC-4, -5, -7, -9) and class IIb (HDAC-6 and HDAC-10). These subclasses can shuttle between the cytosol and nucleus of the heart, skeletal muscle, and brain tissue, and are linked with cardiac defects.[48] Class III HDACs (Sirt1-Sirt7) are a class of NAD^+ dependent enzymes found in both nucleus and cytoplasm while class IV HDACs (HDAC-11) are structurally distinct from the other groups and also localized to the nucleus and cytoplasm.[49, 50] Under the current paradigm class I HDAC enzymes are considered mediators of hypertrophy whereas class II HDACs are generally regarded as anti-hypertrophic.[20, 51] Similar to HATs such as p300 and Cbp, several HDAC enzymes are known to interact with cardiac transcription factors and co-regulatory determinants to control expression of genes associated with hypertrophy and heart failure.[18, 20]

Recent studies describe numerous key co-regulatory components of the heart that serve distinct functions in gene expression. Cardiac-specific deletion of class IIa HDACs in mice increased expression of genes regulated by the cardiac transcription factor, Mef2 and concomitant sensitivity to cardiac hypertrophy. By contrast, transgenic expression of class IIa HDACs prevented activation of Mef2 target genes to attenuate cardiac hypertrophy.[52, 53] Although these data suggest that inhibition of HDAC activity would increase cardiac hypertrophy, recent studies of pan-HDAC inhibition in mouse models described an anti-hypertrophic role mediated by transcriptional changes in gene expression.[54] These experimental observations importantly founded the hypothesis that distinct histone deacetylase activities could mediate pro- and anti-hypertrophic signaling within the stressed myocardium. Accordingly, class I HDAC inhibition alone effectively attenuated cardiac hypertrophy

by Angiotensin II infusion and aortic banding in pre-clinical models.[18, 45] These observations suggest that pro-hypertrophic effects of class I HDACs to be of higher catalytic efficiency than the anti-hypertrophic role of class II HDACs. Development of class-selective HDAC inhibitors resulted in the identification of stress-responsive roles for many HDAC enzymes as well as the genes and proteins associated with these enzymes in cardiovascular diseases. **Table 1** lists the HDAC enzymes whose expression and function are regulated during hypertrophy and associated with heart disease. Although clinical trials with HDAC inhibitors reported promising improvements in ventricular function in heart failing patients, poor drug tolerance often results in side effects such as nausea, fatigue, thrombocytopenia and limited patient survival.[55, 56] Because HDACs are required for normal cellular function and operate in multiple cell types of the heart, understanding the precise molecular targets of individual HDAC isoforms is essential to the development of selective inhibitors specific to cardiomyocytes for better therapy in the clinic.

1.2.6 HDAC inhibition - current standing and future perspectives

Despite initial characterization as chromatin modifiers, HDACs are now known to strongly recognize and deacetylate non-histone proteins such as transcription factors and contractile proteins. The distinct class-specificity and diverse substrate binding of HDAC enzymes confer versatility in mediating stress responsive signaling through a wide range of pathways. Identifying pathways regulated by HDAC enzymes including cardiac apoptosis, autophagy and inflammation offer improvements for potential therapeutic manipulation. Moreover, both the class I and class II HDACs may participate in regulating hypertrophy since mice genetically deleted for HDAC5 and HDAC9 developed hypertrophy in response to aortic banding and calcium signaling, however not in response to the β-adrenergic agonist isoproterenol-mediated induction.[57] Strikingly, administration of the HDAC inhibitor Trichostatin A (TSA) blocked induction of hypertrophy under all these stimulating conditions.[57] These observations indicate that class II HDACs may participate in regulating a specific subset of hypertrophy pathways depending on the nature of pathological stimuli. The pro-hypertrophic HDAC1 and HDAC2 are required for normal embryonic development since mice null for these enzymes died at 9.5 embryonic days.[58]

Moreover, cardiac specific deletion of class I HDACs resulted in neonatal lethality. These results indicate class I HDACs, although required for pathological signaling in adult hearts, are developmentally critical as well as required for homeostatic gene expression.

HDAC inhibition to reduce myocyte hypertrophy also affects non-muscle cells within the heart resulting in diverse inflammatory responses associated with toxicity.[59] Crucially, diverse cellular pathways are regulated by HDACs that are essential for normal cell functioning. The requirement for high drug concentrations for certain HDAC inhibitors to effectively reduce disease-inducing pathways is often poorly tolerated.[60] Nevertheless, HDAC inhibition can effectively attenuate pathological insults to cardiomyocyte reducing myocardial hypertrophy, myocyte death and fibrosis. Identification of critical pathological mediators using HDAC inhibitors such as TSA improves knowledge of hypertrophy-associated pathways. Development of molecule-specific inhibitor compounds selective of pathological pathways could address the issue of off-target effects.

1.2.7 Post-translational histone methylation in cardiac pathology

Mechanisms of transcriptional activation and repression by methyl-writing and -erasing enzymes play critical roles in cardiac physiology and pathology.[7, 61] The chromatin landscape is dynamically regulated by histone methylation paralleling temporal gene expression patterns at all different stages within the developing heart.[62, 63] Recent experiments show global changes to chromatin landscape associated with differential histone methylation patterns in the failing myocardium.[17, 21, 22] Histone methyltransferases such as Smyd1 and Ptip are thought to enzymatically regulate gene expression in context of cardiovascular pathogenesis. Post-translational histone methylation established by these and similar enzymes is a dynamic regulatory mark that is removed by histone demethylases (HDMs). This covalent chemical modification is diversely linked with the regulation of gene transcription depending on the residue modified. Methylation of H3K4 is often associated with gene expression, whereas addition of the methyl-moiety to H3K9 and H3K27 are linked with transcriptionally repressive chromatin conformations.[28]

For example, trimethylation of H3K4 (H3K4me3) is indispensable for expression of *Kcnip2*, a gene encoding Kv-channel interacting protein 2 required for cardiac repolarization.[7] Expression of *Kcnip2* is reduced under heart failing conditions and associated with reduced H3K4me3 modification at the promoter. By contrast, ischaemic reperfusion in mouse models induced the expression of the G9a HMT and concomitant H3K9me3 enrichment at the *Sirt-1* promoter paralleling *Sirt-1* transcriptional repression.[64]

The specific methylation of H3K27 by the Ezh2 polycomb-group (PcG) HMT is required for cardiomyocyte lineage-specification during mouse embryogenesis.[65] Genetic deletion of Ezh2 in mouse heart identified the necessity of the enzyme for suppression of pro-hypertrophic genes including *Anp*, *Bnp* and *β-MHC*.[6] The complexity of cardiac epigenetic regulation is extended by recent observations of H3K36 methylation, typically associated with transcription elongation, co-existing with genomic methylation at critical cardiac genes in the human failing heart.[21] A key finding of the study was that methylation at CpG dinucleotide sequence and H3K36 residues of the *Dux4* locus correlating with mRNA expression in human failing heart could be inhibited by DNA methyltransferase blockade *in vitro*.[21] These results suggest that diverse histone lysine methylating enzymes are required for proper myocardial function, however such enzymes are often deregulated during cardiovascular pathology. Although the co-regulatory complexes that exert H3K36 methylation remain uncharacterized, a growing list of histone modifiers show altered expression and/or functional activity in cardiovascular diseases (**Table 2**).

Distinct classes of enzymes that catalyze demethylation of histone tail residues are also important regulators of cardiac gene expression, exemplified by elevated expression of the Jmjd2a histone demethylase enzyme in mouse hearts with increased pressure-overload.[61] Jmjd2a is an H3K9me3 demethylase that functions in transcriptional activation. In healthy hearts, *Fhl1* gene expression is suppressed by H3K9me3 enrichment at the promoter.[61] In TAC mouse model, experiments showed increased Jmjd2a binding and reduced H3K9me3 modification at the *Fhl1* gene

promoter in parallel with increased *Fhl1* mRNA expression.[61] Co-regulatory complexes similarly mediate transcriptional changes under disease conditions via removal of histone methylation at lysine 27 (H3K27me3).[66]

1.2.8 Lessons from EZH2 knockout mouse models

Co-ordinated actions of polycomb repressive complexes (PRC) and co-regulatory proteins functionally suppress hundreds of genes in humans.[67] These regulatory complexes include two main families, PRC1 and PRC2.[68] PcG-mediated gene silencing is conferred by intrinsic histone methyltransferase activity; the PRC2 holoenzyme is a complex of HMTs that include Suz12 and Eed with either Ezh2 or Ezh1 required for H3K27me3 modification.[67, 68] In the adult mouse heart, expression of hypertrophy-associated genes (*Anp*, *β-MHC*) and pro-fibrotic genes such as *Tgfβ3* are suppressed by Ezh2-mediated H3K27me3 modification.[6, 65, 69] Genetic deletion of Ezh2 in mice increased cardiomyocyte growth accompanied by induction of hypertrophy-associated gene expression. Moreover, elevated pro-fibrotic gene expression such as *Tgfβ3*, *Spp1* and *Postn* and cardiac fibrosis was observed in Ezh2-deficient mice.[6] Ezh2 is expressed in the heart as early as E9.5 days and specific inactivation in cardiac progenitors is associated with reduced H3K27me3 accumulation during cardiomyocyte differentiation implying a role in cardiac-lineage specification in embryogenesis.[6] Whereas cardiac-specific Ezh2 deletion in adult hearts promotes hypertrophy, its inactivation in cardiac progenitors confers severe heart malformations in later stages of heart development.[6, 69] Such results indicate the epigenetic silencing of genes by Ezh2 as a critical determining factor for the development and function of the heart.

1.2.9 Chromatin complexity of cardiac MHC genes

The cardiac MHC genes, α and β, encode ATPase subunits that assemble with myosin complex to regulate cardiac contractility.[57] Both MHC proteins vary in ATPase activity with *α-MHC* exhibiting three times faster ATPase activity than *β-MHC* isoform.[70] The *α-* and *β- MHC* genes are organized in tandem on chromosome 14 of human and mouse.[71] Expression of these genes is antithetically regulated in the developing, healthy and diseased heart (**Figure 1**). Whereas expression of the *β-*

MHC isoform predominates developing myocardium, α-*MHC* expression is maintained at high levels in adult hearts. Cardiac hypertrophy induces β-*MHC* gene expression with concomitant suppression of α-*MHC* and this isoform shift negatively impacts myocardial contractility.[72] Indeed, human failing hearts express lower α-*MHC* isoform in comparison to healthy individuals.[73, 74] Thus the regulatory mechanisms governing the dynamic interchange between the α- and β- isoforms are highly relevant to myocardial function in health and disease. Remarkable complexity has been observed in the regulation of the *MHC* locus. Recently, non-coding RNA (ncRNA) expression from the intergenic bi-directional promoter (bdP) transcribing *antisense* (*AS*) β-*MHC* transcript was described as a regulator of cardiac *MHC* genes.[75, 76] The intertgenic bdP harbours binding sequences for cardiac transcription factors such as GATA4 and also associates with epigenetic enzymes such as the HDAC2, HDAC9, Brg1 and Ezh2 (**Figure 1**). Furthermore, chromatin remodeling complexes such as the SWI/SNF components directly associate with the intergenic bdP in the hypertrophied heart.[19, 31] Recent findings by assays using mouse ventricular tissues suggest that Ezh2 functions in the suppression of β-*MHC* in normal adult heart tissues.[6] Cardiac-specific inactivation of Ezh2 in mice is associated with increased β-*MHC* and reduced α-*MHC* gene expression and cardiac hypertrophy. Consistent with these observations, the reactivation of hypertrophy markers in Ezh2 knockout mice is associated with reduced H3K27me3 at promoters of genes such as *Anp* and *Bnp* suggesting Ezh2-mediated gene suppression is required for cardiac homeostasis.[6] Further work examining the interaction of ncRNA and epigenetic factors that recognize and regulate the expression of *MHC* will further reveal the signaling cues in physiological and pathological hypertrophy.

1.2.10 Conclusions

Characterization of specific modulators and transcriptional outcomes associated with chromatin modification in the heart offers novel potential for therapeutic treatment of cardiac disease. Current understanding of transcriptional changes in the diseased myocardium implicates specific enzymes and modifications in the complex regulation of heart specific promoters and transcription factors. HDAC inhibition has shown

promise having been successfully translated from pre-clinical to clinical studies, however numerous and severe off-target effects are reported. Evidently further investigation of distinct HDAC classes allowing identification of specific targets and inhibitors is required. Inhibition of histone methylatransferases such as Ezh2 using pharmacological compounds shown promising results in cancer treatment.[77] Only recently, a function for this enzyme in the heart has been reported, however the role in cardiovascular disease requires further clarification. With a multitude of enzymes and specific modification of histone tails characterized in vertebrates, it is likely that an extensive network of chromatinized factors govern transcriptional changes associated with myocardial stress.

1.2.11 References

1. Tabibiazar R, Wagner RA, Liao A, Quertermous T. Transcriptional profiling of the heart reveals chamber-specific gene expression patterns. *Circ Res* 2003;**93**:1193-1201.
2. Bruneau BG, Logan M, Davis N, Levi T, Tabin CJ, Seidman JG, *et al.* Chamber-specific cardiac expression of Tbx5 and heart defects in Holt-Oram syndrome. *Dev Biol* 1999;**211**:100-108.
3. Bruneau BG. Transcriptional regulation of vertebrate cardiac morphogenesis. *Circ Res* 2002;**90**:509-519.
4. Akazawa H, Komuro I. Cardiac transcription factor Csx/Nkx2-5: Its role in cardiac development and diseases. *Pharmacol Ther* 2005;**107**:252-268.
5. Anversa P, Leri A, Kajstura J. Cardiac regeneration. *J Am Coll Cardiol* 2006;**47**:1769-1776.
6. Delgado-Olguin P, Huang Y, Li X, Christodoulou D, Seidman CE, Seidman JG, *et al.* Epigenetic repression of cardiac progenitor gene expression by Ezh2 is required for postnatal cardiac homeostasis. *Nat Genet* 2012;**44**:343-347.
7. Stein AB, Jones TA, Herron TJ, Patel SR, Day SM, Noujaim SF, *et al.* Loss of H3K4 methylation destabilizes gene expression patterns and physiological functions in adult murine cardiomyocytes. *J Clin Invest* 2011;**121**:2641-2650.
8. Zaidi S, Choi M, Wakimoto H, Ma L, Jiang J, Overton JD, *et al.* De novo mutations in histone-modifying genes in congenital heart disease. *Nature* 2013;**498**:220-223.
9. Kehat I, Molkentin JD. Molecular pathways underlying cardiac remodeling during pathophysiological stimulation. *Circulation* 2010;**122**:2727-2735.
10. Cohn JN, Ferrari R, Sharpe N. Cardiac remodeling--concepts and clinical implications: a consensus paper from an international forum on cardiac remodeling. Behalf of an International Forum on Cardiac Remodeling. *J Am Coll Cardiol* 2000;**35**:569-582.
11. Gardin JM, Lauer MS. Left ventricular hypertrophy: the next treatable, silent killer? *JAMA* 2004;**292**:2396-2398.
12. Frey N, Olson EN. Cardiac hypertrophy: the good, the bad, and the ugly. *Annu Rev Physiol* 2003;**65**:45-79.
13. Li HL, Liu C, de Couto G, Ouzounian M, Sun M, Wang AB, *et al.* Curcumin prevents and reverses murine cardiac hypertrophy. *J Clin Invest* 2008;**118**:879-893.
14. Heineke J, Molkentin JD. Regulation of cardiac hypertrophy by intracellular signalling pathways. *Nat Rev Mol Cell Biol* 2006;**7**:589-600.
15. Insel PA, Hammond HK. Beta-adrenergic receptors in heart failure. *J Clin Invest* 1993;**92**:2564.
16. Sipido KR, Volders PG, Vos MA, Verdonck F. Altered Na/Ca exchange activity in cardiac hypertrophy and heart failure: a new target for therapy? *Cardiovasc Res* 2002;**53**:782-805.
17. Han P, Hang CT, Yang J, Chang CP. Chromatin remodeling in cardiovascular development and physiology. *Circ Res* 2011;**108**:378-396.
18. McKinsey TA. Therapeutic potential for HDAC inhibitors in the heart. *Annu Rev Pharmacol Toxicol* 2012;**52**:303-319.
19. Hang CT, Yang J, Han P, Cheng HL, Shang C, Ashley E, *et al.* Chromatin regulation by Brg1 underlies heart muscle development and disease. *Nature* 2010;**466**:62-67.
20. Backs J, Olson EN. Control of cardiac growth by histone acetylation/deacetylation. *Circ Res* 2006;**98**:15-24.

21. Movassagh M, Choy MK, Knowles DA, Cordeddu L, Haider S, Down T, *et al.* Distinct epigenomic features in end-stage failing human hearts. *Circulation* 2011;**124**:2411-2422.
22. Kaneda R, Takada S, Yamashita Y, Choi YL, Nonaka-Sarukawa M, Soda M, *et al.* Genome-wide histone methylation profile for heart failure. *Genes Cells* 2009;**14**:69-77.
23. McKinsey TA, Zhang CL, Olson EN. MEF2: a calcium-dependent regulator of cell division, differentiation and death. *Trends Biochem Sci* 2002;**27**:40-47.
24. McKinsey TA, Zhang CL, Lu J, Olson EN. Signal-dependent nuclear export of a histone deacetylase regulates muscle differentiation. *Nature* 2000;**408**:106-111.
25. Dai YS, Markham BE. p300 Functions as a coactivator of transcription factor GATA-4. *J Biol Chem* 2001;**276**:37178-37185.
26. Saha A, Wittmeyer J, Cairns BR. Chromatin remodelling: the industrial revolution of DNA around histones. *Nat Rev Mol Cell Biol* 2006;**7**:437-447.
27. Clapier CR, Cairns BR. The biology of chromatin remodeling complexes. *Annu Rev Biochem* 2009;**78**:273-304.
28. Campos EI, Reinberg D. Histones: annotating chromatin. *Annual review of genetics* 2009;**43**:559-599.
29. Takeuchi JK, Lou X, Alexander JM, Sugizaki H, Delgado-Olguin P, Holloway AK, *et al.* Chromatin remodelling complex dosage modulates transcription factor function in heart development. *Nature communications* 2011;**2**:187.
30. Gupta MP. Factors controlling cardiac myosin-isoform shift during hypertrophy and heart failure. *J Mol Cell Cardiol* 2007;**43**:388-403.
31. Chang L, Kiriazis H, Gao XM, Du XJ, El-Osta A. Cardiac genes show contextual SWI/SNF interactions with distinguishable gene activities. *Epigenetics* 2011;**6**:760-768.
32. Lai HL, Grachoff M, McGinley AL, Khan FF, Warren CM, Chowdhury SA, *et al.* Maintenance of adult cardiac function requires the chromatin factor Asxl2. *J Mol Cell Cardiol* 2012;**53**:734-741.
33. Sayed D, He M, Yang Z, Lin L, Abdellatif M. Transcriptional regulation patterns revealed by high resolution chromatin immunoprecipitation during cardiac hypertrophy. *J Biol Chem* 2013;**288**:2546-2558.
34. Schlesinger J, Schueler M, Grunert M, Fischer JJ, Zhang Q, Krueger T, *et al.* The cardiac transcription network modulated by Gata4, Mef2a, Nkx2.5, Srf, histone modifications, and microRNAs. *PLoS Genet* 2011;**7**:e1001313.
35. Mathiyalagan P, Chang L, Du XJ, El-Osta A. Cardiac ventricular chambers are epigenetically distinguishable. *Cell Cycle* 2010;**9**:612-617.
36. Yao TP, Oh SP, Fuchs M, Zhou ND, Ch'ng LE, Newsome D, *et al.* Gene dosage-dependent embryonic development and proliferation defects in mice lacking the transcriptional integrator p300. *Cell* 1998;**93**:361-372.
37. Gusterson RJ, Jazrawi E, Adcock IM, Latchman DS. The transcriptional co-activators CREB-binding protein (CBP) and p300 play a critical role in cardiac hypertrophy that is dependent on their histone acetyltransferase activity. *J Biol Chem* 2003;**278**:6838-6847.
38. Slepak TI, Webster KA, Zang J, Prentice H, O'Dowd A, Hicks MN, *et al.* Control of cardiac-specific transcription by p300 through myocyte enhancer factor-2D. *J Biol Chem* 2001;**276**:7575-7585.

39. Sartorelli V, Huang J, Hamamori Y, Kedes L. Molecular mechanisms of myogenic coactivation by p300: direct interaction with the activation domain of MyoD and with the MADS box of MEF2C. *Mol Cell Biol* 1997;**17**:1010-1026.
40. Chandrasekaran S, Peterson RE, Mani SK, Addy B, Buchholz AL, Xu L*, et al.* Histone deacetylases facilitate sodium/calcium exchanger up-regulation in adult cardiomyocytes. *FASEB J* 2009;**23**:3851-3864.
41. Sunagawa Y, Morimoto T, Takaya T, Kaichi S, Wada H, Kawamura T*, et al.* Cyclin-dependent kinase-9 is a component of the p300/GATA4 complex required for phenylephrine-induced hypertrophy in cardiomyocytes. *J Biol Chem* 2010;**285**:9556-9568.
42. Morimoto T, Sunagawa Y, Kawamura T, Takaya T, Wada H, Nagasawa A*, et al.* The dietary compound curcumin inhibits p300 histone acetyltransferase activity and prevents heart failure in rats. *J Clin Invest* 2008;**118**:868-878.
43. Sunagawa Y, Morimoto T, Wada H, Takaya T, Katanasaka Y, Kawamura T*, et al.* A natural p300-specific histone acetyltransferase inhibitor, curcumin, in addition to angiotensin-converting enzyme inhibitor, exerts beneficial effects on left ventricular systolic function after myocardial infarction in rats. *Circ J* 2011;**75**:2151-2159.
44. McKinsey TA, Kass DA. Small-molecule therapies for cardiac hypertrophy: moving beneath the cell surface. *Nat Rev Drug Discov* 2007;**6**:617-635.
45. Kee HJ, Sohn IS, Nam KI, Park JE, Qian YR, Yin Z*, et al.* Inhibition of histone deacetylation blocks cardiac hypertrophy induced by angiotensin II infusion and aortic banding. *Circulation* 2006;**113**:51-59.
46. Glenn DJ, Wang F, Chen S, Nishimoto M, Gardner DG. Endothelin-stimulated human B-type natriuretic peptide gene expression is mediated by Yin Yang 1 in association with histone deacetylase 2. *Hypertension* 2009;**53**:549-555.
47. Choudhary C, Kumar C, Gnad F, Nielsen ML, Rehman M, Walther TC*, et al.* Lysine acetylation targets protein complexes and co-regulates major cellular functions. *Science* 2009;**325**:834-840.
48. Marks PA, Xu WS. Histone deacetylase inhibitors: Potential in cancer therapy. *J Cell Biochem* 2009;**107**:600-608.
49. Gregoretti IV, Lee YM, Goodson HV. Molecular evolution of the histone deacetylase family: functional implications of phylogenetic analysis. *J Mol Biol* 2004;**338**:17-31.
50. Dokmanovic M, Clarke C, Marks PA. Histone deacetylase inhibitors: overview and perspectives. *Mol Cancer Res* 2007;**5**:981-989.
51. Kee HJ, Kook H. Roles and targets of class I and IIa histone deacetylases in cardiac hypertrophy. *J Biomed Biotechnol* 2011;**2011**:928326.
52. Backs J, Song K, Bezprozvannaya S, Chang S, Olson EN. CaM kinase II selectively signals to histone deacetylase 4 during cardiomyocyte hypertrophy. *J Clin Invest* 2006;**116**:1853-1864.
53. Zhang CL, McKinsey TA, Chang S, Antos CL, Hill JA, Olson EN. Class II histone deacetylases act as signal-responsive repressors of cardiac hypertrophy. *Cell* 2002;**110**:479-488.
54. Antos CL, McKinsey TA, Dreitz M, Hollingsworth LM, Zhang CL, Schreiber K*, et al.* Dose-dependent blockade to cardiomyocyte hypertrophy by histone deacetylase inhibitors. *J Biol Chem* 2003;**278**:28930-28937.
55. Giles F, Fischer T, Cortes J, Garcia-Manero G, Beck J, Ravandi F*, et al.* A phase I study of intravenous LBH589, a novel cinnamic hydroxamic acid analogue

histone deacetylase inhibitor, in patients with refractory hematologic malignancies. *Clin Cancer Res* 2006;**12**:4628-4635.
56. Klimek VM, Fircanis S, Maslak P, Guernah I, Baum M, Wu N*, et al.* Tolerability, pharmacodynamics, and pharmacokinetics studies of depsipeptide (romidepsin) in patients with acute myelogenous leukemia or advanced myelodysplastic syndromes. *Clin Cancer Res* 2008;**14**:826-832.
57. Chang S, McKinsey TA, Zhang CL, Richardson JA, Hill JA, Olson EN. Histone deacetylases 5 and 9 govern responsiveness of the heart to a subset of stress signals and play redundant roles in heart development. *Mol Cell Biol* 2004;**24**:8467-8476.
58. Montgomery RL, Davis CA, Potthoff MJ, Haberland M, Fielitz J, Qi X*, et al.* Histone deacetylases 1 and 2 redundantly regulate cardiac morphogenesis, growth, and contractility. *Genes Dev* 2007;**21**:1790-1802.
59. Steele NL, Plumb JA, Vidal L, Tjornelund J, Knoblauch P, Rasmussen A*, et al.* A phase 1 pharmacokinetic and pharmacodynamic study of the histone deacetylase inhibitor belinostat in patients with advanced solid tumors. *Clin Cancer Res* 2008;**14**:804-810.
60. Neal JW, Sequist LV. Complex role of histone deacetylase inhibitors in the treatment of non-small-cell lung cancer. *J Clin Oncol* 2012;**30**:2280-2282.
61. Zhang QJ, Chen HZ, Wang L, Liu DP, Hill JA, Liu ZP. The histone trimethyllysine demethylase JMJD2A promotes cardiac hypertrophy in response to hypertrophic stimuli in mice. *J Clin Invest* 2011;**121**:2447-2456.
62. Wamstad JA, Alexander JM, Truty RM, Shrikumar A, Li F, Eilertson KE*, et al.* Dynamic and coordinated epigenetic regulation of developmental transitions in the cardiac lineage. *Cell* 2012;**151**:206-220.
63. Paige SL, Thomas S, Stoick-Cooper CL, Wang H, Maves L, Sandstrom R*, et al.* A temporal chromatin signature in human embryonic stem cells identifies regulators of cardiac development. *Cell* 2012;**151**:221-232.
64. Das M, Das S, Lekli I, Das DK. Caveolin induces cardioprotection through epigenetic regulation. *J Cell Mol Med* 2012;**16**:888-895.
65. Chen L, Ma Y, Kim EY, Yu W, Schwartz RJ, Qian L*, et al.* Conditional ablation of Ezh2 in murine hearts reveals its essential roles in endocardial cushion formation, cardiomyocyte proliferation and survival. *PLoS One* 2012;**7**:e31005.
66. Ohtani K, Vlachojannis GJ, Koyanagi M, Boeckel JN, Urbich C, Farcas R*, et al.* Epigenetic regulation of endothelial lineage committed genes in pro-angiogenic hematopoietic and endothelial progenitor cells. *Circ Res* 2011;**109**:1219-1229.
67. Simon JA, Kingston RE. Mechanisms of polycomb gene silencing: knowns and unknowns. *Nat Rev Mol Cell Biol* 2009;**10**:697-708.
68. Margueron R, Reinberg D. The Polycomb complex PRC2 and its mark in life. *Nature* 2011;**469**:343-349.
69. He A, Ma Q, Cao J, von Gise A, Zhou P, Xie H*, et al.* Polycomb repressive complex 2 regulates normal development of the mouse heart. *Circ Res* 2012;**110**:406-415.
70. Rundell VL, Manaves V, Martin AF, de Tombe PP. Impact of beta-myosin heavy chain isoform expression on cross-bridge cycling kinetics. *Am J Physiol Heart Circ Physiol* 2005;**288**:H896-903.
71. Mahdavi V, Chambers AP, Nadal-Ginard B. Cardiac alpha- and beta-myosin heavy chain genes are organized in tandem. *Proc Natl Acad Sci U S A* 1984;**81**:2626-2630.

72. Krenz M, Robbins J. Impact of beta-myosin heavy chain expression on cardiac function during stress. *J Am Coll Cardiol* 2004;**44**:2390-2397.
73. Lowes BD, Minobe W, Abraham WT, Rizeq MN, Bohlmeyer TJ, Quaife RA*, et al.* Changes in gene expression in the intact human heart. Downregulation of alpha-myosin heavy chain in hypertrophied, failing ventricular myocardium. *J Clin Invest* 1997;**100**:2315-2324.
74. Miyata S, Minobe W, Bristow MR, Leinwand LA. Myosin heavy chain isoform expression in the failing and nonfailing human heart. *Circ Res* 2000;**86**:386-390.
75. Haddad F, Bodell PW, Qin AX, Giger JM, Baldwin KM. Role of antisense RNA in coordinating cardiac myosin heavy chain gene switching. *J Biol Chem* 2003;**278**:37132-37138.
76. Haddad F, Qin AX, Bodell PW, Zhang LY, Guo H, Giger JM*, et al.* Regulation of antisense RNA expression during cardiac MHC gene switching in response to pressure overload. *Am J Physiol Heart Circ Physiol* 2006;**290**:H2351-2361.
77. Knutson SK, Wigle TJ, Warholic NM, Sneeringer CJ, Allain CJ, Klaus CR*, et al.* A selective inhibitor of EZH2 blocks H3K27 methylation and kills mutant lymphoma cells. *Nature chemical biology* 2012;**8**:890-896.
78. Haddad F, Qin AX, Bodell PW, Jiang W, Giger JM, Baldwin KM. Intergenic transcription and developmental regulation of cardiac myosin heavy chain genes. *Am J Physiol Heart Circ Physiol* 2008;**294**:H29-40.
79. Giger JM, Bodell PW, Baldwin KM, Haddad F. The CAAT-binding transcription factor 1/nuclear factor 1 binding site is important in beta-myosin heavy chain antisense promoter regulation in rats. *Exp Physiol* 2009;**94**:1163-1173.
80. Dai YS, Cserjesi P, Markham BE, Molkentin JD. The transcription factors GATA4 and dHAND physically interact to synergistically activate cardiac gene expression through a p300-dependent mechanism. *J Biol Chem* 2002;**277**:24390-24398.
81. Kim TG, Jung J, Mysliwiec MR, Kang S, Lee Y. Jumonji represses alpha-cardiac myosin heavy chain expression via inhibiting MEF2 activity. *Biochem Biophys Res Commun* 2005;**329**:544-553.
82. Huang WY, Liew CC. A conserved GATA motif in a tissue-specific DNase I hypersensitive site of the cardiac alpha-myosin heavy chain gene. *Biochem J* 1997;**325 (Pt 1)**:47-51.
83. Huang WY, Liew CC. Chromatin remodelling of the cardiac beta-myosin heavy chain gene. *Biochem J* 1998;**330 (Pt 2)**:871-876.
84. van Rooij E, Quiat D, Johnson BA, Sutherland LB, Qi X, Richardson JA*, et al.* A family of microRNAs encoded by myosin genes governs myosin expression and muscle performance. *Dev Cell* 2009;**17**:662-673.
85. Cao DJ, Wang ZV, Battiprolu PK, Jiang N, Morales CR, Kong Y*, et al.* Histone deacetylase (HDAC) inhibitors attenuate cardiac hypertrophy by suppressing autophagy. *Proc Natl Acad Sci U S A* 2011;**108**:4123-4128.
86. Kee HJ, Kook H. Kruppel-like factor 4 mediates histone deacetylase inhibitor-induced prevention of cardiac hypertrophy. *J Mol Cell Cardiol* 2009;**47**:770-780.
87. Trivedi CM, Luo Y, Yin Z, Zhang M, Zhu W, Wang T*, et al.* Hdac2 regulates the cardiac hypertrophic response by modulating Gsk3 beta activity. *Nat Med* 2007;**13**:324-331.
88. Kee HJ, Eom GH, Joung H, Shin S, Kim JR, Cho YK*, et al.* Activation of histone deacetylase 2 by inducible heat shock protein 70 in cardiac hypertrophy. *Circ Res* 2008;**103**:1259-1269.

89. Zhu H, Shan L, Schiller PW, Mai A, Peng T. Histone deacetylase-3 activation promotes tumor necrosis factor-alpha (TNF-alpha) expression in cardiomyocytes during lipopolysaccharide stimulation. *J Biol Chem* 2010;**285**:9429-9436.
90. Hohl M, Wagner M, Reil JC, Muller SA, Tauchnitz M, Zimmer AM*, et al.* HDAC4 controls histone methylation in response to elevated cardiac load. *J Clin Invest* 2013;**123**:1359-1370.
91. Granger A, Abdullah I, Huebner F, Stout A, Wang T, Huebner T*, et al.* Histone deacetylase inhibition reduces myocardial ischemia-reperfusion injury in mice. *FASEB J* 2008;**22**:3549-3560.
92. Sucharov CC, Dockstader K, McKinsey TA. YY1 protects cardiac myocytes from pathologic hypertrophy by interacting with HDAC5. *Mol Biol Cell* 2008;**19**:4141-4153.
93. Tao R, de Zoeten EF, Ozkaynak E, Chen C, Wang L, Porrett PM*, et al.* Deacetylase inhibition promotes the generation and function of regulatory T cells. *Nat Med* 2007;**13**:1299-1307.
94. Ohtani K, Dimmeler S. Epigenetic regulation of cardiovascular differentiation. *Cardiovasc Res* 2011;**90**:404-412.
95. Borlak J, Thum T. Hallmarks of ion channel gene expression in end-stage heart failure. *FASEB J* 2003;**17**:1592-1608.
96. Costantini DL, Arruda EP, Agarwal P, Kim KH, Zhu Y, Zhu W*, et al.* The homeodomain transcription factor Irx5 establishes the mouse cardiac ventricular repolarization gradient. *Cell* 2005;**123**:347-358.
97. Diehl F, Brown MA, van Amerongen MJ, Novoyatleva T, Wietelmann A, Harriss J*, et al.* Cardiac deletion of Smyd2 is dispensable for mouse heart development. *PLoS One* 2010;**5**:e9748.
98. Nguyen AT, Xiao B, Neppl RL, Kallin EM, Li J, Chen T*, et al.* DOT1L regulates dystrophin expression and is critical for cardiac function. *Genes Dev* 2011;**25**:263-274.

1.2.12 Figure 1. Dynamic chromatin modifications underlie the physiological and pathological MHC gene regulation in the heart.

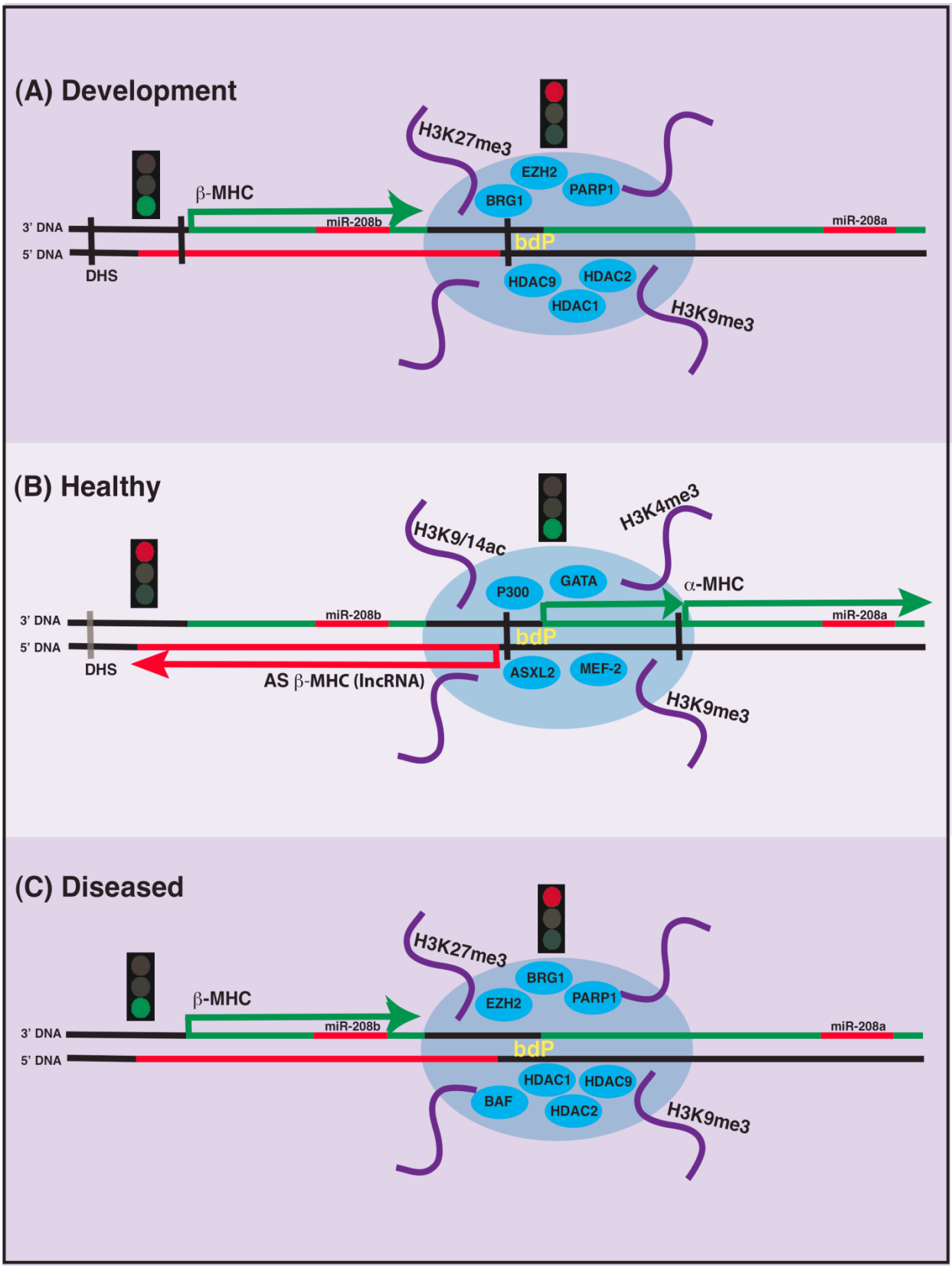

1.2.13 Figure legends

Figure 1. Dynamic chromatin modifications underlie the physiological and pathological MHC gene regulation in the heart.

Protein-coding (green) and non-coding transcripts (red) encoded by cardiac *MHC* genes. The expression of cardiac α- and β-*MHC* genes is dynamically regulated in (A) development (B) health and (C) disease. Binding of several transcription factors and co-regulatory determinants such as Gata, Ctf1/Nf1, Rar, T3R, Mef-2, Hand2, Jarid2 and p300 are identified within the bi-directional promoter (bdP) of the α- and β-*MHC* intergenic region (big blue ellipse).[78-81] Chromatin remodeling proteins such as Brg1 and histone modifiers such as Ezh2 and HDACs have been reported to directly bind to the bdP and thought to mediate pathological MHC gene shift in response to stress. Indeed, the bdP is dynamically regulated for histone modifications such as H3K9/14 acetylation and H3K4, H3K27 and H3K9 methylation. Several DNase Hypersensitive sites (DHS, highlighted in vertical bars) have been mapped to the promoters of β-*MHC* and α-*MHC* genes as well as with the bdP sequence. Presence or absence of DHS correlates with *MHC* expression during heart development and is associated with *MHC* gene expression in adult hearts, however the role of DHS in disease remains undetermined.[82, 83] An additional feature of the *MHC* genes is that both the α- and β-*MHC* genes encode microRNAs, *miRNA-208a* and *miRNA-208b* (red) whose expressions and functions are associated with heart health and disease.[84] The association of epigenetic enzymes as complex within the intergenic bdP is thought to suppress the expression of *AS* β-*MHC* and α-*MHC* genes leaving sense transcription and expression of β-*MHC* gene in cardiac pathology.

1.2.14 Table 1: Histone deacetylation is a key determinant of pathological gene expression in the heart

HDAC activity in disease (↑/↓)	Disease association	Target gene/protein	Study model
HDAC1 (↑)	Cardiac hypertrophy, Autophagy	(**a**) *Ncx*1 (↑)[40] (**b**) *Beclin* 1 (↑)[85]	(**a**) *In vivo* TAC and β-adrenergic infusions (**b**) *In vitro* PE induction and HDAC1 over expression
HDAC2 (↑)	Cardiac Hypertrophy, fibrosis and autophagy	(**a**) Klf (↓)→ *Anp* (↑)[86] (**b**) Yy1 (↑) → *Bnp* (↓)[46] (**c**) Inpp5f (↓)→ *Gsk3β* (↓)[87] (**d**) *Atg5* & *Beclin 1* genes (↑)[85] Hsp70 (↑)[88]	(**a**) Cardiomyocyte Phenylephrine treatment, *In vivo* aortic constriction[45] (**b**) Cardiomyocyte endothelin stimulation (**c**) Isoproterenol and TAC induction of cardiac hypertrophy in HDAC2 null/Tg mice (**d**) *In vitro* PE induction, TAC in Beclin 1-Tg mice; *In vivo* hypertrophy induction with isoproterenol, AngII or TAC.
HDAC3 (↑)	Contractile dysfunction, hypertrophy and fibrosis	Tnfα (↑)[89]	Cardiomyocyte lipopolysaccharide stimulation
HDAC4 (↑)	Ischemia DISCUSS JMJDs here	Suv39H1[90] Hif1a (↑)[91]	Ischemic reperfusion in mice, Hypoxia induction in HDAC4 suppressed cardiomyocytes
HDAC5 (↑)	Hypertrophy, Ischemia	Nkx2.5/p300 → *Ncx1* (↑)[40]	*In vivo* TAC and β-adrenergic infusions *In vitro* PE induction[92]
HDAC9 (↑)	Cardiac allograft rejection	Foxp3 (↓) → regulatory T-cell production (↓)[93]	HDAC9 null mice, human cardiac allograft

1.2.15 Table 2. Role of histone methylation and demethylation in cardiac pathology

Enzyme & activity in disease (↑/↓)	Histone Modification	Disease association	Target gene/protein (↑/↓)	Study model	Global histone profile in model	Role in disease
G9a (↑)[64]	H3K9me	Ischemia	*Sirtuin-1* (↓)	Cav-1 null mice and ischemic reperfusion	H3K9me3 (↑)	Pro
Ezh2[6]	H3K27me3	Unknown	*Anp, Bnp, α- and β-MHC*	Ezh2 null mice hearts	Unknown	Unknown
Asxl2[32] **(↓)**	H3K27me3	Ischemic and idiopathic DCM	*α- and β-MHC*	Asxl2 null mice hearts	H3K27me3 (↓)	Unknown
Jmjd2a[61, 90] **(↑)**	H3K9 demethylase	Hypertrophy, ICM	*Anp gene Fhl1* gene (↑)	TAC mice	Unknown	Pro
Jmjd1a[90] **(↑) Jmjd2b**[90] **(↑)**	H3K9demethylase	ICM, DCM	*Anp, Bnp*	Human failing myocardium, TAC mice	H3K9me3 (↓)	Pro
Utx & Jmjd3 (↑)[94]	H3K27 demethylase	Hypoxia	*eNOS* (↑)	Hypoxia induction in PAC	H3K27me1,2,3 (↓)	Pro
Ptip (↓)[7]	Cofactor of H3K4 methyltransferase, KMT2C/D	Electrophysiological property, Ventricular arrhythmia	*Kcnip2* (↓)	Cardiomyocyte sensitization with Isoproterenol/caffeine	H3K4me3 (↓)	Anti
Smyd1 (↑)[95]	H3K4 methyltransferase	Arrhythmia, depolarization[96]	Ion-channel protein coding genes	Biopsies from ESHF patients	No changes to H3K4me1,2,3	Pro
Smyd2[97]	H3K36me H3K4me	Unknown	Proteins of translation machinery	Smyd2 null mice	No changes to H3K36me1,2,3 H3K4me1,2,3	Unknown
Dot1L (↓)[98]	H3K79 methyltransferase (↓)	DCM	*Dystrophin* (↓)	IDCM	H3K79me2,3 (↓)	Anti
HMT/HDM (Unknown)	H3K4me3 & H3K9me3[22]	Distinguishable genome-wide patterns in ESHF patients	Induced hypertrophic gene expression	ESHF patient explants & Dahl salt-sensitive rats	H3K4me3 & H3K9me3[22]	Unknown
HMT/HDM (Unknown)	H3K36me3[21]	Distinguishable genome-wide patterns in ESHF patients	*Dux4* (↓)	ESHF patient explants (what explants)	H3K36me3[21]	Unknown

IDCM, idiopathic dilated cardiomyopathy; **ESHF**, end-stage heart failure; **TAC**, transverse aortic constriction; **FHL1**, Four-and-a-half LIM domains 1; **Cav1**, caveolin1; **PAC**, proangiogenic cells; **ICM**, Ischemic cardiomyopathy.

1.3 AIMS

Significant literature highlight epigenetic modifications such as the DNA methylation, histone methylation / acetylation in combination with chromatin interactions of ncRNAs modulate the expression of genes implicated in cardiac hypertrophy. Our understanding of epigenetic regulation of genes particularly in the settings of cardiac hypertrophy remains preliminary, although prominently studied in complex diseases such as the cancer. This project was developed with particular interest to address the epigenetic modifications associated with genes implicated in cardiac hypertrophy. The aims and experimental results presented in this thesis progressively address the associations of histone modifications as well as the expression and interaction of ncRNAs investigated in wild-type mouse heart ventricles to pre-clinical models of cardiac hypertrophy and its attenuation by HDAC inhibition.

The aims of this project were to:

(i) Study the chamber-specific gene expression patterns in mouse heart ventricles and determine the histone acetylation and methylation profile associated with gene promoters.

(ii) Determine the histone methylation patterns associated with the gender-specific expression of coding and non-coding transcripts from *MHC* genes in mouse heart ventricles.

(iii) Investigate the role of long ncRNAs in modulating gene transcription by chromatin interaction during cardiac hypertrophy and its attenuation by trichostatin A administration.

CHAPTER TWO

2.1

Cell Cycle 9:3, 612-617; February 1, 2010; © 2010 Landes Bioscience

Cardiac ventricular chambers are epigenetically distinguishable

Prabhu Mathiyalagan, Lisa Chang, Xiao-Jun Du and Assam El-Osta*

Epigenetics in Human Health and Disease Laboratory; Baker IDI Heart and Diabetes Institute; The Alfred Medical Research and Education Precinct; Melbourne, VIC Australia

Key words: chamber specific gene expression, ventricle, chromatin, histone acetylation, epigenetic

The left and right ventricles are muscular chambers of the heart that differ significantly in the extent of pressure workload. The regional and differential distribution of gene expression patterns is critical not only for heart development, but, also in the establishment of cardiac hypertrophy phenotypes. The cells of the myocardium employ elaborate regulatory mechanisms to establish changes in chromatin structure and function, yet, the role of epigenetic modifications and specific gene expression patterns in cardiac ventricles remains poorly understood. We have examined gene expression changes and studied histone H3 and H4 acetylation as well as dimethylation of lysine 4 on histone H3 on promoters of *α-Myosin heavy chain gene* (α-MHC), *β-Myosin heavy chain gene* (β-MHC), *Atrial natriuretic peptide gene* (ANP), *B-type natriuretic peptide gene* (BNP) and *Sarcoplasmic reticulum Ca(2+) ATPase gene* (SERCA2a). The recruitment of histone acetyltransferase (HAT) enzyme p300, which is a transcriptional coactivator, was also studied on the hyperacetylated promoters using immunopurification of soluble chromatin in the left and right ventricles of the mouse. We present evidence for the first time that the pattern of gene expression is closely linked with histone modifications and propose the left and right chambers of the heart are epigenetically distinguishable.

Introduction

The mammalian heart is composed of four chambers, which undergoes spatial and temporal-specific changes in gene expression to handle differing physiological conditions. The complexity of gene expression changes in the left and right ventricles (LV and RV) of the heart is also exemplified during the developmental stages from embryonic development to aging. Recent experimental evidence now suggests that gene expression signatures are exquisitely controlled in the developing and diseased heart. Firstly, a number of proto-oncogenes and early growth response genes, including *atrial natriuretic peptide* (ANP) and β-*myosin heavy chain* (β-MHC) genes are active during the developmental stage, inactivated at maturity and re-activated in the senescent stage.[1] Secondly, under pathological conditions, multiple signaling pathways are activated leading to myocardial hypertrophy, dysfunction, matrix remodeling and ultimately heart failure.[2-4] Thirdly, cardiac myocytes respond to a variety of stresses by hypertrophic growth, during which cells increase in size, rather than dividing, to adopt a demand for an increased workload with distinct patterns in gene expression.[5] Recent studies have revealed different gene expression profiling between the ventricles under baseline and diseased conditions.[6]

Despite these and other recent advances uncovering the signaling pathways and transcription factors that mediate specific gene expression patterns, as well as the events associated with remodelling in the heart, the underlying molecular mechanism still remains poorly defined. Mounting evidence now suggests that chemical variation to chromatin in the form of histone modifications are considered critical to the underlying regulatory events associated with the heart.[7] These studies expand the current understanding of cardiac gene expression by adding a level of epigenomic complexity.[8] The precise nature of cardiac chamber-specific histone acetylation and gene expression remains poorly understood. In this paper we specifically hypothesize that chamber specific gene expression in the heart is distinguishable in the form of hyperacetylation events on histones H3 and H4 as well as methylation of histone H3 that corresponds with increased transcription in the left ventricle. We observe distinguishable hyperacetylation events in the left ventricle of the mouse heart that parallel increased recruitment of the histone acetyltransferase p300 and gene expression.

Results

Transcriptional profiling of the mammalian LV and RV of the heart shows distinct differences in gene expression.[9] Since we were keen to study transcriptional events associated with epigenetic modifications of the histone H3 and H4 tail, and, specifically by histone acetylation, we included in the analysis the α- and β-*MHC* genes, *ANP* and *BNP*, the *SERCA2a* genes. We first determined the level of gene expression by isolating and preparing RNA from carefully dissected LV and RV tissues. To determine which genes had an expression level that was statistically significant between

*Correspondence to: Assam El-Osta; Email: [redacted]
Submitted: 06/29/09; Revised: 10/22/09; Accepted: 11/12/09
Previously published online: www.landesbioscience.com/journals/cc/article/10612

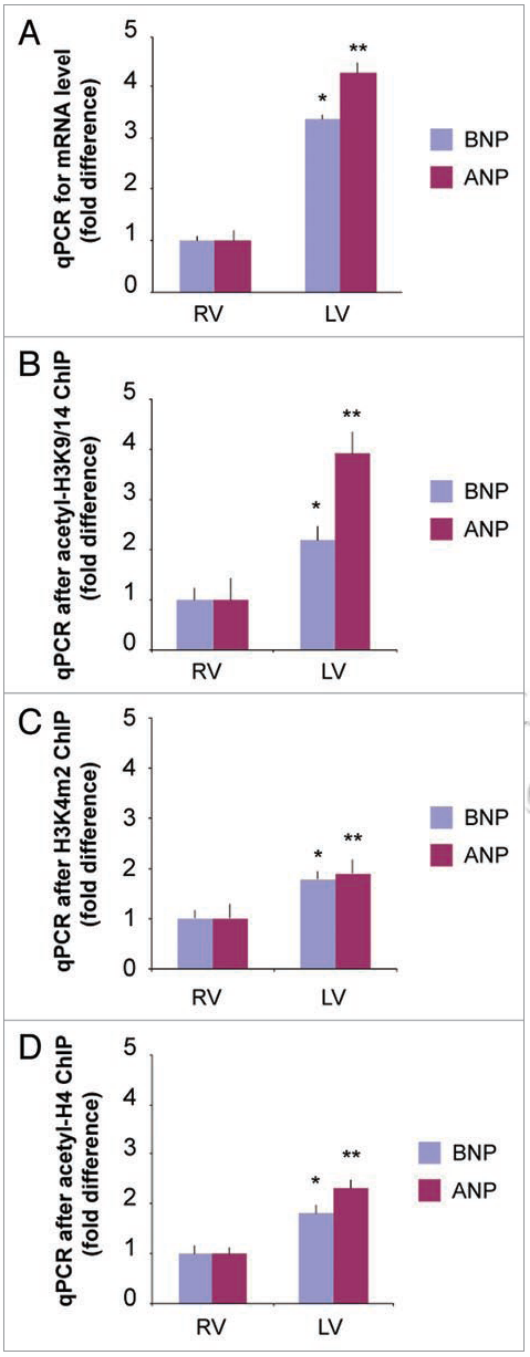

Figure 1. Ventricular chambers of the mouse heart are epigenetically distinct and this is tightly associated with changes in gene expression. (A) BNP and ANP mRNA levels in the LV and RV tissues were assessed by realtime qPCR. *p < 0.0001 versus RV; **p < 0.0023 versus RV. (B) Chromatin immunopurification of acetylated H3K9/K14 histones in the LV and RV tissues assessed by realtime qPCR. *p < 0.0024 versus RV; **p < 0.0005 versus RV. (C) Chromatin immunopurification of H3K4m2 in the LV and RV tissues assessed by realtime qPCR. *p < 0.0053 versus RV; **p < 0.0281 versus RV. (D) Chromatin immunopurification of acetylated H4 in the LV and RV tissues assessed by realtime qPCR. *p < 0.0018 versus RV; **p < 0.0001 versus RV.

LV and RV, we used a quantitative real-time RT-PCR assay to study gene expression. *ANP* and *BNP* expression is tightly associated with increased expression in the hypertrophied heart,[10] however, its mode of expression and transcriptional control remains poorly understood. To determine whether *ANP* and *BNP* gene expression is associated with hyperacetylation of histones to these promoters, we first defined the gene expression levels in the mouse LV and RV dissections. Figure 1A shows that *ANP* and *BNP* genes are differentially expressed, and, these genes are specifically elevated in the LV of the mouse heart. To study histone acetylation changes in greater detail on the *ANP* and *BNP* promoters, we sought the immunopurification of soluble chromatin prepared from the LV and RV of the heart. To determine whether genes are differentially modified at specified histones residues we therefore sought to develop an in vivo method of ChIP from dissected LV and RV tissues. Although ChIP has been used successfully to map histone acetylation profiles in the mammalian genome of different cell types in culture, the application of this assay is significantly more challenging to apply to limited cell numbers from dissected and difficult to homogenize heart tissues. A key feature of the ChIP technique is the optimised conditions set for crosslinking of chromatin with formaldehyde and its sonication to shear genomic DNA into lengths suitable for realtime PCR quantification.

The acetylation of histones is an important posttranslational modification with important functional consequences associated with chromatin structure and transcriptional competence. To specifically determine whether histone acetylation is increased on the *ANP* and *BNP* promoters in cardiomyocytes of the LV, ChIPs were performed with antibody to acetylated H3K9/K14 and the association with these genes were determined by quantitative realtime PCR (Fig. 1B). Isolated soluble chromatin was significantly enriched for acetylated H3K9/K14 with the *ANP* and *BNP* promoters and commensurate with increased gene expression in the LV. Histone H3K4m2 (dimethylation) is typically concordant with transcriptionally active and euchromatic regions of the genome. To specifically examine the identity of methylation marks from LV and RV tissues, we immunopurified chromatin enriched for H3K4m2. Concordant with H3K9/K14 acetylation and gene expression, H3K4m2 was consistently elevated on the *ANP* and *BNP* genes from LV tissues (Fig. 1C). Histone H4 hyperacetylation is often associated as well with changes in gene expression, which is often found to co-exist with H3 acetylation on some genes. To determine the relevance of H4 acetylation, we also immunopurified hyperacetylated H4 chromatin from the LV and RV tissues (Fig. 1D). Consistent with the hyperacetylation data for histone H3 our ChIP analysis indicated that *ANP* and *BNP* promoters were significantly enriched for H4 acetylation. These data suggest that the LV and RV are epigenetically distinct on the *ANP* and *BNP* genes.

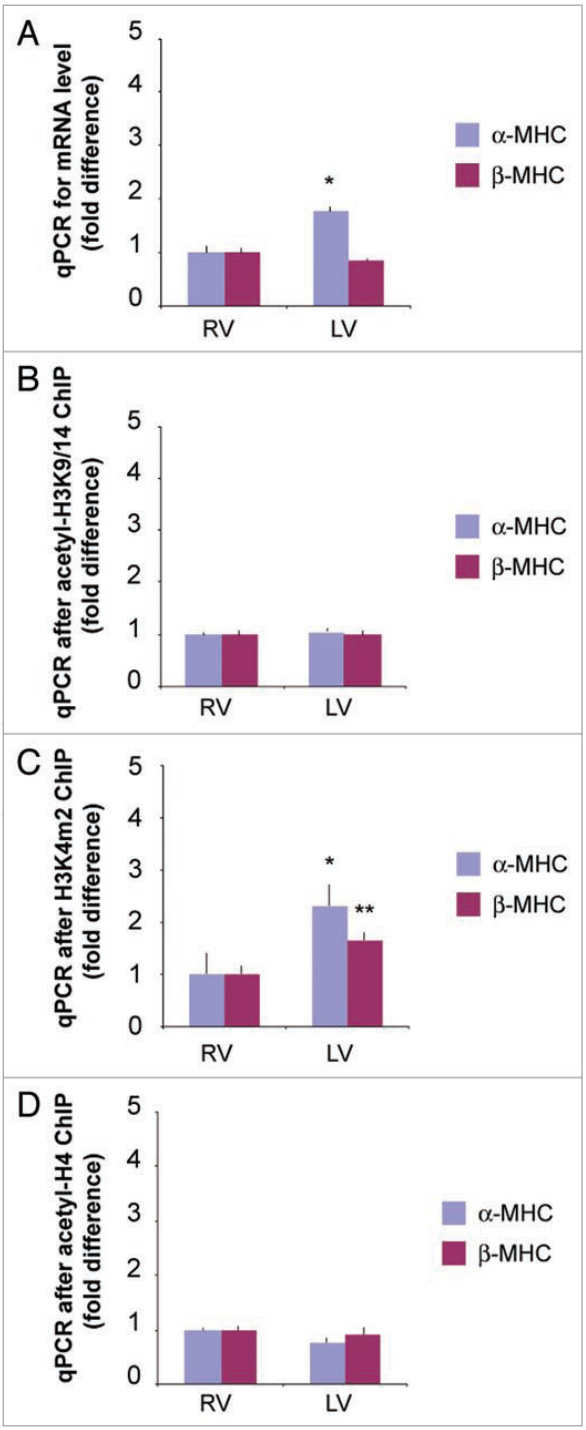

Figure 2. Expression of the myosin heavy chain genes in the ventricular chambers of the mouse heart is not hyperacetylated for H3 and H4 histones. (A) α- and β-MHC mRNA levels in the LV and RV tissues were assessed by realtime qPCR. *p < 0.009 versus RV. (B) Chromatin immunopurification of acetylated H3K9/K14 histones in the LV and RV tissues assessed by realtime qPCR. (C) Chromatin immunopurification of H3K4m2 in the LV and RV tissues assessed by realtime qPCR. *p < 0.0303 versus RV; **p < 0.0091 versus RV. (D) Chromatin immunopurification of acetylated H4 in the LV and RV tissues assessed by realtime qPCR.

Although it has been recently suggested that epigenetic processes might account the expression of the two genes that code for MHC in the heart, the mechanism of regulation remains poorly defined.[11] We reasoned that changes in α- or β-*MHC* gene expression would be correlated with increased histone hyperacetylation on these promoters. Figure 2A shows that α- and β-*MHC* genes are differentially expressed, and, that the α-*MHC* gene is specifically elevated in the LV of the mouse heart. To confirm that increased α-*MHC* gene expression was associated with histone acetylation, chromatin from the LV and RV were immunopurified using an antibody specific for hyperacetylated H3K9/K14, and association with the α- and β-*MHC* promoters were determined using quantitative real time PCR (Fig. 2B). Individual ChIP experiments performed for H3K4m2 show specific enrichment for dimethylation of lysine 4 on histone H3 (Fig. 2C). ChIP analysis indicated that although there is a specific increase in α-*MHC* expression in the LV, there was no association with H3 and H4 hyperacetylation (Fig. 2D). These data suggest that the expression of the α-and β-*MHC* genes is indeed enriched for H3K4m2 and independent of histone hyperacetylation in the LV and RV tissues of these same promoters. Thus, of the genes examined, histone hyperacetylation including dimethylation of H3K4 are enriched on *ANP* and *BNP* gene activity, whereas, H3K4m2 is restricted to α- and β-*MHC* gene sequences.

The results to our experiments thus far indicate that increased expression of the *ANP* and *BNP* genes are correlated with increased histone H3 and H4 hyperacetylation in the LV, and, that the acetylation profile is distinct of that for the active α-*MHC* gene. To differentiate the role of histone acetylation on genes that are increased in the LV, with that of genes that do not significantly alter in expression, we analysed for histone acetylation on the *SERCA2a* promoter in LV and RV tissues. Consistent with the idea that *SERCA2a* expression is comparable, we observed no significant change in gene expression in the LV and RV of the mouse heart (Fig. 3A). To confirm histone hyperacetylation was indeed stable in the LV and RV, ChIP analysis was performed for *SERCA2a* gene promoter region. Although SERCA2a showed enrichment for acetylated histones H3 and H4 in both the ventricles, neither H3 acetylation (Fig. 3B), H3K4m2 (Fig. 3C) nor H4 acetylation (Fig. 3D) showed any difference in enrichment levels associated on *SERCA2a* chromatin in the LV and RV tissues.

p300 histone acetyltranseferase. The results to these experiments indicate that histone acetylation could play a critical role in determining the chromatin structure and its accessibility to transcriptional machinery resulting in gene activation. The histone acetyl-transferase (HAT) p300 knock out mice died between the 9 and 11.5 days of gestation showing its critical role in the developing heart.[14] The histone acetyltransferase activity of p300 was extensively studied in a knock in approach and it showed that only

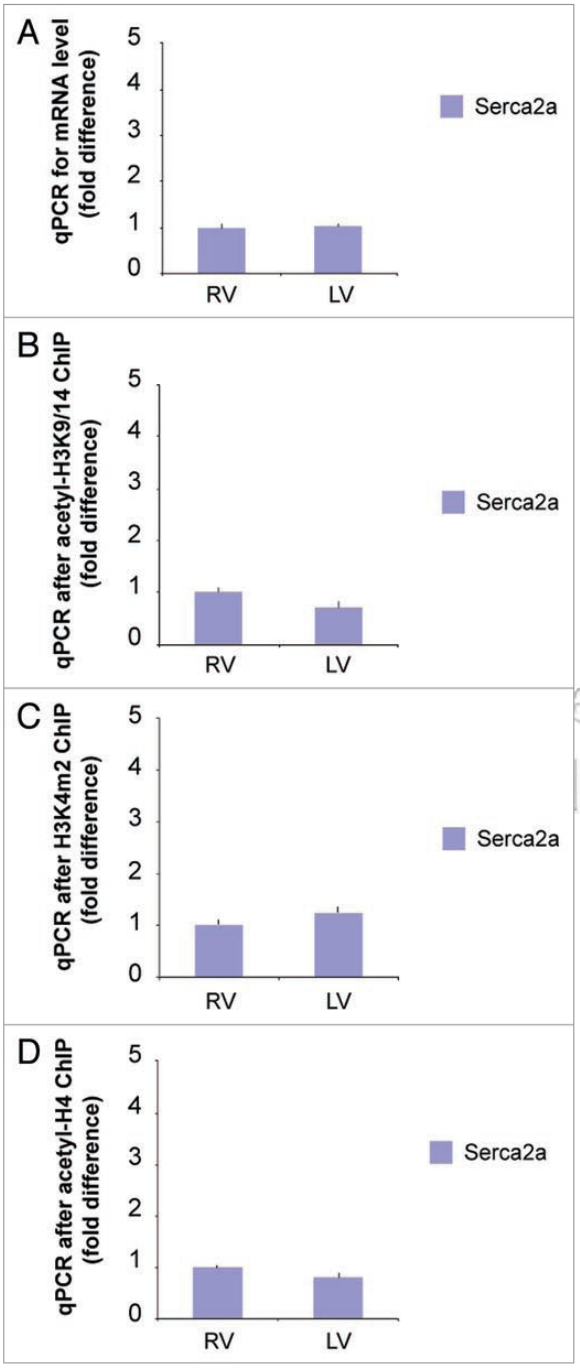

Figure 3. Expression of SERCA2a in the ventricular chambers of the mouse heart is not epigenetically distinct. (A) SERCA2a levels in the LV and RV tissues were assessed by realtime qPCR. (B) Chromatin immunopurification of acetylated H3K9/K14 histones in the LV and RV tissues assessed by realtime qPCR. (C) Chromatin immunopurification of H3K4m2 in the LV and RV tissues assessed by realtime qPCR. (D) Chromatin immunopurification of acetylated H4 in the LV and RV tissues assessed by realtime qPCR.

a single allelic deficient mouse that lacks acetyltransferase (AT) domain in p300 is necessary to result in an abnormal heart. It was also observed that the lethality was irreversible even after p300 delivery showing the importance of AT activity in controlling gene expression.[15] These particular findings interested us towards checking whether they play any important role in determining the acetylation status in cardiac ventricular gene expression. Having already established that immunopurified chromatin from the LV for the *ANP* and *BNP* promoters are specifically enriched with acetylated histones, we wished to determine whether this was consistent with the recruitment of the transcriptional co-activator, p300, which possess histone acetyltransferase activity.[12] The most specific approach to determine the recruitment of p300 on *ANP* and *BNP* promoters is by the immunopurification of soluble chromatin from LV and RV tissues of the mouse heart. Solubilized chromatin from separated ventricles was specifically immunopurified using antibody against p300 acetyltransferase, and the association with the *ANP* and *BNP* promoters was determined by quantitative realtime PCR (Fig. 4). Chromatin from both ANP and BNP promoters were significantly enriched for p300 acetyltransferase. This correlative enrichment of p300 at the same promoter regions of *ANP* and *BNP* which already have been found to be enriched for acetylated H3 and H4 suggests that the ventricular gene expression might in part be controlled by histone acetylating enzymes to maintain a stable acetylation profile. Together, these experimental data indicate that the LV and RV of the mouse heart are epigenetically distinct and this is tightly associated with changes in gene expression.

Discussion

In this study we hypothesized that gene expression changes in LV and RV tissues of the mouse heart could be associated with specific histone modification events, namely H3 and H4 acetylation and dimethylation of lysine 4 on histone H3. Examining five different promoters we could demonstrate that increased *ANP* and *BNP* gene expression in the LV were associated with increased histone acetylation and H3K4m2, whereas, with *SERCA2a* gene expression which did not significantly change in LV and RV tissues show no concordant change in acetylation or dimethylation. Although it has been suggested that the expression of the α- and β-*MHC* genes could be associated with epigenetic changes in the heart with no direct experimental evidence,[11] our results indicate that increased α-*MHC* gene expression in the LV relative to that of RV was correlated with H3K4 methylation.

Asymmetric gene expression patterns in the chambers of the heart provides a mechanism to cope with the differing physiological conditions and has been implicated in the response to phenotypic changes in pressure and volume in the failing myocardium. Furthermore, embryonic heart development is also specified by distinct gene expression patterns, which is critical for proper heart formation. Although we are beginning to understand how gene expression signatures are coordinated during the different developmental stages or patterned with in cardiac pathophysiology,

we still do not know the molecular mechanisms that direct these changes in ventricular tissues. Using a specialized ChIP procedure we determined that solubilized chromatin immunopurified with antibodies that specifically recognize acetylated H3 and H4 histones show increased acetylation of *ANP* and *BNP* in the LV. The close correlation between increased histone acetylation and the commensurate changes with gene expression is most easily explained by the recruitment of the p300 histone acetyltransferase[12] on these promoters in the LV. *ANP* and *BNP* are commonly used as markers for pathological myocardial hypertrophy. However, this change in gene expression is not accompanied with upregulation of β-MHC, a more reliable gene marker for fetal heart or for pathological hypertrophy. The expression of ANP and BNP are correlative with work-load pressure.

Recent evidence now suggests that chromatin variation, and, more specifically histone modifications are unique properties in the gene regulatory events linking the functional consequences of chromatin structure and gene expression changes with cardiac function.[6,13] The distinct epigenetic changes that we have identified show for the first time that the identity of the LV and RV tissues is not only specified by changes in gene expression, but also in the histone modifications on specific promoters. Understanding the elaborate mechanisms that regulate structural and chemical variation of chromatin in the heart remains poorly understood and remains a significant challenge to determine how the epigenetic code determines normal development and function of the heart, and how epigenetic changes interplays with physiological and pathophysiological phenotypes of the heart.

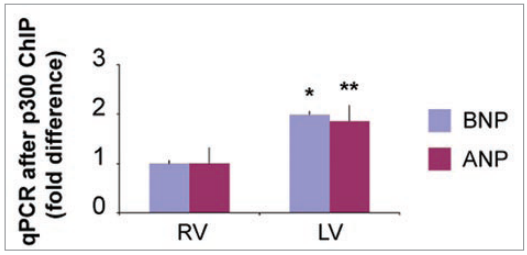

Figure 4. Histone acetyltransferase p300 is recruited and increased on the active ANP and BNP genes in the left ventricle determined by ChIP assay. Chromatin immunopurification of p300 acetyltransferase in the LV and RV tissues assessed by realtime qPCR. *p < 0.0001 versus RV; **p < 0.0533 versus RV.

Materials and Methods

Preparation of ventricles. We used the 8-week-old mice of Swiss Webster strain (Pelfreeze Biologicals). Atria were removed from the ventricular base. RV was carefully dissected from the LV by cutting down the interface of tricuspid valve.

Total RNA preparation. Approximately 30 mg of tissue from RV and LV were homogenized separately to a clear solution in TriZol and cells were opened in the presence of RNaseIn (Promega). Total RNA was prepared using RNeasy minikit preparation columns (Qiagen). DNA in total RNA was subsequently digested using Turbo Dnase kit (Ambion). First strand cDNA synthesis was performed for 1 μg of purified total RNA from each pool using M-MLV Reverse transcriptase kit (Invitrogen, Cat-28025-02).

Real-time quantitative PCR analysis for gene expression. Following first strand cDNA synthesis, SYBR Green real-time quantitative PCR was performed using the 7500 Fast SYBR green Real-time PCR system (Applied biosystems prism 7500) using cDNA primers specific for genes α-*MHC*, β-*MHC*, *BNP*, *ANP* and *SERCA2a* in LV and RV tissues. Endogenous control gene 18S ribosomal RNA[9] and GAPDH were included for normalization. Data showed no significant variation between both of the tested controls. The primer sequences were, for α-MHC, forward: 5′-CCA CCT GGG CAA GTC TAA CAA, reverse: 5′-TGT AGT CCA CGG TGC CAG C; for β-MHC, forward: 5′-GAT GTT TTT GTG CCC GAT GA, reverse: 5′-ACC GTC TTG CCA TTC TCC G-3′; for BNP, forward: 5′-TCC AGA GCA ATT CAA GAT GCA, reverse: 5′-CTT TTG TGA GGC CTT GGT CC; for ANP, forward: 5′-ACA GCC AAG GAG GAA AAG GC; reverse: 5′-CCA CAG TGG CAA TGT GAC CA; for SERCA2a, forward: 5′-CCC CCT GGG AGA ATA TCT GG, reverse: 5′-GAT CTG GAA AAT GAG CGG CA; for GAPDH, forward: 5′-TGA AGC AGG CAT CTG AGG G; reverse: 5′-CGA AGG TGG AAG AGT GGG AG; for 18S rRNA, forward: 5′-TCG GAA CTG AGG CCA TGA TT-3′; reverse: 5′-CTT TCG CTC TGG TCC GTC TT-3′.

Chromatin immunoprecipitation. An equal amount of tissue as a starting material (approximately 100 mg) from LV and RV were diced separately in ice cold PBS (w/o calcium and magnesium ions) and fixed with 1% formaldehyde for 10 minutes. Crosslinking was quenched by treating the tissue with 0.1 M glycine for 10 minutes. Tissue resuspended in SDS lysis buffer containing 1% SDS, 10 mM EDTA, 50 mM Tris-HCl pH 8 containing protease Inhibitor cocktail (Cayman). Tissue were homogenized (Polytron PT 2100) and cell lysis was performed in ice for 15 minutes. Chromatin shearing was performed by sonication (Diagenode, Denmark) to obtain chromatin fragments range from 200–500 bp in length using conditions set to high power, constantly for 35 minutes. Soluble chromatin was resuspended in ChIP dilution buffer containing 0.01% SDS, 1.1% Triton X-100, 1.2 mM EDTA, 16.7 mM Tris-HCl pH 8.0 and 167 mM NaCl. Soluble chromatin immunoprecipitation (ChIP) was carried out on sheared chromatin diluted 10 times in ChIP dilution buffer with protease inhibitors with the following antibodies: H3K4me2 (Abcam 7766), H3K9/K14Ac (Upstate 06-599), H4Ac (Upstate 06-866) and p300 (Upstate 05-257). Protein A/G magnetic beads (Dynabeads, Invitrogen) also included capturing Ab-chromatin complex. The non-specific IgG control included as negative control. 1/10th of the chromatin used to IP was kept frozen as input material for realtime interpretations. After chromatin IP, the samples were given a sequence of five washes beginning with low and high salt wash buffers containing 0.1% SDS, 1% Triton X-100, 2 mM EDTA, 20 mM Tris-HCl pH 8.0 with 150 mM and 500 mM NaCl respectively. Following low and high salt washes, the beads were given lithium chloride wash which contains 0.25 M LiCl, 1% Tergitol, 1% deoxycholic

acid, 1 mM EDTA and 10 mM Tris-HCl ph 8.0 followed by TE buffer (pH-8.0) wash and TE + 0.01% SDS wash. All these washes were carried out by rotation at 4 degrees except for final washing with TE + 0.01% SDS at room temperature. Washed chromatin IP beads and input sample were reverse crosslinked and eluted in ChIP elution buffer containing 20 mM Tris-HCl, pH 7.5, 5 mM EDTA, 50 mM NaCl, 1% SDS for 2 hours at 62°C on a thermomixer (Thermomixer comfort, eppendorf) that was set to 1,400 rpm. Proteinase K (Invitrogen) was included in the elution buffer for reversing protein-DNA cross-links.

Real time quantitative PCR analysis for ChIP DNA. Once elution and purification of input, antibody bound DNA, and IgG fractions were performed, SYBR Green quantitative real time analysis using primers specific for promoter region of genes α-*MHC,* β-*MHC, BNP, ANP* and *SERCA2a* were carried out. The amplified sequences with regards to the transcriptional start site were, for *ANP,* -45 to +54; for *BNP, -194 to -32; for* α-*MHC,* -1385 to -1124; for β-*MHC,* -760 to -659; for *SERCA2a,* +434 to +484. Approximately we used 10 ng of input DNA and 0.5–1 ng of immunoprecipitated DNA for one real time PCR reaction. The sequences of primers for ChIP DNA were, for α-*MHC*, forward: 5'-CTC TAT CTG CCC ATC GGC C; reverse: 5'-CTC AGT GCT CCA GCC CCT T; for β-*MHC*, forward: 5'-TGT TGT AGG TGG CTC CGA GAA; reverse: 5'-AGA CTA ACA ACC TCC GAG CCC; for *BNP*, forward: 5'-AGC TCA GCC GGC AGG AAT; reverse: 5'-CGT GTT CTC CCT TGT CTC GC; for *ANP*, forward: 5'-GTG GGC AGA GAC AGC AAA CA; reverse: AAG CCA AAA GGC CAA GAC G; for *SERCA2a*, forward: 5'-CGT TTC TTG TGC TCC CCA AA; reverse: 5'-GCT GGG TCA TCA CTT CTG CC.

PCR-reaction conditions. PCR amplification was performed using ABI Prism 7500. 2 pmol of each forward and reverse primer was added to a total volume of 20 µl reaction containing 2x Fast-SYBR green (Applied Biosystems).

Data analysis and statistics. ChIP recoveries from specified antibodies in both LV and RV were calculated as % of the relative input material. % of input in negative control ChIPs performed with non-specific IgG antibodies was <1% of the ChIPs performed with relevant antibody, and was considered as negligible. Since both the ventricles showed a considerable level of enrichment giving a Ct (cycle threshold) value of about 28 on ChIP samples compared to 24 in the Input samples, the relative enrichment between the two ventricles was calculated by doing the ratio of ChIP recoveries in LV and RV. The fold difference in enrichment or ratio between tissues can be analysed with a simplified method using the formula $2^{-[(CT_{RV\text{-}input} - CT_{RV\text{-}ChIP}) - (CT_{LV\text{-}input} - CT_{LV\text{-}ChIP})]}$. Data are shown as +/-SE. Statistical significance and p-values were calculated by unpaired t-tests using Graphpad prism.

Acknowledgements

The authors acknowledge grant support from the National Health and Medical Research Council (NHMRC) of Australia. X.J.D. and A.E.-O. are NHMRC fellows.

References

1. Lakatta EG, Sollott SJ. Perspectives on mammalian cardiovascular aging: humans to molecules. Comp Biochem Physiol A Mol Integr Physiol 2002; 132:699-721.
2. Chien KR, Knowlton KU, Zhu H, Chien S. Regulation of cardiac gene expression during myocardial growth and hypertrophy: molecular studies of an adaptive physiologic response. FASEB J 1991; 5:3037-46.
3. Bristow MR, Minobe WA, Raynolds MV, Port JD, Rasmussen R, Ray PE, et al. Reduced beta1 receptor messenger RNA abundance in the failing human heart. J Clin Invest 1993; 92:2737-45.
4. Tan FL, Moravec CS, Li J, Apperson-Hansen C, McCarthy PM, Young JB, et al. The gene expression fingerprint of human heart failure. Proc Natl Acad Sci USA 2002; 99:11387-92.
5. Ooi L, Wood IC. Chromatin switching and transcriptional regulation in disease. Biochem Soc Trans 2008; 36:599-602.
6. Kaufman BD, Desai M, Reddy S, Osorio JC, Chen JM, Mosca RS, et al. Genomic profiling of left and right ventricular hypertrophy in congenital heart disease. J Card Fail 2008; 14:760-7.
7. Haberland M, Montgomery RL, Olson EN. The many roles of histone deacetylases in development and physiology: implications for disease and therapy. Nat Rev Genet 2009; 10:32-42.
8. Jenuwein T, Allis CD. Translating the histone code. Science 2001; 293:1074-80.
9. Tabibiazar R, Wagner RA, Liao A, Quertermous T. Transcriptional profiling of the heart reveals chamber-specific gene expression patterns. Circulation Res 2003; 93:1193-201.
10. Kuhn M, Voss M, Mitko D, Stypmann J, Schmid C, Kawaguchi N, et al. Left ventricular assist device support reverses altered cardiac expression and function of natriuretic peptides and receptors in end-stage heart failure. Cardiovasc Res 2004; 64:308-14.
11. Haddad F, Qin AX, Bodell PW, Jiang W, Giger JM, Baldwin KM. Intergenic transcription and developmental regulation of cardiac myosin heavy chain genes. Am J Physiol Heart Circ Physiol 2008; 294:29-40.
12. Ogryzko VV, Schiltz RL, Russanova V, Howard BH, Nakatani Y. The transcriptional coactivators p300 and CBP are histone acetyltransferases. Cell 1996; 87:953-9.
13. McKinsey TA, Olson EN. Cardiac histone acetylation—therapeutic opportunities abound. Trends Genet 2004; 20:206-13.
14. Yao T-P, Oh SP, Fuchs M, Zhou N-D, Ch'ng L-E, Newsome D, et al. Gene dosage-dependent embryonic development and proliferation defects in mice lacking the transcriptional integrator p300. Cell 1998; 93:361-72.
15. Shikama N, Lutz W, Kretzschmar R, Sauter N, Roth J-F, Marino S, et al. Essential function of p300 acetyltransferase activity in heart, lung and small intestine formation. EMBO J 2003; 22:5175-85.

2.2 Conclusion

The results presented in this chapter show post-translational histone modifications in left and right chambers of the heart regulate chamber-specific gene expression patterns. The next aim of this study was to determine whether or not the post-translational modifications regulate gender-specific gene expression patterns in mouse heart ventricles. Experiments to this end were conducted in the male and female mouse ventricles and gene expression was assessed. These results are presented in the upcoming Chapter Three.

CHAPTER THREE

Antisense Non-coding RNA and H3K27me3 Modification Distinguish Sexually Dimorphic Cardiac Myosin Heavy Chain Gene Expression

3.1 Introduction

Gender differences in cardiovascular health and disease are well documented and understanding of these differences is likely to improve therapeutics in men and women.[1] In general, females are regarded as less vulnerable to pathological cardiac remodeling and the male disadvantage has been recently linked to hormonal regulation.[2] Indeed, cardiac pathogenesis such as cardiomyocyte apoptosis and necrosis characteristic of hypertrophy are known to occur predominantly in male hearts than in females under disease conditions.[3] The primary determinant of sex-specific molecular mechanisms are sex steroid hormone receptors that present in cardiomyocytes. Sex steroid hormones such as estrogen, progesterone and testosterone mediate several cardiac metabolic pathways including stress responsive signaling.[4] As a result, male and female hearts respond distinctly to sex-specific hormones as well as to their varying levels within individuals leading to intracellular signaling pathways that significantly differ between the two genders. Distinct activation in signaling pathways ultimately affects nuclear processes including gene expression, collectively driving the susceptibility in males.[5]

Disease induced sex-specific gene expression has been well studied in rodent models. For example, age-matched male and female mice exposed to increased ventricular pressure overload developed a similar hypertrophic phenotype in both genders however the expression of hypertrophy markers such as *Anp* and *β-MHC* was higher in males compared to female hearts.[6] The same study reports significant down regulation of the calcium-channel protein-coding gene *Serca2a* in males compared to the females. In diabetic rats with contractile dysfunction of the heart, expression of *β-MHC* was higher in males compared to females and thought to contribute to increased severity in male rat hearts.[7] These molecular distinctions between genders during disease pathogenesis implicate potential imbalances to

treatment responses in men and women.[8] We hypothesized that epigenetic mechanisms such as post-translational histone modifications associated with the expression of non-coding RNAs (ncRNAs) in the heart could mediate sex-specific regulation of gene expression.

In this study, we determined the gender-specific expression patterns of genes implicated in cardiac hypertrophy such as *Anp*, *Bnp*, *Serca2a*, α-*MHC* and β-*MHC* in the left and right ventricles (LV and RV) of mouse heart. Expression of ncRNA encoded within cardiac *MHC* genes has been recently linked with MHC isoform shift in normal and pathological left ventricles.[9] The expression of RNA from the antisense DNA strand complementary to the β-*MHC* gene using a bi-directional promoter (bdP) is associated with α-*MHC* to β-*MHC* shift. We measured the sense (mRNA) and antisense (ncRNA) transcript expression of cardiac *MHC* genes in mouse left ventricles. The study further examined the promoters of *MHC* genes and report that the bdP of the *MHC* intergenic region is differentially maintained for gene transcription in male and female ventricles. Chromatin immunoprecipitation (ChIP) of intergenic bdP support our hypothesis that specific histone modifications are associated with the differential expression of cardiac *MHC* genes in male and female mouse hearts. We also show that the ncRNA expression from the cardiac MHC genes is regulated distinctly in both genders.

3.2 Methods

3.2.1 Animal models

For studies involving Swiss Webster (SW) mice ventricles, hearts isolated from 8-weeks old age matched male and female mice were purchased (Pelfreeze Biologicals). For C57BL/6 study, we obtained hearts from 4-weeks old male and female mice. Hearts from both strains were stored at -80^{o}C. At least four mice per group were sacrificed and ventricular tissues were extracted. Gene expression and ChIP assays were separately performed using ventricular tissues obtained from each group. Experiments were repeated at least four times using ventricular tissues extracted from different animals from each group.

3.2.2 Preparation of ventricular tissues

Hearts were thawed on ice before analysis. The ventricular segment was carefully separated from the atrial compartment using iris scissors. Excessive blood from ventricles was removed by washing with ice-cold PBS$^{w/o\ Ca2+/Mg2+}$ several times. LV and RV tissues were then carefully dissected by cutting down the tricuspid valve interface. The isolated LV and RV tissues were immediately processed further for RNA extraction and chromatin immunoprecipitation procedures.

3.2.3 Total RNA extraction and qRT-PCR

The left and right ventricular tissues (~30 mg) isolated from male and female mice were suspended in ice-cold PBS$^{w/o\ Ca2+/Mg2+}$ and cut into small pieces. Diced LV and RV tissues were then suspended in Trizol reagent (Ambion) and homogenized in separate tubes until the suspension became clear. At this stage, RNase inhibitor (SUPERase-In, Ambion) was added and cells were let to stand on ice for 15 minutes to promote lysis. Chloroform (Sigma) was added to the preparation at a 1:5 ratio (chloroform:trizol) and vortexed vigorously for 1-2 minutes. Samples were left in eppendorf shaker for 10 minutes with brief mixing of samples once every two minutes. Samples were then centrifuged at maximum speed for 15 minutes at 4^{o}C and the supernatant containing the aqueous phase was carefully removed and added to two volumes of isopropanol. The solution was gently mixed and incubated at room temperature for 15 minutes on rotation. The samples containing total RNA were precipitated at -80^{o}C for at least 30 minutes before proceeding with next step. Precipitated RNA was then pelleted by centrifugation at maximum speed for 30 minutes. Pellets were washed with 500μl ethanol (70 %) and centrifuged again at maximum speed for 25 minutes. Pellets were then dissolved in 50-100μl of nuclease free water and the concentration of RNA was quantified using a fluorometer (Qubit, Invitrogen). DNA in total RNA was digested using Turbo DNase protocol (Ambion). For cDNA synthesis using random primers, high capacity cDNA reverse transcription kit (Applied Biosystems) was used according to manufacturer's recommendations. For strand-specific RNA quantification, strand-specific primers were used according to the manufacturers instructions (Thermoscript, Invitrogen).

3.2.4 Chromatin Immunoprecipitation

Comparable amount of LV and RV tissues (~100 mg) were diced to tiny pieces in ice-cold PBS$^{w/o\ Ca2+/Mg2+}$ followed by chromatin fixation at room temperature using 1% formaldehyde. Excessive formaldehyde was quenched using 0.1M glycine. Tissue samples were washed with ice-cold PBS$^{w/o\ Ca2+/Mg2+}$ to remove glycine. The samples were resuspended in ice-cold PBS$^{w/o\ Ca2+/Mg2+}$ (1 ml) and homogenized to a clear solution in presence of protease inhibitor cocktail (Cayman). Homogenate was pelleted and resuspended in SDS lysis buffer (1% SDS, 10mM EDTA, 50mM Tris-HCl, pH 8) and incubated on ice for 10 minutes. Homogenates were separated into 300μl volumes in eppendorf and sonicated at maximum power, constantly for 30 minutes using diagenode bioruptor (Denmark). Soluble chromatin as supernatant was collected carefully after centrifugation and shearing of chromatin was ensured in the range of 300-500bp using MultiNA (Shimadzu). Approximately 5μg of chromatin was suspended in ChIP dilution buffer (0.01% SDS, 1.1% Triton X-100, 1.2 mM EDTA, 16.7 mM Tris-HCl pH 8 and 167 mM NaCl) and immunopurification of histone modifications was performed using specific antibodies: H3K4me3 (Abcam ab8580), H3K9me3 (Abcam ab8898) and H3K27me3 (Millipore 07-449). Non-specific IgG was included for each reaction as control. The antibody-chromatin-proteinA/G conjugates were subjected to a series of five washes using 1) low salt buffer 2) high salt buffer 3) lithium chloride buffer 4) TE buffer and 5) TE + 0.01% SDS. Crosslinks within the immunopurified conjugates as well as equivalent amounts of input chromatin were reversed using ChIP elution buffer (20 mM Tris-HCl pH7.5, 5 mM EDTA, 50 mM NaCl, 1% SDS) and incubation for 2 hours at 62^{o}C in a thermomixer (Thermomixer comfort, eppendorf) set at 1400rpm in presence of proteinase K (Invitrogen). The reverse crosslinked DNA was then purified using DNA binding columns according to the manufacturer's recommendations (Nucleospin). Purified DNA is eluted in nuclease free water and final concentration was measured using a fluorometer.

3.2.5 Realtime qPCR assays for ChIP enriched DNA

Relative enrichment of DNA in input, ChIP and IgG samples was quantified using Fast SYBR Green qRT-PCR system (ABI Prism 7500). The primer sequences used to amplify the cardiac myosin heavy chain gene sequences are: Primer A (-3.3 kb α-*MHC*): CAAGAGAAAGCAGACAACAG and CGGACTCACTCACTCTTTTT, Primer B (-2.7 kb α-*MHC*): AGGGAGGATCACACTGGATG and TGAGGCTCTACCACCAGTCC,
Primer C (-2.2 kb α-*MHC*): ATGGTCCTTCTCACCTGTGG and GGTTTGCCCTCTTCTTCCTT, Primer D (-1.9 kb α-*MHC*): CCACTACCCATACCAAGTTT and TATGTCACTGCCTGGTTCT,
Primer E (-1.7 kb α-*MHC*): GAGCCTCAAGTGACCTCCAG and CTCCAAGGGACCTGATTCAA, Primer F (-1.2 kb α-*MHC*): TCAGTCTGCAGAGCCCCTAT and GGCTGAGGGAGAAAGGGTAT, Primer G (-0.8 kb α-*MHC*): GCTGTGCAGCTGTTCAGTTC and CAGGCCATCATCCAATCTCT, Primer H (-0.3 kb α-*MHC*): TATTAAGCCTGGAAGAGAAG and GCAGATAGAGGAGAGACAGG, Primer I (-0.1 kb α-*MHC*): CTCTATCTGCCCATCGGCC and CTCAGTGCTCCAGCCCCTT, Primer J (+0.1kb α-*MHC*): CACCTAGAAGGAAACTGC and CCAGTGTTTCTTGTGGAA, Primer K (+0.7 kb α-*MHC*): CAATCTTCCAGTGAGCCACA and CTGGACGGAGAGAGGAACAG, Primer L (1.4 kb α-*MHC*) CTTAGGGAAAGGGGTTGGAG and GGAAGACAGCGTCTTTCTGG.

3.2.6 Data analysis and statistics

Enrichment of bdP sequences in ChIP purified material using specific antibodies was calculated as percent ratio relative to input chromatin. Enrichment in non-specific IgG controls was ensured to be negligible. Percent input ratio was calculated for control and treatment groups after ChIP and fold enrichment data was generated by normalizing treatment groups to control by ΔΔCt method using $2^{-[(Ct_{control\ Input}-Ct_{control\ bound})-(Ct_{treatment\ Input}-Ct_{treatment\ bound})]}$, where Ct is the cycle threshold as determined by realtime qPCR. Resulted fold enrichment data from each group has been evaluated with a two-tailed, unpaired Student's t test using QuickCalcs

(GraphPad). Data presented as Mean±SEM for each group. A value of $p < 0.05$ was considered statistically significant.

3.3 Results

3.3.1 Gender-specific *MHC* gene expression in SW strain

To determine the level of gene expression between the two genders, we quantified relative mRNA levels for *Anp*, *Bnp*, *Serca2a*, α-*MHC* and β-*MHC* genes using realtime qPCR (qRT-PCR). Firstly, the expression pattern for the genes between the two genders was compared in LV tissue of the mice heart. In LV, the expression of *Anp*, *Bnp* and *Serca2a* genes was comparable in male and female mice (**Figure 1A**), while the expression of β-*MHC* in male LVs was found to be higher than in female LV tissues (**Figure 1B**). Conversely, α-*MHC* gene expression is down regulated in male LV. We then assessed the gene expression in total RNA extracted from right ventricles of male and female mice. Consistent with patterns observed for LV, the *Anp*, *Bnp* and *Serca2a* genes show comparable mRNA expression in male and female RV (**Figure 1C**). The expression of β-*MHC* gene is high while the expression of α-*MHC* gene is maintained at low levels in male RV (**Figure 1D**). These data suggest that the expression of β-*MHC* is maintained at high levels in both LV and RV of male mice, whereas α-*MHC* gene expression is higher in female ventricular tissues. The gene expression profile in male and female hearts was conducted using ventricular tissues obtained from Swiss Webster mice, an outbred strain with high degree of genetic heterogeneity.[10] We asked if the sex-specific difference in cardiac *MHC* gene expression is indeed consistent between inbred and outbred mouse strains.

3.3.2 Gender-specific MHC gene expression in C57BL/6 strain

We assessed mRNA expression for *Anp*, *Bnp*, *Serca2a*, α-*MHC* and β-*MHC* genes in LV isolated from male and female C57BL/6 mice. The expression of natriuretic peptide genes, *Anp* and *Bnp* is higher in male LV compared to female LV tissues (**Figure 2A**). Paralleling the SW strain, the β-*MHC* gene expression was maintained at high levels while α-*MHC* expression was lower in male LV obtained from C57BL/6 mice (**Figure 2B**). We then quantified gene expression in total RNA extracted from

male and female RV of C57BL/6 mice. The expression of *Anp* was higher in male RV than in female RV (**Figure 2C**). The expression of *Bnp* and *Serca2a* genes showed no difference between the two genders. The expression of *β-MHC* gene is higher when compared to female RV whereas the *α-MHC* gene showed no difference in expression (**Figure 2D**).

3.3.3 Differential expression of *AS β-MHC* transcript between the genders

The results so far suggest differential expression of cardiac genes in male and female mice. Our gene expression data suggest variable mRNA expression for *Anp* and *Bnp* genes in the two strains of mice studied. The variability in gene expression between distinct strains such as the inbred and outbred is well documented, particularly for genes implicated in cardiovascular biology.[11-13] Here we show increased expression of *β-MHC* and down regulated *α-MHC* expression in male LV isolated from both strains. We assessed if the expression of *antisense β-MHC* (*AS β-MHC*) in male and female LV. Using strand-specific RNA detection and amplification by PCR, the sense and *AS β-MHC* RNA could be detected and quantitatively compared between the two genders. As described in **Figure 3**, the expression of *AS β-MHC* gene in male C57BL/6 mice was down regulated. This is consistent with recent reports and suggestive of an inverse correlation in the expression of *AS β-MHC* transcript with the transcription of *β-MHC* gene.[9, 14, 15] We then determined if this differential expression of cardiac *MHC* genes in male and female LV could be associated with epigenetic mechanisms such as post-translational modification of histones.

3.3.4 Histone H3K27 tri-methylation of bdP distinguishes MHC gene expression

We assessed if the bdP that produces *AS β-MHC* transcript show specific histone modifications. The transcription start site (TSS) for *AS β-MHC* gene is mapped approximately 2kb upstream to the *α-MHC* gene.[14, 15] Chromatin immunoprecipitation with antibodies specific to histone modifications revealed increased enrichment for H3K4me3 marks at the bdP in male C57BL/6 mice (**Figure 4A**). The H3K4me3 mark is generally associated with actively transcribing genes, however in male C57BL/6

LV, the expressions of *AS β-MHC* and *α-MHC* genes were reduced[16] Conversely, the repressive H3K9me3 modification was reduced at the *MHC* intergenic bdP sequence isolated from male LV tissue (**Figure 4B**). We next examined for additional histone modifications and report specific association of H3K27me3 modifications within the intergenic bdP of cardiac *MHC* genes in male LV tissue (**Figure 4C**). We then examined for additional histone modifications and report specific association of H3K27me3 modifications within the intergenic bdP of cardiac *MHC* genes in male LV tissue (**Figure 4C**). Strikingly, ChIP results revealed enrichment for H3K27me3 at two specific regions; one corresponding to the bdP at C and D regions (~1kb downstream to *AS β-MHC* TSS) and the second peak observed at regions G and H (~1kb upstream to *α-MHC* TSS). This observation is consistent with reduced expression of *AS β-MHC* and *α-MHC* genes in male mice because H3K27me3 is strongly associated with transcriptional repression.[17] Collectively these data suggest that the *MHC* intergenic region is maintained as H3K4me3 enriched chromatin, whereas the transcriptional repression of *AS β-MHC* and *α-MHC* genes is determined by H3K27me3 modification that spatially distinguishes these gene promoters in male left ventricles.

3.3.5 Discussion

Our experiments in LV tissues prepared from male and female mice associate post-translational histone modifications with the differential expression of genes between the two genders. Specifically, chromatin immunopurification of histone proteins suggests H3K27me3 as a key distinguishing modification of the intergenic bdP of cardiac *MHC* genes. This difference in H3K27me3 enrichment is correlative to the expression of *α-MHC* and *β-MHC* genes in male and female mouse LV. Importantly, we show that the expression of a long ncRNA, *AS β-MHC* is differentially regulated in male and female LV tissue. These data suggest epigenetic mechanisms such as histone modifications and long ncRNA expression as additional mediators underlying the complexity of gender-based myosin heavy chain gene expression. Epigenetic regulation of gender-specific gene expression has been observed in a variety of tissues such as the liver and kidney, and the majority of genes involved in drug metabolism and osmotic regulation exhibit differential expression in male and female

mice.[18] In the heart, epigenetic transcriptional regulation during developmental stages is tightly coordinated.[19] However, very little is known of the epigenetic mechanisms regulating gender-specific gene expression. Our experiments reveal a new level of epigenetic complexity in driving gender-based regulation of transcription.

The function of ncRNAs during development and disease has emerged as a key topic in recent years. Non-coding RNAs such as *Braveheart* and *AS β-MHC* regulate key gene expression patterns in the development and disease of the heart.[9, 20] Here we show that the expression of *AS β-MHC* transcript is regulated in a gender-specific manner. Importantly, emerging literature indicate ncRNAs to be key functional RNAs that specifically mediate H3K27me3 modifications and thereby epigenetic silencing of gene expression in a variety of tissues.[21] Notably, expression of ncRNAs is regulated during disease conditions and the contribution to disease pathogenesis offers tremendous potential to therapeutically manipulate these transcripts.[22] Here we describe for the first time that the expression of a long ncRNA is regulated in a sex-specific pattern.

Key cardiac genes in mouse ventricles show differences in expression patterns when compared between the different strains of inbred and outbred mice. These observations are not striking because significant literature identify and discuss these variabilities in gene expression across different strains of mice. In our studies, the expression of *Anp* and *Bnp* genes showed increased levels in male ventricles of C57BL/6 mice whereas SW mice show no differences in expression levels between the two genders. Studies that compared gene expression between five different inbred mouse strains resulted in 88 differentially expressed genes out of 6144 genes expressed in all the mice.[23]

A strong epigenetic link to cardiac *MHC* gene regulation has been established. Features of open and closed chromatin state such as the presence or absence of DNase hypersensitive site (DHS) have been observed within the intergenic bdP region of *α*- and *β-MHC* genes, and are thought to correlate with gene expression.[24] Recently, histone modifications such as hyperacetylation (H3K9/14ac) and

methylation (H3K4me3, H3K9me3) have been demonstrated to associate with the *MHC* intergenic regions and are thought to regulate the transcription of *MHC* genes under altered thyroid states.[15] Our data on chromatin modifications are consistent with these observations for H3K4me3, however these observations do not correlate with the expression of *AS* β*-MHC* and α*-MHC* genes. Indeed, the expression of these genes in male and female left ventricles is associated with H3K27me3 modifications.

3.3.6 References

1. Okin PM, Gerdts E, Kjeldsen SE, Julius S, Edelman JM, Dahlof B*, et al.* Gender differences in regression of electrocardiographic left ventricular hypertrophy during antihypertensive therapy. *Hypertension* 2008;**52**:100-106.
2. Tomaszewski M, Charchar FJ, Maric C, Kuzniewicz R, Gola M, Grzeszczak W*, et al.* Association between lipid profile and circulating concentrations of estrogens in young men. *Atherosclerosis* 2009;**203**:257-262.
3. Guerra S, Leri A, Wang X, Finato N, Di Loreto C, Beltrami CA*, et al.* Myocyte death in the failing human heart is gender dependent. *Circ Res* 1999;**85**:856-866.
4. Mendelsohn ME, Karas RH. Molecular and cellular basis of cardiovascular gender differences. *Science* 2005;**308**:1583-1587.
5. Piro M, Della Bona R, Abbate A, Biasucci LM, Crea F. Sex-related differences in myocardial remodeling. *J Am Coll Cardiol* 2010;**55**:1057-1065.
6. Weinberg EO, Thienelt CD, Katz SE, Bartunek J, Tajima M, Rohrbach S*, et al.* Gender differences in molecular remodeling in pressure overload hypertrophy. *J Am Coll Cardiol* 1999;**34**:264-273.
7. Zhong Y, Reiser PJ, Matlib MA. Gender differences in myosin heavy chain-beta and phosphorylated phospholamban in diabetic rat hearts. *Am J Physiol Heart Circ Physiol* 2003;**285**:H2688-2693.
8. Schirmer SH, Hohl M, Bohm M. Gender differences in heart failure: paving the way towards personalized medicine? *Eur Heart J* 2010;**31**:1165-1167.
9. Haddad F, Qin AX, Bodell PW, Zhang LY, Guo H, Giger JM*, et al.* Regulation of antisense RNA expression during cardiac MHC gene switching in response to pressure overload. *Am J Physiol Heart Circ Physiol* 2006;**290**:H2351-2361.
10. Chia R, Achilli F, Festing MF, Fisher EM. The origins and uses of mouse outbred stocks. *Nat Genet* 2005;**37**:1181-1186.
11. Tabibiazar R, Wagner RA, Spin JM, Ashley EA, Narasimhan B, Rubin EM*, et al.* Mouse strain-specific differences in vascular wall gene expression and their relationship to vascular disease. *Arterioscler Thromb Vasc Biol* 2005;**25**:302-308.
12. Yuan Z, Miyoshi T, Bao Y, Sheehan JP, Matsumoto AH, Shi W. Microarray analysis of gene expression in mouse aorta reveals role of the calcium signaling pathway in control of atherosclerosis susceptibility. *Am J Physiol Heart Circ Physiol* 2009;**296**:H1336-1343.
13. Pavlidis P, Noble WS. Analysis of strain and regional variation in gene expression in mouse brain. *Genome Biol* 2001;**2**:RESEARCH0042.
14. Haddad F, Bodell PW, Qin AX, Giger JM, Baldwin KM. Role of antisense RNA in coordinating cardiac myosin heavy chain gene switching. *J Biol Chem* 2003;**278**:37132-37138.
15. Haddad F, Jiang W, Bodell PW, Qin AX, Baldwin KM. Cardiac myosin heavy chain gene regulation by thyroid hormone involves altered histone modifications. *Am J Physiol Heart Circ Physiol* 2010;**299**:H1968-1980.
16. van Ingen H, van Schaik FM, Wienk H, Ballering J, Rehmann H, Dechesne AC*, et al.* Structural insight into the recognition of the H3K4me3 mark by the TFIID subunit TAF3. *Structure* 2008;**16**:1245-1256.
17. Mikkelsen TS, Ku M, Jaffe DB, Issac B, Lieberman E, Giannoukos G*, et al.* Genome-wide maps of chromatin state in pluripotent and lineage-committed cells. *Nature* 2007;**448**:553-560.

18. Rinn JL, Rozowsky JS, Laurenzi IJ, Petersen PH, Zou K, Zhong W, *et al.* Major molecular differences between mammalian sexes are involved in drug metabolism and renal function. *Dev Cell* 2004;**6**:791-800.
19. Wamstad JA, Alexander JM, Truty RM, Shrikumar A, Li F, Eilertson KE, *et al.* Dynamic and coordinated epigenetic regulation of developmental transitions in the cardiac lineage. *Cell* 2012;**151**:206-220.
20. Klattenhoff CA, Scheuermann JC, Surface LE, Bradley RK, Fields PA, Steinhauser ML, *et al.* Braveheart, a long noncoding RNA required for cardiovascular lineage commitment. *Cell* 2013;**152**:570-583.
21. Pandey RR, Mondal T, Mohammad F, Enroth S, Redrup L, Komorowski J, *et al.* Kcnq1ot1 antisense noncoding RNA mediates lineage-specific transcriptional silencing through chromatin-level regulation. *Mol Cell* 2008;**32**:232-246.
22. Wahlestedt C. Targeting long non-coding RNA to therapeutically upregulate gene expression. *Nat Rev Drug Discov* 2013;**12**:433-446.
23. Turk R, t Hoen PA, Sterrenburg E, de Menezes RX, de Meijer EJ, Boer JM, *et al.* Gene expression variation between mouse inbred strains. *BMC Genomics* 2004;**5**:57.
24. Huang WY, Liew CC. A conserved GATA motif in a tissue-specific DNase I hypersensitive site of the cardiac alpha-myosin heavy chain gene. *Biochem J* 1997;**325 (Pt 1)**:47-51.

3.3.7 Figure Legends

Figure 1. Differential ventricular expression of cardiac MHC genes in the male and female Swiss Webster mice. (**A**) Relative mRNA expression for ANP, BNP and SERCA2a genes in male and female mouse LV determined by qRTPCR. (**B**) Relative mRNA expression for cardiac α- and β-MHC genes in male and female mouse LV determined by qRT-PCR. (**C**) Relative mRNA expression for ANP, BNP and SERCA2a genes in male and female mouse RV determined by qRT-PCR. (**D**) Relative mRNA expression for cardiac α- and β-MHC genes in male and female mouse RV determined by qRT-PCR. *P<0.003. All experiments were independently performed, N=7.

Figure 2. Differential gene expression in male and female C57BL/6 mice. (**A**) Relative mRNA expression for *ANP*, *BNP* and *SERCA2a* genes in male and female mouse LV determined by qRT-PCR. (**B**) Relative mRNA expression for cardiac α- and β-*MHC* genes in male and female mouse LV determined by qRT-PCR. (**C**) Relative mRNA expression for *ANP*, *BNP* and *SERCA2a* genes in male and female mouse RV determined by qRTPCR. (**D**) Relative mRNA expression for cardiac α- and β-*MHC* genes in male and female mouse RV determined by qRT-PCR. *P<0.001. All experiments were independently performed, N=5.

Figure 3. Relative expression of *AS β-MHC* in male and female LV tissue isolated from C57BL/6 mice. Total RNA extracted from male and female LV tissues were amplified for *AS β-MHC* using strand-specific PCR assay and relative expression was assessed by qRT-PCR. N=5; *p<0.0029.

Figure 4. The intergenic bdP of cardiac MHC genes show association of specific histone modifications. (**A**) Schematic illustration of primer positions (A-L) used for ChIP walk. (**B**) H3K4me3-ChIP, *P<0.01; **P<0.02 (**C**) H3K9me3-ChIP, *P<0.003; **P<0.02 and (**D**) H3K27me3-ChIP assays in C57BL/6 male and female LV tissue assessed by qRT-PCR. *P<0.02; **P<0.03. N=4.

3.3.8

Figure 1

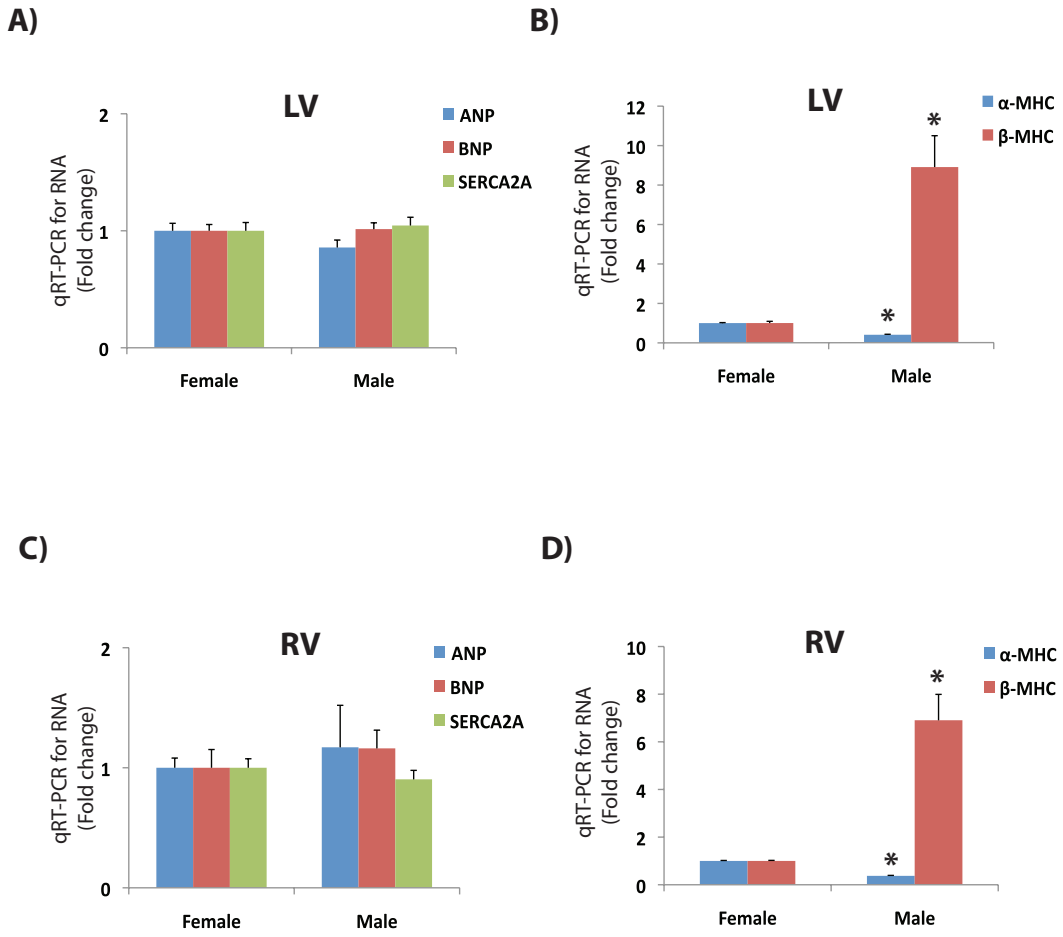
A)
LV
ANP
BNP
SERCA2A
qRT-PCR for RNA (Fold change)
2
1
0
Female
Male
B)
LV
α-MHC
β-MHC
qRT-PCR for RNA (Fold change)
12
10
8
6
4
2
0
*
*
Female
Male
C)
RV
ANP
BNP
SERCA2A
qRT-PCR for RNA (Fold change)
2
1
0
Female
Male
D)
RV
α-MHC
β-MHC
qRT-PCR for RNA (Fold change)
10
8
6
4
2
0
*
*
Female
Male

3.3.9

Figure 2

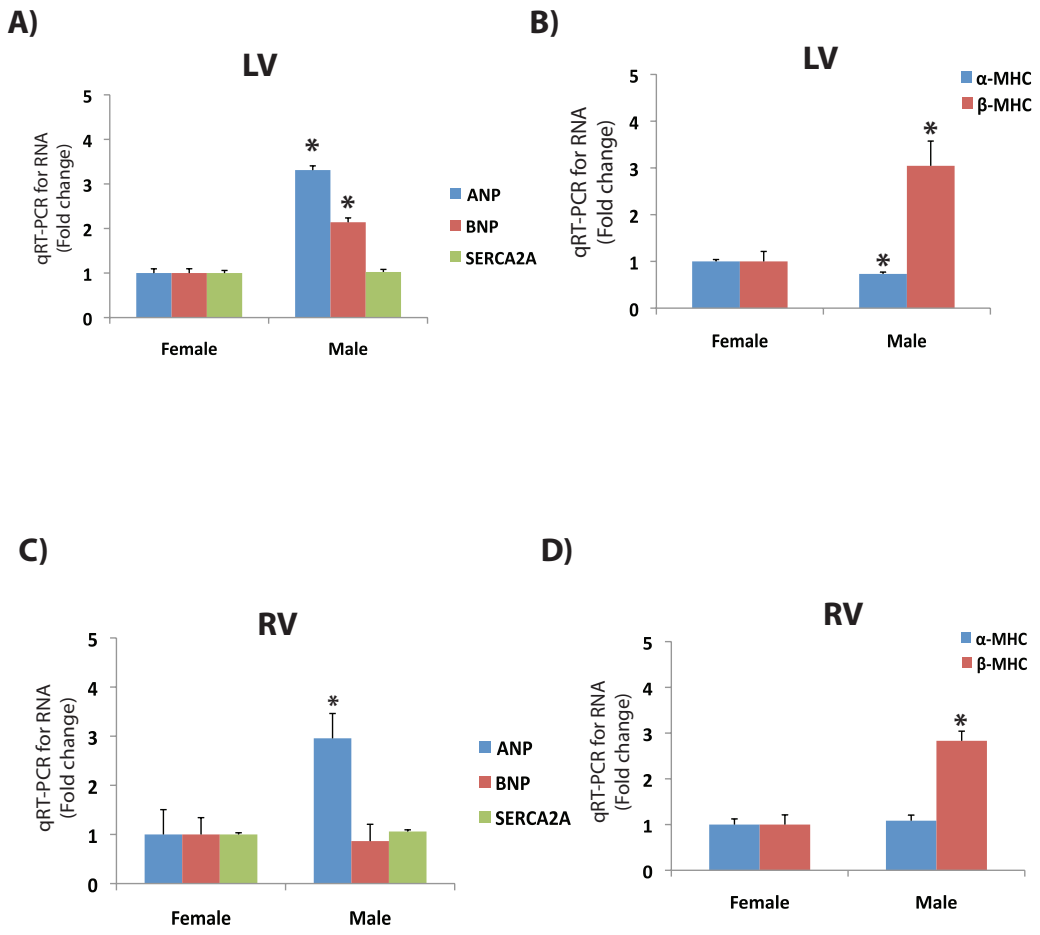
A)
LV
qRT-PCR for RNA (Fold change)
0
1
2
3
4
5
Female
Male
ANP
BNP
SERCA2A
B)
LV
α-MHC
β-MHC
C)
RV
D)
RV

3.3.10

Figure 3

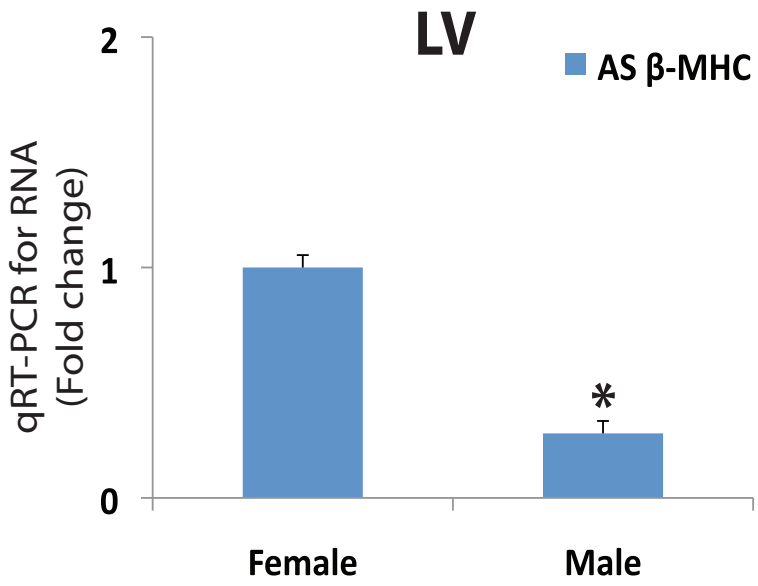

3.3.11

Figure 4

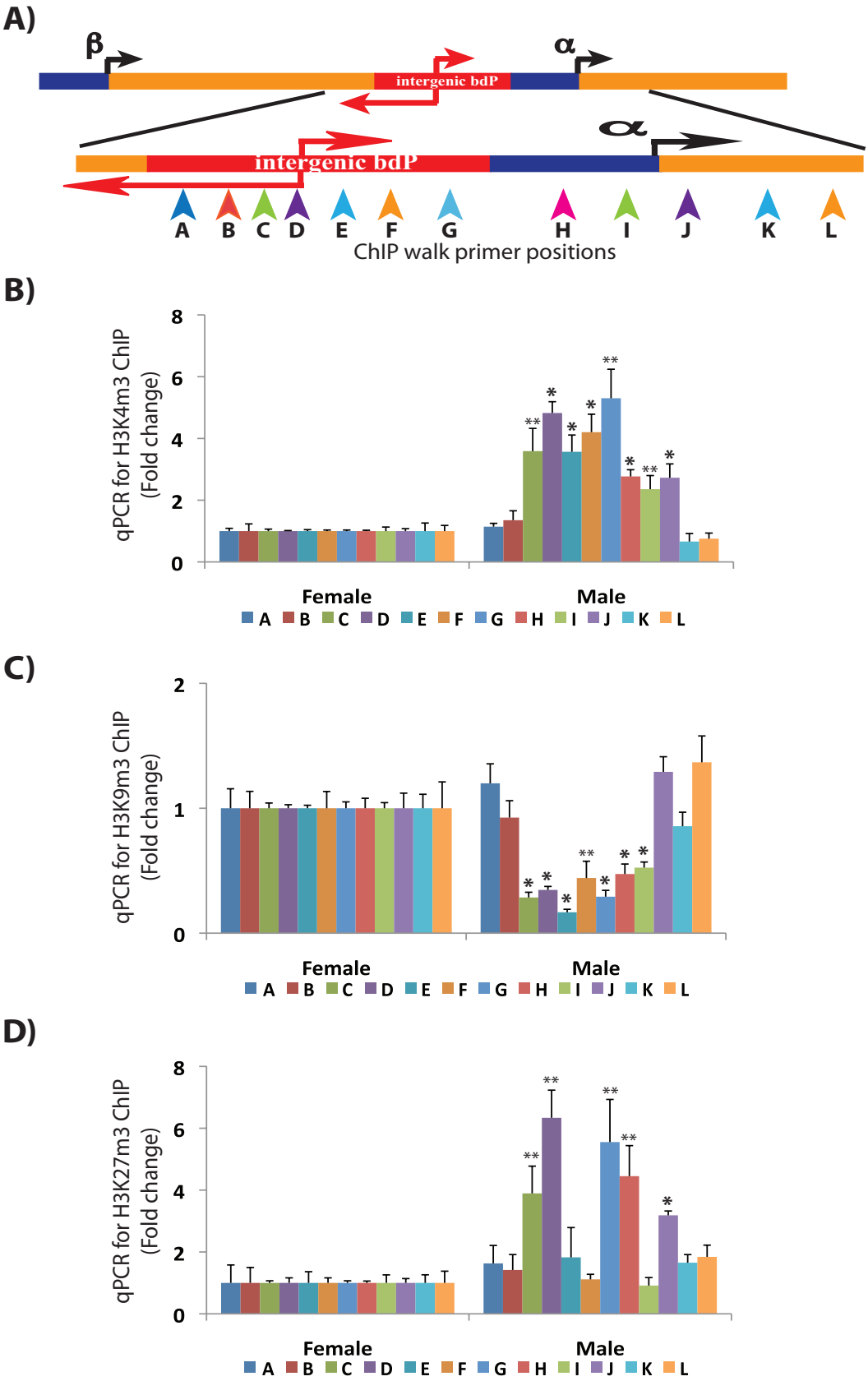

3.4 Conclusion

The results obtained from male and female LV tissues suggest strong epigenetic regulation conferred by post-translational H3K27me3 modifications associated with the *MHC* intergenic bi-directional promoter. The next aim was to assess the hypothesis whether the H3K27me3 histone modifications at the intergenic bdP of *MHC* genes and/or elsewhere in the genome could be regulated during pathological hypertrophy in the heart. Because the isoform shift in *MHC* expression is associated with pathological hypertrophy, we explored the interaction of ncRNAs and H3K27me3 modifications in detail in a mouse model of pressure overload using transcverse aortic constriction (TAC) and studied the patterns by administering histone deacetylase inhibitor, Trichostatin A (TSA) in TAC mice. These results are the focus of the upcoming Chapter four.

CHAPTER FOUR

4.1

Nucleic Acids Research Advance Access published October 16, 2013

Nucleic Acids Research, 2013, 1–14
doi:10.1093/nar/gkt896

The primary microRNA-208b interacts with Polycomb-group protein, Ezh2, to regulate gene expression in the heart

Prabhu Mathiyalagan[1], Jun Okabe[1], Lisa Chang[1], Yidan Su[2], Xiao-Jun Du[2,4] and Assam El-Osta[1,3,4,*]

[1]Epigenetics in Human Health and Disease Laboratory, The Alfred Medical Research and Education Precinct, Melbourne, Victoria 3004, Australia, [2]Experimental Cardiology, Baker IDI Heart and Diabetes Institute, The Alfred Medical Research and Education Precinct, Melbourne, Victoria 3004, Australia, [3]Department of Pathology, The University of Melbourne, Parkville, Victoria, Australia and [4]Central Clinical School, Faculty of Medicine, Monash University, Victoria, Australia

Received June 9, 2013; Revised and Accepted September 12, 2013

ABSTRACT

The Polycomb-group protein, Ezh2, is required for epigenetic gene silencing in the adult heart by unknown mechanism. We investigated the role of Ezh2 and non-coding RNAs in a mouse model of pressure overload using transverse aortic constriction (TAC) attenuated by the prototypical histone deacetylase inhibitor, trichostatin A (TSA). Chromatin immunoprecipitation of TAC and TAC+TSA hearts suggests interaction of Ezh2 and primary microRNA-208b (pri-miR-208b) in the regulation of hypertrophic gene expression. RNAi silencing of pri-miR-208b and Ezh2 validate pri-miR-208b-mediated transcriptional silencing of genes implicated in cardiac hypertrophy including the suppression of the bi-directional promoter (bdP) of the cardiac myosin heavy chain genes. In TAC mouse heart, TSA attenuated Ezh2 binding to bdP and restored *antisense β-MHC* and *α-MHC* gene expression. RNA-chromatin immunoprecipitation experiments in TAC hearts also show increased pri-miR-208b dependent-chromatin binding. These results are the first description by which primary miR interactions serve to integrate chromatin modifications and the transcriptional response to distinct signaling cues in the heart. These studies provide a framework for MHC expression and regulation of genes implicated in pathological remodeling of ventricular hypertrophy.

INTRODUCTION

The heart undergoes dramatic remodeling under physiological and pathological stress that is associated with changes in gene function (1). Pressure overload by transverse aortic constriction (TAC) upregulates the expression of hypertrophy markers such as *Anp* (*Nppa*) and *Bnp* (*Nppb*), whereas it downregulates *Serca2a* gene expression (2). Cardiac hypertrophy is associated with a shift in myosin heavy chain (MHC) gene expression (3). Chromatin-modifying enzymes and non-coding RNAs (ncRNAs) are thought to mediate gene regulatory functions in cardiac hypertrophy (4,5). Chromatin remodeling complexes such as Brg1 and HDAC enzymes are known to regulate genes implicated in hypertrophy by directly associating to the intergenic bi-directional promoter (bdP) of the *α*- and *β-MHC* genes (6). Expression of antisense (AS) RNA (*AS β-MHC*) from the bdP is associated with *β-MHC* gene expression in hypertrophic and hypothyroid animals (7,8). Together with the evolutionary conserved *Myh7b* gene, these three myosin genes are regulated by MyomiRs, a family of intronic miRNAs (miR-208a, miR-208b and miR-499) that govern cardiac hypertrophy, growth and muscle performance (9,10).

The histone methyltransferase enzyme, Ezh2, regulates gene expression in mature cardiomyocytes (11). Although the functional relevance of the polycomb-group (PcG) histone methyltransferase enzyme, Ezh2, in the healthy heart was recently shown, its role in heart disease remains poorly characterized. Ezh2-deficient mice show increased cardiac growth with upregulated expression of hypertrophic and fibrotic genes such as *Anp*, *Bnp*, *β-MHC* and *Tgfb3* (12). How these genes are precisely regulated by Ezh2 as well as the underlying mechanisms in the hypertrophied heart is not well understood. To study the role of Ezh2, we induced pressure overload by TAC in mice and attenuated the hypertrophy-associated gene expression using histone deacetylase (HDAC) inhibitors. HDAC inhibitors such as trichostatin A (TSA) can reverse pathological hypertrophy and ameliorate cardiac function (13).

*To whom correspondence should be addressed. [redacted]

Structurally diverse HDAC inhibitors can attenuate the induction of hypertrophy markers such as *Anp*, *Bnp* and the embryonic *β-MHC* genes (14–16).

In this study, we examined the expression of a number of genes implicated in cardiac hypertrophy and assessed chromatin interaction of long ncRNAs in complex with PcG silencing proteins such as Ezh2. Results from TAC animals as well as *in vitro* loss-of-function studies suggest a novel role for Ezh2 and the primary microRNA-208b (pri-miR-208b) transcript. Administration of TSA in TAC mice attenuated the expression of pressure overload-induced hypertrophic and fibrotic genes. These results describe for the first time the interaction of pri-miR-208b targeting specific chromatin modifications and regulation of genes implicated in pathological remodeling of ventricular hypertrophy. These studies provide new insights for specific long non-coding RNAs (lncRNAs) underlying the exchange of regulatory complexes involved with chromatin modification and the control of gene transcription in cardiac hypertrophy.

MATERIALS AND METHODS

TAC surgery

Chronic pressure overload was induced by transverse aorta constriction (TAC) performed on C57BL6 male mice at 10–12 weeks of age. TAC mice were injected subcutaneously with either dimethyl sulfoxide (DMSO) or TSA (dissolved in 50% DMSO), twice daily at 0.6 mg/kg/day for a period of 4 weeks. Establishment of hypertrophy and attenuation by TSA was confirmed by echocardiography by measuring left ventricular (LV) wall thickness and dimensions end-diastole and end-systole (17). Sham control animals underwent the same surgical procedures without constriction of the aorta and exhibited no hypertrophy. Non-invasive echocardiographic test was performed at the end of the 4-week study period. Mice were anesthetized with isoflurane (4% for induction and 1.7% for maintenance). Using iE33 ultrasound system (Philips) and a 15-MHz liner-array transducer, 2D short-axis view of the left ventricle (LV) was obtained and M-mode traces were acquired as we previously described (18). LV diameters at diastole and systole (LVDd, LVDs) or wall thickness at diastole was measured, and fractional shortening and LV mass were calculated. Results are presented as mean ±SEM.

Sca1+ cell fractionation and isolation

Stem cell antigen-1 positive (Sca-1+) progenitor cells were isolated by magnetic activated cell sorting system using anti-Sca-1 microbeads (Miltenyi Biotech) from differentiated mouse embryonic stem cells by the removal of 103 U/ml leukemia inhibitory factor (ESGRO, Millapore), as previously described (19). In all, 80–95% of isolated cells positive for Sca1 antigen were evaluated by flow cytometry and immunostaining. Sca-1+ and mES cells were cultured on 1% gelatin-coated dishes with Dulbecco's modified Eagle's medium supplemented with ES-qualified fetal bovine serum (FBS), knockout serum replacement, non-essential amino acids, antibiotics (penicillin/streptomycin) and β-mercaptoethanol (Gibco) at 37°C in humid air with 5% CO_2. To obtain higher numbers of Sca-1+ cells, these cells were allowed to grow in culture without leukemia inhibitory factor for two to eight population doublings.

Mouse neonatal ventricular cardiomyocyte isolation, culture and treatment

Day 1—C57BL/6 pups were sacrificed by single cut decapitation procedure and their chests were opened. Hearts were suspended in Hanks solution. Ventricles were carefully dissected and suspended into Hanks+ Trypsin solution followed by 4°C incubation overnight on the orbital shaker. Day 2—Tissues were suspended in Hanks+Collagenase medium for tissue dissociation, and resulting cell suspension was collected. This step was repeated until complete tissue dissociation was achieved. The digested extract was pelleted, and adding Dulbecco's modified Eagle's medium/10% fetal calf serum (FCS) deactivated the collagenase. The cells were plated in P150 culture dish and incubated for 50 min at 37°C to allow fibroblasts to adhere to the bottom of the dish. Cell suspension was collected and incubated again for 45 min at 37°C to allow the remaining fibroblasts to adhere to the dish. After second incubation, cell suspension was collected into a sterile container. Bromodeoxyuridine (Brdu) (3.15 mg/ml) 100 ul/10 ml media was added, and cells were plated at the density of 0.5×10^6/ml, 2 ml/well (6-well plate). Cardiomyocytes were allowed to settle for 2–3 days followed by serum starvation before TSA treatment was initiated. The serum-starved neonatal ventricular cardiomyocytes were incubated for 48 h in media containing DMSO (vehicle) or TSA (100 nM).

Total RNA preparation

For *in vivo* studies, mice heart LV tissue was homogenized in Trizol reagent (Invitrogen) in the presence of RNase inhibitor (SUPERase-In, Ambion). For *in vitro* studies, cultured mouse cardiac progenitor cells were trypsinized and pelleted by centrifugation, and then resuspended with Trizol reagent. Vigorous phenol–chloroform treatment to obtain RNA-containing aqueous phase was followed by purification of RNA using RNeasy Mini Kit preparation columns (Qiagen). DNase treatment ensured removal of residual DNA, and total RNA was accurately quantified using Qubit fluorometer (Invitrogen).

RNA quantification by quantitative reverse transcriptase-polymerase chain reaction

For gene expression studies, total RNA (1–2 μg) was reverse transcribed using high capacity cDNA synthesis kit (Applied Biosystems) in a 20-μl reaction volume containing random primers. For strand-specific quantitative reverse transcriptase-polymerase chain reaction (qRT-PCR) of MHC genes, forward and reverse primers were included in separate reactions, and cDNA synthesis was performed at 60°C using Thermoscript cDNA preparation system (Invitrogen) and real-time quantification was

performed using Fast SyBr-Green qPCR system (Applied Biosystems). Gene expression levels are expressed as fold difference where relative RNA levels between the control and treatment groups were normalized. The specificity of template amplification was assessed by melt curve analysis. To ensure the RNA strand-specific cDNA synthesis, negative primer controls and negative enzyme controls were included and assessed for negligible non-specific amplification. Oligonucleotide sequences are listed in Supplementary Data. For miR detection, ~10 ng of RNA was included in Taqman MicroRNA Reverse transcription kit (PN 4366596). miR-specific RT reactions were carried out for miR-208a (RT000511), miR-208b (RT002290) and control small ncRNA snoRNA135 (RT001230). Relative levels were amplified in PCR using Taqman small RNA Assays for miR-208a (TM000511), miR-208b (TM002290) and snoRNA135 (TM001230). The pri-miR-208b transcript was detected using strand-specific amplification as well as Taqman primary microRNA assays (Applied Biosystems).

Chromatin immunoprecipitation

For *in vivo* studies, LV tissue was carefully dissected and finely diced. Formaldehyde fixation (1%) was carried out in phosphate buffered saline (w/o Ca^{2+}/Mg^{2+}) by rotation for 10 min at room temperature, and quenching of excessive formaldehyde was achieved using glycine (0.125 M) (17,20). Fixed tissues were washed with ice-cold phosphate buffered saline and homogenized to a clear solution in warm sodium dodecyl sulphate (SDS) lysis buffer containing 1% SDS, 10 mM ethylenediaminetetraacetic acid (EDTA), 50 mM Tris–HCl, pH 8, containing protease inhibitor cocktail (Cayman). Homogenate was placed on ice to ensure proper cell lysis. For *in vitro* studies, cultured cells (~80% confluent) were formaldehyde (1%) fixed and quenched by adding glycine. Collected cell pellet was lysed in warm SDS lysis buffer. Cell lysates prepared from LV as well as from cultured cells were separated into 300-µl aliquots, and sonication of chromatin was achieved using the bioruptor (Diagnode) with constant power settings. Sheared soluble chromatin was size-fractionated using MultiNA (Shimadzu) to ensure proper sonication of chromatin (~500 bp). Soluble chromatin (5-µg) was resuspended in chromatin immunoprecipitation (ChIP) dilution buffer containing 0.01% SDS, 1.1% Triton X-100, 1.2 mM EDTA, 16.7 mM Tris–HCl, pH 8.0, and 167 mM NaCl. Immunopurification of soluble chromatin was performed using antibodies for specific histone modifications, H3K9/14ac (Millipore 06-599), H3K4m3 (Abcam ab8580), H3K9m3 (Abcam ab8898) and H3K27m3 (Millipore 07-449). Antibodies for histone-modifying enzymes are Ezh2 (Abnova PAB0648), HDAC2 (Sigma H3159) and HDAC1 (Upstate 06-720). The antibody-bound chromatin fraction was precipitated using dynabeads coated with protein A/G (Invitrogen). Conjugates were washed with increasing salt conditions followed by LiCl and SDS washes. Input and antibody-bound isolates were heated at 64°C/2 h in elution buffer containing proteinase K, and the reverse cross-linked DNA was purified by column fractionation (Nucleospin). ChIP-enriched DNA sequences were detected by amplification using real-time qPCR system. Percentage input (% input) was calculated for each ChIP experiment, and results are expressed as relative fold enrichment/ratio for the target sequences compared between the treated versus control groups. The non-specific IgG immunoprecipitation served as control for non-specific background enrichment.

Chromatin RNA immunoprecipitation (RNA-ChIP)

Mice heart LV tissue and cardiac stem cells were formaldehyde fixed, quenched with glycine and resuspended with SDS lysis buffer as described above. To ensure RNA integrity and to protect from RNase degradation, only freshly prepared buffers containing RNase inhibitors were used. Cell lysates were sonicated in the size optimized for RNA (~1000-bp long), and residual DNA from sheared chromatin was removed by mild DNase treatment. Antibodies that recognize histone H3 (Abcam ab1791) and Ezh2 (Abnova PAB0648) were used in the immunoprecipitation procedure (4°C/4–5 h) to purify RNA associated with chromatin. Conjugates were reverse cross-linked, and RNA was purified using Qiagen RNeasy columns followed by removal of DNA (Roche). Strand-specific reverse transcription of chromatin-associated RNAs and input RNA was performed using Thermoscript reverse transcription protocol (Invitrogen). Relative enrichment of long ncRNAs such as *AS β-MHC* and pri-miR-208b was assessed using qRT-PCR. Strand-specific amplification was ensured using controls as described above.

short-hairpin RNA-mediated knockdown strategy

The knockdown of Ezh2 protein, ncRNAs *AS β-MHC* and pri-miR-208b in Sca1+ vascular progenitors was achieved by MISSION short-hairpin RNA (shRNA) expressing lentivirus vectors (Sigma) as described previously (21). Target sequences are as follows: Ezh2, 5′-GCTAGG CTAATTGGGACC-3′ (TRCN0000039041), shRNA for *AS β RNA* 5′-CTGCTAGTTAGTATCCTACGC-3′ and shRNA for miR-208b 5′-CCGAATATAAGACGAACA AAA-3′. The knockdown of Ezh2 in the cells was verified by qRT-PCR and immunoblots. The knockdown of *AS β-MHC* and pri-miR-208b was verified by strand-specific qRT-PCR assays, as described above. Cells transduced with the MISSION Non-target shRNA control vector (Sigma) served as controls.

Nuclear and cytoplasmic cellular fractionation

Preparation of cytosolic and nuclear fractions was performed as described previously (21). Sca-1+ cells (1×10^7) were resuspended in hypotonic buffer containing 5 mM Tris HCl, pH 7.5, 20 mM KCl, 2 mM MgCl2, 0.25 mM EDTA, 0.125 mM ethylene glycol tetraacetic acid (EGTA), 1 mM Dithiothreitol (DTT), 0.5 mM Phenylmethanesulfonylfluoride (PMSF), 0.05% NP-40 and protease inhibitor (Cayman) for 10 min at 4°C. The cytosolic fraction (supernatant) and the nuclear pellet were separated by centrifugation at 600 *g* for 5 min. The pellet was extracted with buffer containing 20 mM Hepes

KOH, pH 7.9, 25% glycerol, 520 mM KCl, 5 mM MgCl2, 0.1 mM EDTA, 1 mM DTT, 0.5 mM PMSF, 0.2% NP-40 and protease inhibitor for 15 min at 4 °C. The nuclear fraction was recovered by centrifugation at 15 000 *g* for 15 min. The nuclear and cytosolic fractions were verified by immunoblot procedure using anti-Brm and anti-MeCP2 (nuclear markers) as well as anti-glyceraldehyde 3-phosphate dehydrogenase (GAPDH) (cytoplasmic marker) antibodies.

In vitro dsDNA/RNA binding assay

The intergenic bdP fragment (~2 kb) corresponding to positions −726 to −2756 relative to *α-MHC* transcription start site was amplified using PCR. One picomole of intergenic bdP fragment was incubated at 37°C for 30 min with 100 pmol of pri-miR-208b (CCUCUCAGG GAAGCUUUUUGCUCGCGUUAUGUUU-BiotinTg) or non-specific (UCCCCUGUGGGUGGGGGUGGGG GGUCUUU-BiotinTg) RNA oligonucleotides (Sigma). The RNA/DNA hybrids were immunoprecipitated using streptavidin-coated beads (Life technologies) in the presence or absence of RNase H or RNase V1. The bdP sequence was amplified using real-time qPCR, and the fold enrichment was determined between the specific and non-specific oligo-enriched samples.

Statistical analysis

Data were presented as ±SEM in each group. All data were evaluated with a two-tailed, unpaired Student's *t*-test using QuickCalcs (GraphPad). Statistical significance was obtained by comparing groups viz Sham versus TAC and TAC versus TAC+TSA. For *in vitro* studies, data compared viz non-targets versus shRNA and shRNA versus shRNA+TSA. A value of $P < 0.05$ was considered statistically significant.

RESULTS

TSA regulates the hypertrophy-induced expression of MHC ncRNAs

The mouse pressure overload model by TAC accelerated LV hypertrophy and heart failure (Table 1). Administration of TSA following TAC surgery reduced the severity of cardiac hypertrophy (Figure 1A). In TAC animals, we examined the expression of hypertrophy-associated genes, and demonstrated that increased *Anp*, *Bnp* and reduced *Serca2a* mRNA expression were attenuated by TSA (Supplementary Figure S1) (13). We confirmed in TAC animals that induction of hypertrophy altered MHC gene expression (elevated *β-MHC* as well as reduced *α-MHC* gene expression) was attenuated by TSA. Consistent with previous reports (7), expression of *AS β-MHC* from the bdP of the MHC intergenic region was reduced in TAC animals and TSA prevented this reduction. We quantified the expression of miR and report the induction of pri-miR-208b and miR-208b transcripts but not miR-208a in TAC animals were attenuated by TSA administration (Figure 1B) (22). The epigenetic regulation of *Anp*, *Bnp* and MHC genes by Ezh2 enzyme in wild-type animals was recently reported (11,12). The PcG protein, Ezh2, trimethylates histone H3 at Lysine 27 (H3K27m3) and mediates gene suppression (23). In TAC animals, we examined the interaction of Ezh2 as well as H3K27m3 modification on *Anp*, *Bnp* and MHC gene promoters by ChIP-qPCR. Ezh2 binding was reduced in hypertrophic animals on the *Anp* and *Bnp* genes and this was not recovered in TSA-administered mice (Figure 1C). We also assessed H3K27m3 on *Anp* and *Bnp* promoters by ChIP and observed consistent reduction in TAC mice as well as in TSA-administered animals (Figure 1D). These results suggest that the induction of *Anp* and *Bnp* genes in TAC animals is associated with reduced Ezh2 binding and H3K27m3 modification.

Table 1. Echocardiographic parameters and LV mass in TAC exposed TSA hearts

ECG parameters	Sham	TAC + vehicle	TAC + TSA
Number	10	12	12
Heart rate (beats/min)	578 ± 12	565 ± 11	552 ± 8
LVDd (mm)	4.1 ± 0.05	4.5 ± 0.1*	3.9 ± 0.07*,†
LVDs (mm)	2.7 ± 0.08	3.6 ± 0.2*	2.6 ± 0.08†
Fractional shortening (%)	34 ± 1	20 ± 1*	32 ± 1†
Wall thickness (mm)	0.72 ± 0.02	1.01 ± 0.04*	0.90 ± 0.02*
LV mass (mg)	116 ± 4	208 ± 13*	147 ± 6*,†

TAC, transverse aortic constriction; LVDd and LVDs, left ventricular diameter at diastole or systole; *$P < 0.01$ versus Sham group; †$P < 0.05$ versus TAC + vehicle group.

Expression of *AS β-MHC* is determined by the binding of Ezh2 at the bdP

We screened the intergenic bdP region of the MHC genes by ChIP-qPCR (Figure 2A). We report increased Ezh2 interaction on the intergenic bdP in TAC animals and this was attenuated in TSA-administered mice (Figure 2B). This binding pattern was consistent with H3K27m3 enrichment (Figure 2C). We determined additional repressive histone marks. We report unremarkable enrichment of H3K9m3 on the bdP in TAC mice (Supplementary Figure S2). Ezh2 was recently demonstrated to interact with HDAC complexes on suppressed genes (24,25). To test the interaction of HDACs on the bdP sequence, LV chromatin was immunopurified from TAC mice using antibodies that recognize HDACs. The intergenic bdP was enriched for HDAC2 binding and not HDAC1 in TAC mice, which was abrogated by TSA (Figure 2D). Consistent with the changes in HDAC2 binding to the bdP, reduced binding on *Anp* and *Bnp* promoters in TAC and TSA mice was observed (Figure 2E). However, neither Ezh2 nor HDAC2 mRNA expression were altered in these mice (Supplementary Figure S3). In summary, these results suggest the reduced binding of Ezh2 and HDAC2 correlates with the induction of *Anp* and *Bnp* genes, whereas, the increased binding of these determinants participate in the suppression of *AS β-MHC* and *α-MHC* gene expression in the hypertrophic heart.

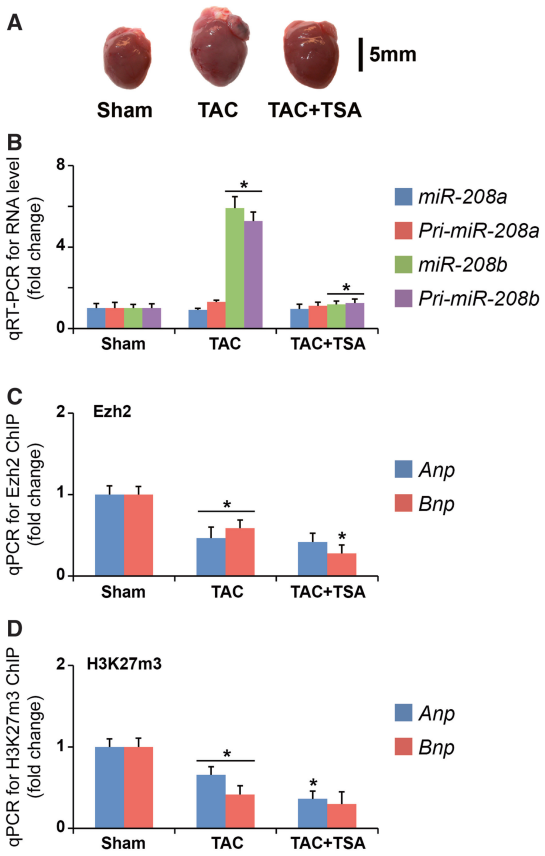

Figure 1. TAC-induced hypertrophy is associated with the release of Ezh2 at *ANP* and *BNP* genes. (**A**) Pressure overload-induced cardiac hypertrophy in mice was attenuated by TSA administration. Image of Sham (control) and TAC hearts as well as reduced left arterial thrombus following TSA administration (black bar = 5 mm). (**B**) Hypertrophy-induced expression of miR-208b and pri-miR-208b transcripts in the LV of TAC mice was attenuated by TSA administration; $^{*}P < 0.001$. (**C**) ChIP for Ezh2 enzyme followed by real-time qPCR for *Anp* and *Bnp* promoters shows reduced binding of Ezh2 in TAC mice; $^{*}P < 0.02$. (**D**) ChIP for H3K27m3 followed by real-time qPCR for *Anp* and *Bnp* promoters shows reduced H3K27m3 enrichment in TAC mice. ($n = 4$); $^{*}P < 0.02$.

The *AS β-MHC* transcript associates with chromatin

Recent evidence suggests that ncRNAs serve to integrate transcriptional responses conferred by chromatin modification (26). Notably, Ezh2 is thought to associate with long ncRNAs to regulate gene expression (27,28). To determine whether ncRNA expression in the hypertrophied heart could be directing Ezh2 methyltransferase to the bdP, soluble chromatin from LVs of TAC mice was immunoprecipitated using histone H3 antibody. Specific interaction of the *AS β-MHC* with chromatin was distinguishable from the sense *β-MHC* transcript (Supplementary Figure S4). The *AS β-MHC* transcript is >5 kb in length; therefore, we designed primers targeting the 5′- and 3′-ends of the transcript to examine chromatin-dependent association in TAC animals as well as in animals treated with TSA (Figure 2F). We detected two regions (end 1 and end 2) at the 3′ sequence of *AS β-MHC* transcript interacting with chromatin and this was reduced in LV chromatin isolated from TAC animals (Figure 2G). To extend these studies to the 5′-end, we validated the interaction of the *AS β-MHC* transcript with chromatin isolated from LV tissue. Increased association of the *AS β-MHC* transcript with chromatin in TSA-administered TAC mice was consistent with *β-MHC* expression. These results suggest that the *AS β-MHC* transcript could be interacting with the *β-MHC* gene to regulate histone modifications and gene expression. The *β-MHC* gene contains sense strand specificity, which is thought to also regulate its gene expression, so we examined two ncRNA transcripts that originate from the sense strand, a long pri-miR-208b as well as the short miR-208b. The interaction of the pri-miR-208b with chromatin was determined by RNA-ChIP using histone H3 antibody. TSA administration in TAC mice attenuated pri-miR-208b interaction with chromatin (Figure 2H). In contrast, the mature 22-nt miR-208b sequence was undetectable in chromatin isolated from the LV tissue of these animals. Next, we examined whether pri-miR-208b binds to Ezh2 enzyme in the heart. The immunopurification of soluble chromatin using antibody that recognizes Ezh2 shows specific interaction of pri-miR-208b transcript in the hypertrophic heart and this could be attenuated by the HDAC inhibitor, TSA. Taken together, these data suggest several scenarios that could mediate the expression of genes associated with hypertrophy. First, the Ezh2 methyltransferase directly suppresses the expression of target genes including *AS β-MHC* and *α-MHC* in response to hypertrophy. Alternatively, the expression of ncRNAs such as *AS β-MHC* and/or pri-miR-208b transcript could direct Ezh2 interaction to distinct gene promoters such as the intergenic bdP.

Interaction of *AS β-MHC* at the bdP is independent of Ezh2

We explored chromatin-associated RNAs in Sca1+ progenitor cells because the immunoprecipitation procedure requires significant numbers of adult heart cells and the integrity of soluble chromatin was reduced because of collagenase treatments in cardiomyocyte isolation procedures (29). Ezh2 loss-of-function experiments using shRNA (Ezh2KD) were performed in mouse Sca1+ progenitor cells (Supplementary Figure S5). Ezh2 knockdown efficiency (93%) was determined using qRT-PCR (Figure 3A). ChIP results showed significant binding of Ezh2 at the intergenic bdP in non-target cells. We observed reduced *AS β-MHC* and *α-MHC* expression in Ezh2KD cells (Figure 3A). In Ezh2KD cells, HDAC inhibition by TSA increased the expression of *AS β-MHC* and *α-MHC* genes and this was consistent with the enrichment of histone H3K9/14ac and H3K4m3 at the intergenic bdP (Supplementary Figures S6 and S7). This observation corresponds with Ezh2 binding to the bdP suppressing *AS*

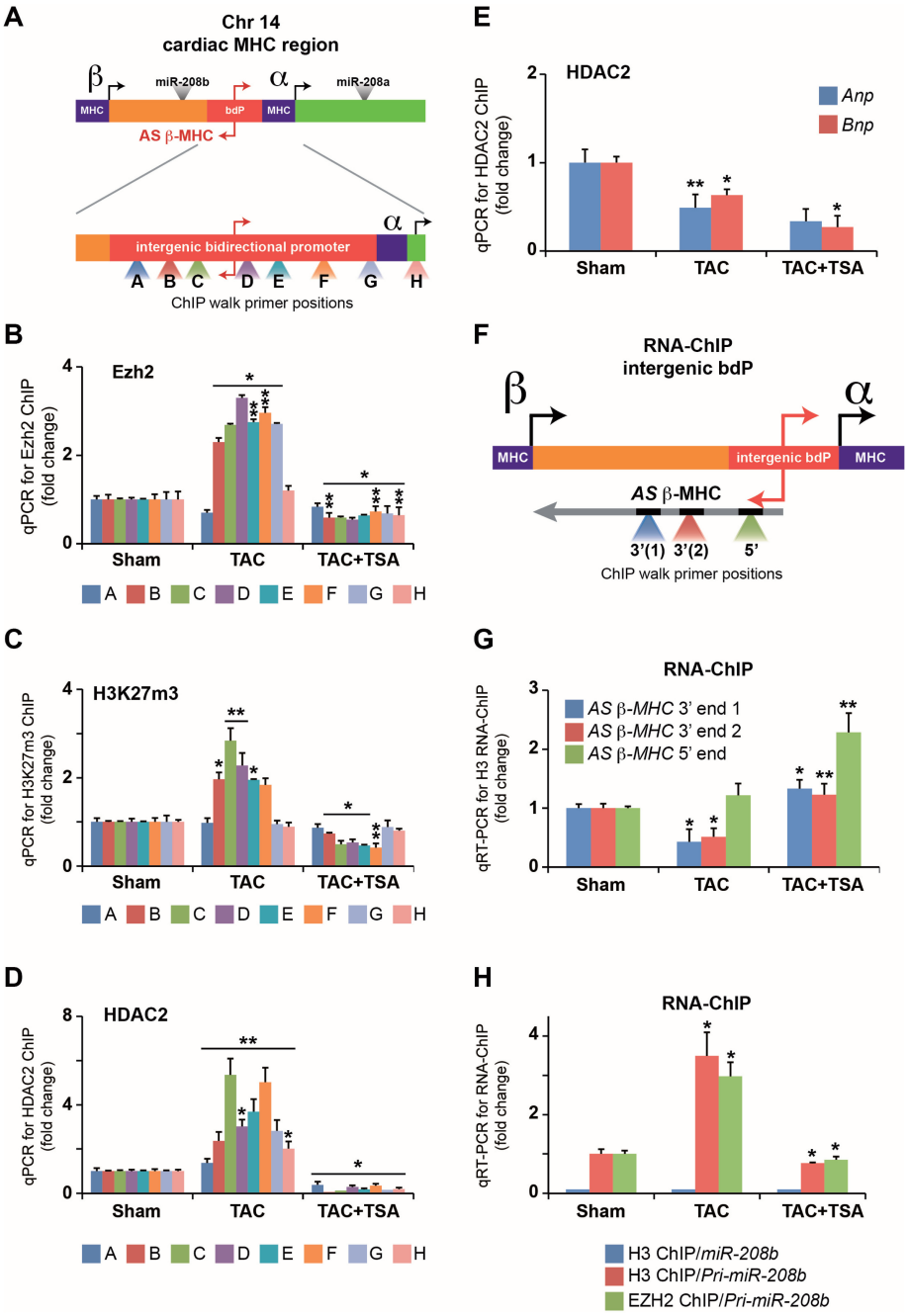

Figure 2. Pathological hypertrophy induced α- to β-*MHC* shift is associated with the interaction of Ezh2 with the intergenic bdP. (**A**) Schematic representation of the cardiac MHC genomic region on chromosome 14 showing primer positions (A–H) used for ChIP walk. (**B**) Enrichment of intergenic bdP sequence was determined by real-time qPCR after Ezh2-ChIP, (**C**) H3K27m3-ChIP and (**D**) HDAC2-ChIP. $*P < 0.01$; $**P < 0.03$. (**E**) Real-time qPCR for *Anp* and *Bnp* promoters was performed after HDAC2-ChIP. $*P < 0.008$; $**P < 0.03$. (**F**) Schematic representation of the chromatin binding of *AS β-MHC* transcript and primer positions (3' and 5') used in qRT-PCR after RNA-ChIP. (**G**) Chromatin-dependent association of *AS β-MHC* transcript after histone H3 RNA-ChIP. $*P < 0.006$; $**P < 0.01$. (**H**) Interaction of pri-miR-208b with chromatin by RNA-ChIP using antibodies that recognize histone H3 and Ezh2 in the LV of TAC mice. $*P < 0.01$. All experiments independently performed $n = 4$.

β-MHC, whereas the activation of *AS β-MHC* requires H3K9/14ac modification in Ezh2KD cells. Ezh2 knockdown significantly reduced H3K27m3 enrichment at the intergenic bdP (Figure 3B). Consistent with our *in vivo* experimental results, we observed increased expression of *Anp* and *Bnp* genes in Ezh2KD cells (Figure 3C). ChIP experiments show reduced H3K27m3 on the *Anp* and *Bnp* genes in these cells (Figure 3D). Stimulation by TSA increased H3K9/14ac (Figure 3E). Taken together, these experimental results suggest Ezh2 confers chromatin silencing events by H3K27m3 to regulate transcriptional responses. Expression of profibrotic genes such as *Tgfb3*, *Spp1* as well as *Sln and Six1* is thought to be regulated by Ezh2 in the adult mouse heart (12). We report in Ezh2KD cells, *Tgfb3* was upregulated, whereas *Spp1* and *Six1* genes were suppressed. In TAC animals, the expression of *Tgfb3*, *Spp1* and *Sln* was increased while TSA administration attenuated gene expression (Figure 3F). These results in the mouse are consistent with *in vitro* observations and suggest Ezh2 could play a role in regulating H3K27m3-mediated gene expression in the hypertrophied heart. We hypothesized that Ezh2 binding confers the expression of hypertrophic as well as profibrotic genes through interaction with ncRNAs, such as *AS β-MHC* and pri-miR-208b. To test this, we examined the interaction of both transcripts associated with immunoprecipitated soluble chromatin prepared from Ezh2-deficient cells. The specific interaction of *AS β-MHC* transcript at the 3′-end remained unchanged on chromatin (Figure 3G). Interestingly, TSA increased *AS β-MHC* expression as well as its interaction with chromatin which was correlated with reduced *β-MHC* gene expression. We observed a strong reduction of interacting pri-miR-208b transcript on chromatin, which was not changed by TSA treatment. These results suggest that the interaction of *AS β-MHC* transcript with chromatin inversely correlates with *β-MHC* gene expression in TAC+TSA animals. In addition, experiments in Ezh2KD cells also indicate the interaction of pri-miR-208b transcript with chromatin was dependent on Ezh2 enzyme. In conclusion, the *AS β-MHC* interaction with chromatin was associated with *β-MHC* gene expression in mice and this was regulated by Ezh2 binding at the intergenic bdP in pathological hypertrophy.

Because *AS β-MHC* transcript binding to chromatin is reduced in the hypertrophic heart, we hypothesized that knockdown of *AS β-MHC* (*AS β-MHC* KD) could regulate the binding of Ezh2 at key cardiac genes. To do this, we used shRNA-mediated knockdown strategy to achieve efficient reduction of the *AS β-MHC* (86%) transcript. Knockdown of *AS β-MHC* did not alter Ezh2 binding nor its determinant H3K27m3 on the intergenic bdP as determined by ChIP-qPCR (Supplementary Figures S8 and S9). These results indicate that Ezh2 binding to intergenic bdP as well as to *Anp* and *Bnp* genes occurs independently of *AS β-MHC* transcript. Compatible with our hypothesis that *AS β-MHC* transcript is not guiding the interaction of Ezh2 with chromatin, we show reduced association of the *AS β-MHC* transcript with chromatin in *AS β-MHC* KD cells (Supplementary Figure S10). Interestingly, the interaction of the pri-miR-208b transcript with chromatin remained unaltered in *AS β-MHC* KD cells, whereas TSA exposure reduced this association. These data suggest that the *AS β-MHC* transcript does not guide Ezh2 to the bdP of the *MHC* gene.

Interaction of Ezh2 with chromatin is determined by pri-miR-208b

Next, we examined whether pri-miR-208b could direct Ezh2-mediated H3K27m3 modification on key cardiac genes. Primary miR transcripts are processed to mature miRNAs processed to mature miRNAs (~22 nt in length) by RNase III family enzymes such as Drosha and Dicer (30). Using shRNA construct, we targeted the knockdown of the pri-miR-208b and miR-208b transcripts (90% reduction) in 208b-KD cells (Figure 4A). We used RNA-ChIP to determine the association of pri-miR-208b transcript with chromatin and show significant reduction in 208b-KD cells (Figure 4B). We then examined gene expression by qRT-PCR. While miR-208b deletion in mice show no changes in MHC gene expression (10), the loss of pri-miR-208b in 208b-KD cells increased the expression of bdP (*AS β-MHC* and *α-MHC* genes) and downregulated *β-MHC* (Figure 4A). We examined whether the chromatin interaction of *AS β-MHC* transcript resulted in *β-MHC* suppression in these cells. Association of the *AS β-MHC* transcript with chromatin was increased and inversely correlated with *β-MHC* gene expression in 208b-KD cells (Figure 4B). These changes to MHC gene expression suggest that the chromatin interaction of pri-miR-208b may be critical for epigenetic regulation of the intergenic bdP. Next, we assessed whether the loss of pri-miR-208b transcript altered Ezh2 and H3K27m3 association with the intergenic bdP region. ChIP results confirmed reduced Ezh2 binding at the bdP (Figure 4C) and this was consistent with reduced H3K27m3 modification in 208b-KD cells (Figure 4D). This was associated with H3K27m3 marks in these cells (Figure 4D). Release of Ezh2 from the intergenic region was consistent with H3K9/14ac increase in TSA-stimulated cells and increased *AS β-MHC* and *α-MHC* gene expression (Figure 4E). These results suggest the interaction of Ezh2 with the intergenic bdP requires pri-miR-208b transcript for gene silencing. We then determined whether the loss of pri-miR-208b transcript could deregulate other Ezh2 gene targets, and show increased *Anp* and *Bnp* gene expression (Figure 5A). Furthermore, additional Ezh2-regulated genes including the expression of *Tgfb3* and *Spp1* genes were increased, whereas *Six1* and *Sln* remained unchanged in 208b-KD cells. Taken together, these experimental results support the idea that the pri-miR-208b transcript regulates gene expression by its interaction with Ezh2 and chromatin. Consistent with this idea, binding of Ezh2 and its determinant, H3K27m3, was reduced on the *Anp* and *Bnp* promoters in 208b-KD cells (Figure 5B and C). Therefore, the loss of pri-miR-208b results in changes to expression of Ezh2-regulated genes such as *Anp, Bnp, Tgfb3, Spp1* as well as *AS β-MHC* and *α-MHC* genes. We examined whether pri-

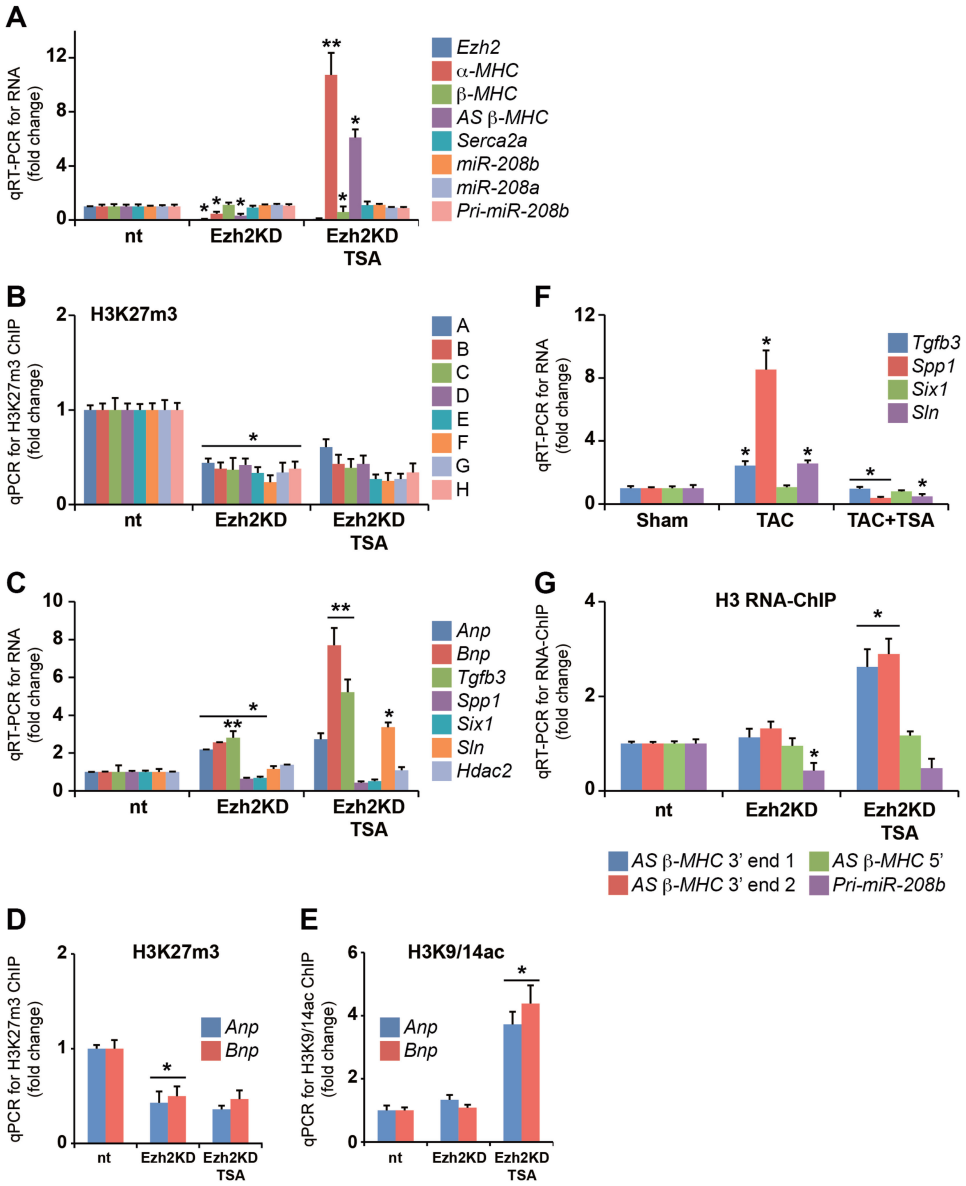

Figure 3. Chromatin association of *AS β-MHC* transcript is independent of Ezh2 and regulates *β-MHC* gene expression. (**A**) Gene expression was assessed by qRT-PCR in non-target (nt), Ezh2-deficient (Ezh2KD) and Ezh2KD cells stimulated with TSA. $*P < 0.001$; $**P < 0.01$. (**B**) H3K27m3-ChIP for intergenic bdP in Ezh2KD cells. $*P < 0.001$; $**P < 0.01$. (**C**) qRT-PCR detection of mRNA for Ezh2-regulated genes. $*P < 0.001$; $**P < 0.015$. (**D**) H3K27m3-ChIP for *Anp* and *Bnp* promoters in non-target (nt), Ezh2-deficient (Ezh2KD) and Ezh2KD cells stimulated with TSA; $*P < 0.015$. (**E**) H3K9/14ac-ChIP for *Anp* and *Bnp* promoters in non-target (nt), Ezh2-deficient (Ezh2KD) and Ezh2KD cells stimulated with TSA; $*P < 0.005$. (**F**) mRNA expression for Ezh2 cardiac gene targets determined by qRT-PCR in mice LV. $*P < 0.005$. (**G**) Loss of Ezh2 reduces the binding of pri-miR-208b but not *AS β-MHC* on chromatin binding of pri-miR-208b, whereas the binding of *AS β-MHC* transcript remained unaffected. $*P < 0.01$. All experiments independently performed $n = 5$.

miR-208b-dependent chromatin binding of Ezh2 could regulate the expression of cardiac stem cell markers in TAC animals because an essential role for Ezh2 in adult muscle and neuronal regeneration after injury has been recently documented (31,32). Increased expression of endogenous cardiac stem cell (eCSC) genes such as *Oct4* and *Sox2* was observed, whereas *Nanog* was downregulated in 208b-KD cells (Figure 5D). TSA administration

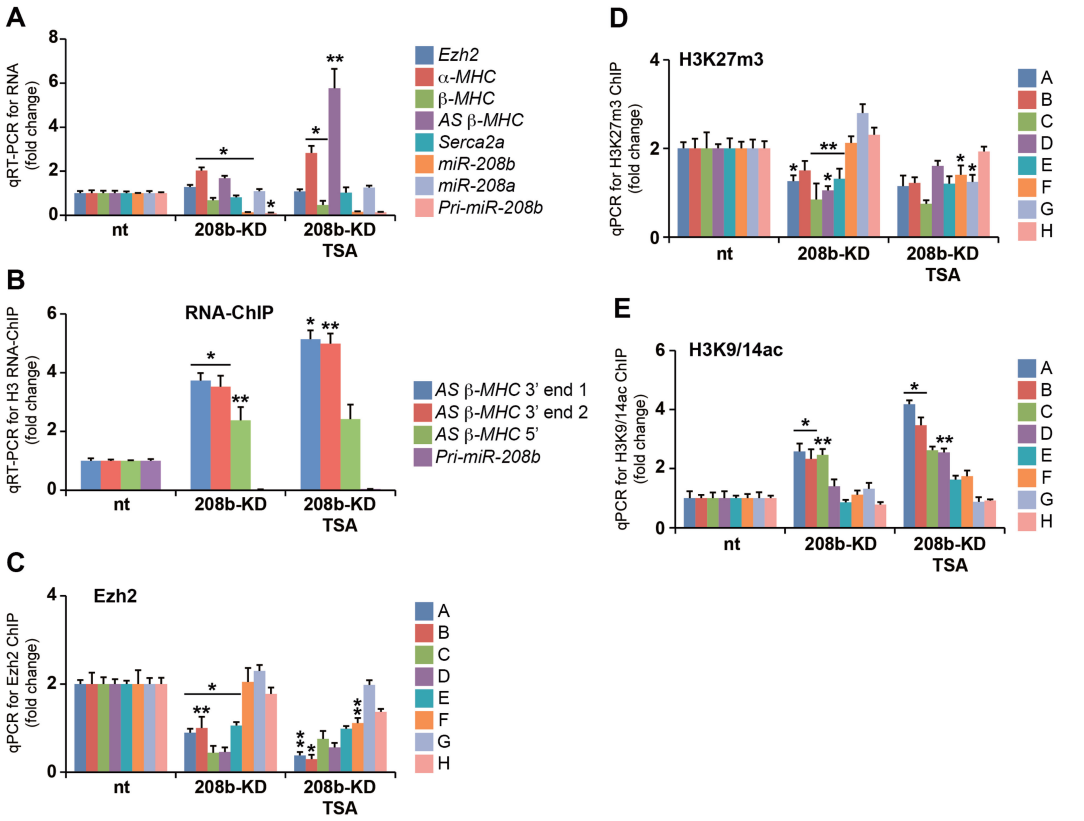

Figure 4. Loss of pri-miR-208b transcript reduces the interaction of Ezh2 binding at the intergenic bdP. (**A**) qRT-PCR for RNA levels in 208b-KD cells shows activation of *AS β-MHC* and *α-MHC* genes. $*P < 0.01$; $**P < 0.02$. (**B**) RNA-ChIP in 208b-KD cells shows increased chromatin binding for *AS β-MHC* transcript. $*P < 0.01$; $**P < 0.02$. (**C**) Ezh2-ChIP in 208b-KD cells was assessed for intergenic bdP. $*P < 0.001$; $**P < 0.004$. (**D**) H3K27m3-ChIP showing reduced enrichment for bdP sequence. $*P < 0.01$; $**P < 0.02$. (**E**) H3K9/14ac-ChIP for intergenic bdP in 208b-KD cells. $*P < 0.001$; $**P < 0.01$. All experiments independently performed $n = 5$.

downregulated the expression of *Oct4* and *Sox2* while de-repressing *Nanog* expression in 208b-KD cells. We extended these observations in LVs of TAC mice and report increased *Oct4, Sox2* and decreased *Nanog* expression consistent with our *in vitro* observations (Figure 5E). Release of Ezh2 from gene targets in TAC animals as well as the activation of Ezh2-regulated genes in 208b-KD cells suggests that the pri-miR-208b transcript could regulate the chromatin binding of the Ezh2 enzyme. The precise role of pri-miR-208b in regulating eCSC marker expression remains to be investigated.

Regulation by pri-miR-208b transcript

Our results suggest a regulatory function for the pri-miR-208b at the transcriptional level mediated by the PcG protein, Ezh2 as well as post-transcriptional regulation in the hypertrophied heart. To further characterize the functions of *pri-miR-208b*, we studied gene expression changes in 208b-KD cells because mature miRNAs suppress mRNA expression by binding to 3′-UTR sequences (30). Because miR-208b is a repressive determinant of *Med13* (*THRAP1*) genes (9,10), we examined gene expression in 208b-KD cells. Figure 6A shows elevated *Med13* expression in 208b-KD cells suggesting regulation is dependent on mature miR-208b. We also assessed the expression of exonic and intronic *Med13* gene sequences. The expression of intronic *Med13* does not change in 208b-KD cells (Figure 6B). These data suggest that miR-208b silences *Med13* expression post-transcriptionally. In contrast, we observed elevated expression of intronic and exonic sequences of the *α-MHC* gene in 208b-KD cells (Figure 6B) suggesting that pri-miR-208b transcriptionally regulates gene expression. These data are also consistent with reduced Ezh2 interaction at the bdP in 208b-KD cells (Figure 4C). The expression of Ezh2 remains unchanged in 208b-KD cells (Figure 4A). To determine whether gene targets of pri-miR-208b are regulated transcriptionally, we isolated

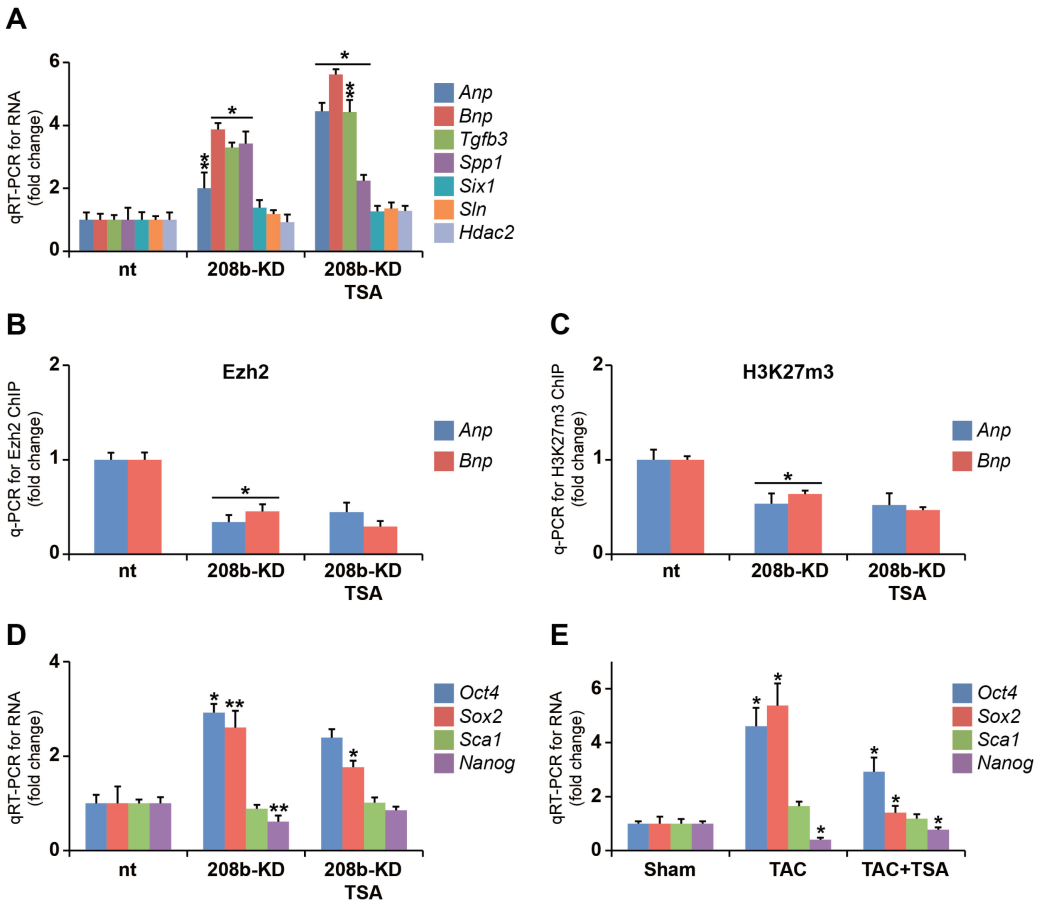

Figure 5. Loss of pri-miR-208b is associated with the expression of Ezh2 gene targets. (**A**) Relative mRNA expression of Ezh2 gene targets was assessed by qRT-PCR in 208b-KD cells. $^{*}P < 0.003$; $^{**}P < 0.015$. (**B**) Ezh2 binding to *Anp* and *Bnp* promoters was reduced in 208b-KD cells; $^{*}P < 0.002$. (**C**) H3K27m3-ChIP in 208b-KD cells followed by real-time qPCR detection of *Anp* and *Bnp* promoters; $^{*}P < 0.01$. (**D**) Loss of pri-miR-208b is associated with the expression of stem cell genes. $^{*}P < 0.007$. (**E**) mRNA expression for eCSC markers in Sham, TAC and TAC+TSA mice. $^{*}P < 0.001$; $^{**}P < 0.01$. All experiments independently performed $n = 5$.

nuclear and cytosolic RNAs (21). We observe predominant expression of miR-208b in cytosolic fractions of Sca1+ cells, whereas the pri-miR-208b transcript was detected in both the nuclear and cytosolic preparations (Figure 6C). As expected, the expression of snoRNA was enriched in the nuclear compartment (Supplementary Figure S11), whereas the expression of 18s rRNA was cytosolic (Supplementary Figure S12). As controls for the nuclear and cytosolic fractions, we show by protein immunoblotting the isolation of Brm and GAPDH, respectively (Supplementary Figure S13). Taken together, these results suggest the mature miR-208b transcript is less likely to regulate gene silencing in the nucleus. We then examined whether pri-miR-208b transcript could directly interact with the intergenic bdP sequence. First, *in silico* analysis indicates specific 5′-end complementarity between the pri-miR-208b transcript and the intergenic bdP at sequences –1227 to –1330 relative to the α-MHC transcription start site (Figure 6D). Second, we designed a synthetic RNA oligomer using the pri-miR-208b sequence to determine its binding efficiency to the bdP using *in vitro* dsDNA/RNA immunoprecipitation assay. This procedure involves hybridization of biotin-incorporated RNA oligonucleotides with DNA, which are immunoprecipitated with streptavidin beads (33). Following immunoprecipitation, the isolates are treated with ribonucleases, RNase H or RNase V1. The endonuclease RNase H specifically catalyzes the cleavage of RNA in RNA/DNA hybrids, whereas the RNase V1 enzyme does not distinguish base-paired RNA/DNA hybrids. To quantify enrichment of the bdP, we used qPCR. Immunoprecipitation indicates the pri-miR-208b sequence interacts specifically with the bdP, which was confirmed by RNase H cleavage, as shown in Figure 6E.

Similarly, treatment with the RNase V1 ribonuclease abolished bdP enrichment. Taken together, these results suggest the pri-miR-208b transcript interacts with the bdP template.

These results show for the first time that the association of the pri-miR-208b transcript with Ezh2 enzyme is linked to changes in gene function in the hypertrophied LV. This concept is supported by the observation that loss of pri-miR-208b transcript is associated with altered chromatin binding of Ezh2 and derepression of Ezh2-regulated genes. However, the chromatin interaction of *AS β-MHC* occurs independent of pri-miR-208b and Ezh2 enzyme. To date, there is little information regarding the chromatin interaction of primary miRNAs regulating epigenetic states and gene expression. Besides functioning as precursor transcripts for miR processing, the current data support novel chromatin regulatory roles for primary miR transcripts in the hypertrophied heart.

While our laboratory is intensely refining the techniques to isolate heart-derived cardiomyocytes for the specific purpose to study chromatin-associated RNAs from small cell numbers, many of the current observations published use considerably larger numbers of cultured cells (34,35). To explore the mechanism of gene regulation, we studied the mouse neonatal ventricular cardiomyocytes to show that gene expression changes were consistent with our observations with Sca1+ cells. For example, we observed the upregulation of *α-MHC* and *AS β-MHC* in TSA-stimulated cells as well as the downregulation of *Anp* genes (Supplementary Figure S14). TSA stimulation did not change the expression of *pri-miR-208a* and *pri-miR-208b* transcripts. While our studies highlight similarities

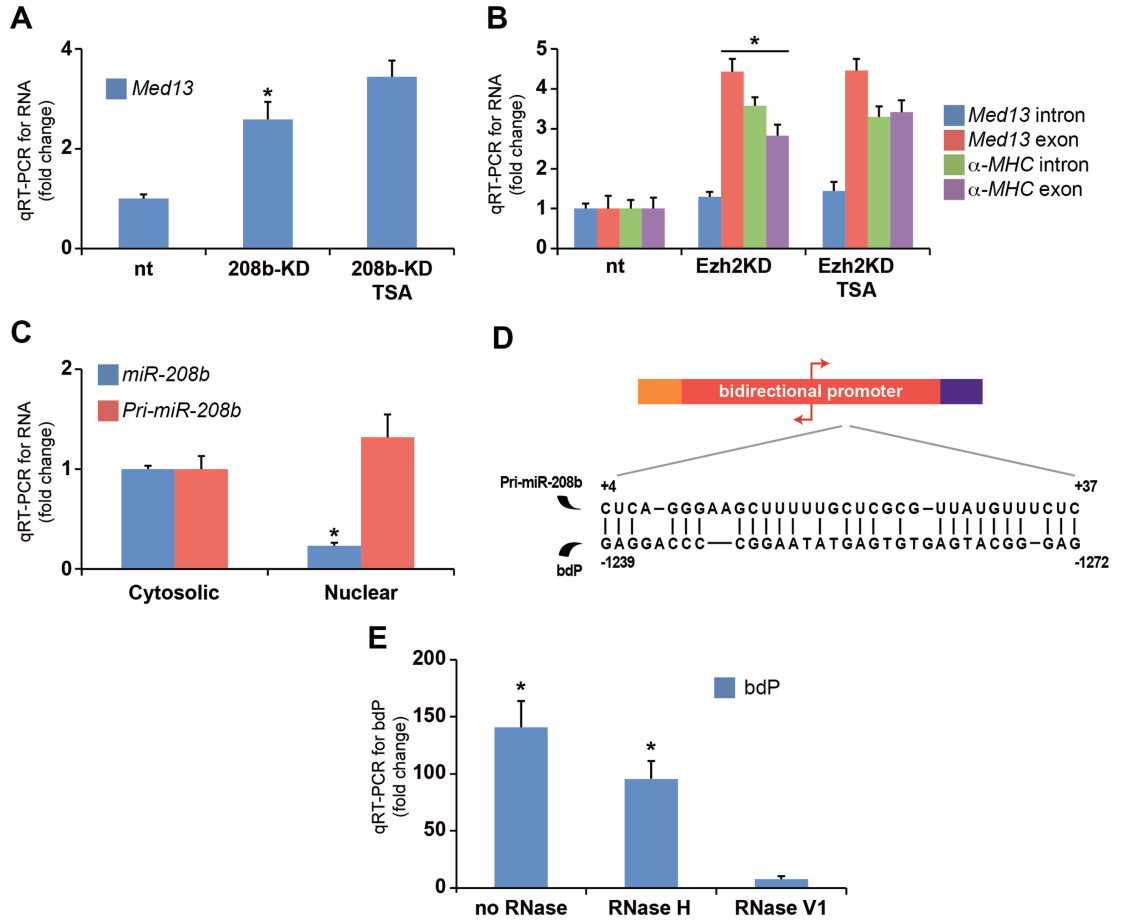

Figure 6. Regulation by regulation by pri-miR-208b transcript. (**A**) Increased expression of *Med13* gene in 208b-KD cells; $^*P < 0.0038$ (**B**) qRT-PCR of exonic and intronic sequences shows transcriptional activation of *α-MHC* gene in 208b-KD cells; $^*P < 0.0005$ (**C**) Wild-type Sca1+ cells were assessed for miR expression in cytosolic and nuclear fractions. $^*P < 0.0007$. (**D**) Pri-miR-208b recognition sequence within the bdP. (**E**) *In vitro* dsDNA/RNA binding assay using biotin-tagged RNA oligomers followed by real-time qPCR of the bdP sequence. Fold enrichment was calculated relative to non-specific oligonucleotide binding. $^*P < 0.0038$. All experiments independently performed $n = 4$.

between terminally differentiated muscle and Sca1+ progenitor cells, we cannot rule out other regulatory differences mediating chromatin-associated ncRNAs.

DISCUSSION

The PcG protein, Ezh2, is a key regulatory enzyme required for tissue-specific gene silencing. We observed binding of Ezh2 to the *Anp* and *Bnp* genes in LV tissues isolated from adult hearts. Pressure overload by TAC surgery results in the activation of fetal genes such as *Anp* and *Bnp* consistent with reduced binding of Ezh2 on these genes. Conversely, the repression of adult genes such as *α-MHC* and *AS β-MHC* in TAC animals is associated with increased Ezh2 binding and H3K27m3 modification at the bdP (Figure 7). Although HDAC inhibition by TSA is known to attenuate the induction of fetal genes and repression of adult-specific genes such as *α-MHC*, the precise molecular regulators targeted by TSA still remain poorly understood. We show that derepression of *α-MHC* and *AS β-MHC* genes by TSA is associated with the release of Ezh2 and H3K27m3 modification at MHC genes. The chromatin binding of Ezh2 in the adult heart is essential for maintaining the homeostatic gene expression.

As shown in Figure 7, MHC chromatin content as well as specific co-regulatory complexes serve to integrate ncRNAs to distinct transcriptional responses in the hypertrophied heart. We propose that the pri-miR-208b transcript as a substrate for histone modification (36). We observed the pri-miR-208b transcript mediates the *α-* to *β-MHC* switch in the hypertrophied heart. HDAC inhibition by TSA attenuates pri-miR-208b dependent-chromatin binding in TAC animals. In the hypertrophied heart, recruitment of Ezh2 is mediated by pri-miR-208b chromatin interaction. *In vitro* silencing of either the pri-miR-208b transcript or Ezh2 enzyme are associated with gene expression changes that were comparable with pri-miR-208b and Ezh2 knockdown. Specifically, the reduced chromatin interaction of pri-miR-208b transcript in miR-208b-KD cells alters Ezh2 binding to target genes. This was associated with the derepression of Ezh2-regulated genes in pri-miR-208b knockdown cells. The loss of *AS β-MHC* transcript in cardiac progenitors did not change the expression of Ezh2-regulated genes. This suggests that pri-miR-208b could regulate the binding of Ezh2 and H3K27m3 at genes. Experimental results derived from TAC animals suggest increased chromatin interaction of pri-miR-208b transcript could mediate the release of Ezh2 from *Anp* and *Bnp* genes, while increase Ezh2 binding to the bdP in the hypertrophied heart.

Recent evidence suggests that antisense transcription is critical for H3K27m3-mediated silencing (37). The long ncRNA, *HOTAIR*, interacts with Ezh2 (34,35,38). While, a mouse ortholog to the *HOTAIR* transcript (*mHOTAIR*) has been reported, its the function in the heart remains uncharacterized (39). We report no appreciable expression of the *HOTAIR* transcript in our experiments. The molecular basis of ncRNA-dependent chromatin interactions conferring gene-regulating

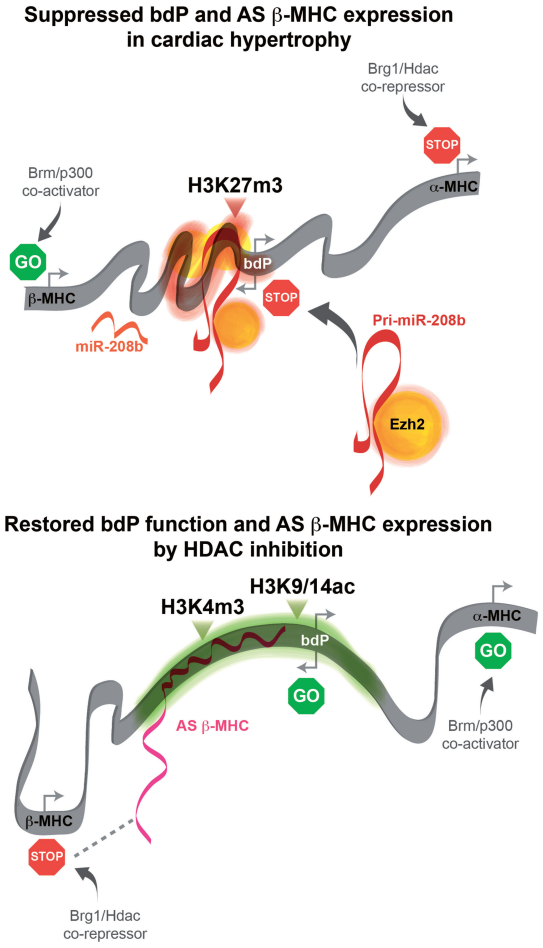

Figure 7. Schematic representation of the α/β MHC gene regulating events at the intergenic bdP mediated by ncRNA. Cardiac hypertrophy is associated with H3K27m3 of intergenic bdP by the PcG methyltransferase protein, Ezh2 and suppression of coding *α-MHC* and non-coding *AS β-MHC* gene expression. Increased expression of pri-miR-208b is associated with Ezh2 interaction at the bdP in cardiac hypertrophy. HDAC inhibition by TSA attenuates cardiac hypertrophy by restoring the expression of *α-MHC* and *AS β-MHC* genes and this is associated with hyperacetylation of the intergenic bdP as well as the release of Ezh2/pri-miR-208b complex. Restoration of *AS β-MHC* expression results in chromatin binding and inhibition of sense *β-MHC* transcription.

epigenetic changes in the heart remains incomplete (40,41). The experimental results presented in this study suggest that ncRNA could guide chromatin-modifying complexes to regulate hypertrophy-associated gene expression (42). Recent studies also indicate that TSA attenuates pathological hypertrophy in mice as well as regulates the co-repressive Brg1-HDAC complexes interacting with the bdP of the intergenic region (6). The mechanism underlying the induction of stem cell population

within the myocardium in response to increased pressure overload is poorly understood; however, it is thought to contribute negatively to ventricular function in the pathological heart (43–45). Our results also suggest a novel role for HDAC inhibition in regulating cardiac stem cell genes by mechanisms that involve ncRNA–chromatin interaction. Not only is this work of direct therapeutic relevance to hypertrophy, but will also be important for our understanding of new mechanisms of gene regulation conferred by interacting ncRNAs that influence chromatin structure and function.

SUPPLEMENTARY DATA

Supplementary Data are available at NAR Online.

ACKNOWLEDGEMENTS

The authors acknowledge grant and fellowship support from the National Health and Medical Research Council (NHMRC) and the National Heart Foundation of Australia (NHF). P.M. was awarded a Monash Graduate Scholarship, and A.E-O. and X-J. D. are NHMRC Senior Research Fellows.

FUNDING

The Victorian Government's Operational Infrastructure Support program (in part). Funding for open access charge: National Health and Medical Research Council and National Heart Foundation of Australia.

Conflict of interest statement. None declared.

REFERENCES

1. Kook,H., Lepore,J.J., Gitler,A.D., Lu,M.M., Wing-Man Yung,W., Mackay,J., Zhou,R., Ferrari,V., Gruber,P. and Epstein,J.A. (2003) Cardiac hypertrophy and histone deacetylase-dependent transcriptional repression mediated by the atypical homeodomain protein Hop. *J. Clin. Invest.*, **112**, 863–871.
2. Frey,N. and Olson,E.N. (2003) Cardiac hypertrophy: the good, the bad, and the ugly. *Annu. Rev. Physiol.*, **65**, 45–79.
3. Gupta,M.P. (2007) Factors controlling cardiac myosin-isoform shift during hypertrophy and heart failure. *J. Mol. Cell Cardiol.*, **43**, 388–403.
4. Luther,H.P. (2005) Role of endogenous antisense RNA in cardiac gene regulation. *J. Mol. Med. (Berl.)*, **83**, 26–32.
5. Han,P., Hang,C.T., Yang,J. and Chang,C.P. (2011) Chromatin remodeling in cardiovascular development and physiology. *Circ. Res.*, **108**, 378–396.
6. Hang,C.T., Yang,J., Han,P., Cheng,H.L., Shang,C., Ashley,E., Zhou,B. and Chang,C.P. (2010) Chromatin regulation by Brg1 underlies heart muscle development and disease. *Nature*, **466**, 62–67.
7. Haddad,F., Qin,A.X., Bodell,P.W., Zhang,L.Y., Guo,H., Giger,J.M. and Baldwin,K.M. (2006) Regulation of antisense RNA expression during cardiac MHC gene switching in response to pressure overload. *Am. J. Physiol. Heart Circ. Physiol.*, **290**, H2351–H2361.
8. Giger,J., Qin,A.X., Bodell,P.W., Baldwin,K.M. and Haddad,F. (2007) Activity of the beta-myosin heavy chain antisense promoter responds to diabetes and hypothyroidism. *Am. J. Physiol. Heart Circ. Physiol.*, **292**, H3065–H3071.
9. Callis,T.E., Pandya,K., Seok,H.Y., Tang,R.H., Tatsuguchi,M., Huang,Z.P., Chen,J.F., Deng,Z., Gunn,B., Shumate,J. *et al.* (2009) MicroRNA-208a is a regulator of cardiac hypertrophy and conduction in mice. *J. Clin. Invest.*, **119**, 2772–2786.
10. van Rooij,E., Quiat,D., Johnson,B.A., Sutherland,L.B., Qi,X., Richardson,J.A., Kelm,R.J. Jr and Olson,E.N. (2009) A family of microRNAs encoded by myosin genes governs myosin expression and muscle performance. *Dev. Cell*, **17**, 662–673.
11. He,A., Ma,Q., Cao,J., von Gise,A., Zhou,P., Xie,H., Zhang,B., Hsing,M., Christodoulou,D.C., Cahan,P. *et al.* (2012) Polycomb repressive complex 2 regulates normal development of the mouse heart. *Circ. Res.*, **110**, 406–415.
12. Delgado-Olguin,P., Huang,Y., Li,X., Christodoulou,D., Seidman,C.E., Seidman,J.G., Tarakhovsky,A. and Bruneau,B.G. (2012) Epigenetic repression of cardiac progenitor gene expression by Ezh2 is required for postnatal cardiac homeostasis. *Nat. Genet.*, **44**, 343–347.
13. Kee,H.J., Sohn,I.S., Nam,K.I., Park,J.E., Qian,Y.R., Yin,Z., Ahn,Y., Jeong,M.H., Bang,Y.J., Kim,N. *et al.* (2006) Inhibition of histone deacetylation blocks cardiac hypertrophy induced by angiotensin II infusion and aortic banding. *Circulation*, **113**, 51–59.
14. Glenn,D.J., Wang,F., Chen,S., Nishimoto,M. and Gardner,D.G. (2009) Endothelin-stimulated human B-type natriuretic peptide gene expression is mediated by Yin Yang 1 in association with histone deacetylase 2. *Hypertension*, **53**, 549–555.
15. Trivedi,C.M., Luo,Y., Yin,Z., Zhang,M., Zhu,W., Wang,T., Floss,T., Goettlicher,M., Noppinger,P.R., Wurst,W. *et al.* (2007) Hdac2 regulates the cardiac hypertrophic response by modulating Gsk3 beta activity. *Nat. Med.*, **13**, 324–331.
16. Davis,F.J., Pillai,J.B., Gupta,M. and Gupta,M.P. (2005) Concurrent opposite effects of trichostatin A, an inhibitor of histone deacetylases, on expression of alpha-MHC and cardiac tubulins: implication for gain in cardiac muscle contractility. *Am. J. Physiol. Heart Circ. Physiol.*, **288**, H1477–H1490.
17. Chang,L., Kiriazis,H., Gao,X.M., Du,X.J. and El-Osta,A. (2011) Cardiac genes show contextual SWI/SNF interactions with distinguishable gene activities. *Epigenetics*, **6**, 760–768.
18. Gao,X.M., Kiriazis,H., Moore,X.L., Feng,X.H., Sheppard,K., Dart,A. and Du,X.J. (2005) Regression of pressure overload-induced left ventricular hypertrophy in mice. *Am. J. Physiol. Heart Circ. Physiol.*, **288**, H2702–H2707.
19. Xiao,Q., Zeng,L., Zhang,Z., Margariti,A., Ali,Z.A., Channon,K.M., Xu,Q. and Hu,Y. (2006) Sca-1+ progenitors derived from embryonic stem cells differentiate into endothelial cells capable of vascular repair after arterial injury. *Arterioscler Thromb. Vasc. Biol.*, **26**, 2244–2251.
20. Mathiyalagan,P., Chang,L., Du,X.J. and El-Osta,A. (2010) Cardiac ventricular chambers are epigenetically distinguishable. *Cell Cycle*, **9**, 612–617.
21. Okabe,J., Orlowski,C., Balcerczyk,A., Tikellis,C., Thomas,M.C., Cooper,M.E. and El-Osta,A. (2012) Distinguishing hyperglycemic changes by Set7 in vascular endothelial cells. *Circ. Res.*, **110**, 1067–1076.
22. Corsten,M.F., Dennert,R., Jochems,S., Kuznetsova,T., Devaux,Y., Hofstra,L., Wagner,D.R., Staessen,J.A., Heymans,S. and Schroen,B. (2010) Circulating MicroRNA-208b and MicroRNA-499 reflect myocardial damage in cardiovascular disease. *Circ. Cardiovasc. Genet.*, **3**, 499–506.
23. Cao,R., Wang,L., Wang,H., Xia,L., Erdjument-Bromage,H., Tempst,P., Jones,R.S. and Zhang,Y. (2002) Role of histone H3 lysine 27 methylation in Polycomb-group silencing. *Science*, **298**, 1039–1043.
24. Varambally,S., Dhanasekaran,S.M., Zhou,M., Barrette,T.R., Kumar-Sinha,C., Sanda,M.G., Ghosh,D., Pienta,K.J., Sewalt,R.G., Otte,A.P. *et al.* (2002) The polycomb group protein EZH2 is involved in progression of prostate cancer. *Nature*, **419**, 624–629.
25. Chng,K.R., Chang,C.W., Tan,S.K., Yang,C., Hong,S.Z., Sng,N.Y. and Cheung,E. (2012) A transcriptional repressor co-regulatory network governing androgen response in prostate cancers. *EMBO J.*, **31**, 2810–2823.
26. Rinn,J.L. and Chang,H.Y. (2012) Genome regulation by long noncoding RNAs. *Annu. Rev. Biochem.*, **81**, 145–166.
27. Margueron,R. and Reinberg,D. (2011) The Polycomb complex PRC2 and its mark in life. *Nature*, **469**, 343–349.

28. Yang,F., Zhang,L., Huo,X.S., Yuan,J.H., Xu,D., Yuan,S.X., Zhu,N., Zhou,W.P., Yang,G.S., Wang,Y.Z. *et al.* (2011) Long noncoding RNA high expression in hepatocellular carcinoma facilitates tumor growth through enhancer of zeste homolog 2 in humans. *Hepatology*, **54**, 1679–1689.
29. Bolli,P., Vardabasso,C., Bernstein,E. and Chaudhry,H.W. (2013) Chromatin immunoprecipitation of adult murine cardiomyocytes. In: Bonifacino,J.S. *et al.* (eds), *Current Protocols in Cell Biology/ Editorial Board.* Wiley, Hoboken, New Jersey, Chapter 17, Unit17 14.
30. Winter,J., Jung,S., Keller,S., Gregory,R.I. and Diederichs,S. (2009) Many roads to maturity: microRNA biogenesis pathways and their regulation. *Nat. Cell. Biol.*, **11**, 228–234.
31. Juan,A.H., Derfoul,A., Feng,X., Ryall,J.G., Dell'Orso,S., Pasut,A., Zare,H., Simone,J.M., Rudnicki,M.A. and Sartorelli,V. (2011) Polycomb EZH2 controls self-renewal and safeguards the transcriptional identity of skeletal muscle stem cells. *Genes Dev.*, **25**, 789–794.
32. Sher,F., Boddeke,E., Olah,M. and Copray,S. (2012) Dynamic changes in Ezh2 gene occupancy underlie its involvement in neural stem cell self-renewal and differentiation towards oligodendrocytes. *PLoS One*, **7**, e40399.
33. Grote,P., Wittler,L., Hendrix,D., Koch,F., Wahrisch,S., Beisaw,A., Macura,K., Blass,G., Kellis,M., Werber,M. *et al.* (2013) The tissue-specific lncRNA Fendrr is an essential regulator of heart and body wall development in the mouse. *Dev. Cell*, **24**, 206–214.
34. Rinn,J.L., Kertesz,M., Wang,J.K., Squazzo,S.L., Xu,X., Brugmann,S.A., Goodnough,L.H., Helms,J.A., Farnham,P.J., Segal,E. *et al.* (2007) Functional demarcation of active and silent chromatin domains in human HOX loci by noncoding RNAs. *Cell*, **129**, 1311–1323.
35. Tsai,M.C., Manor,O., Wan,Y., Mosammaparast,N., Wang,J.K., Lan,F., Shi,Y., Segal,E. and Chang,H.Y. (2010) Long noncoding RNA as modular scaffold of histone modification complexes. *Science*, **329**, 689–693.
36. Mattick,J.S. (2010) RNA as the substrate for epigenome-environment interactions: RNA guidance of epigenetic processes and the expansion of RNA editing in animals underpins development, phenotypic plasticity, learning, and cognition. *Bioessays*, **32**, 548–552.
37. Pandey,R.R., Mondal,T., Mohammad,F., Enroth,S., Redrup,L., Komorowski,J., Nagano,T., Mancini-Dinardo,D. and Kanduri,C. (2008) Kcnq1ot1 antisense noncoding RNA mediates lineage-specific transcriptional silencing through chromatin-level regulation. *Mol. Cell*, **32**, 232–246.
38. Gupta,R.A., Shah,N., Wang,K.C., Kim,J., Horlings,H.M., Wong,D.J., Tsai,M.C., Hung,T., Argani,P., Rinn,J.L. *et al.* (2010) Long non-coding RNA HOTAIR reprograms chromatin state to promote cancer metastasis. *Nature*, **464**, 1071–1076.
39. Schorderet,P. and Duboule,D. (2011) Structural and functional differences in the long non-coding RNA hotair in mouse and human. *PLoS Genet.*, **7**, e1002071.
40. Mercer,T.R., Dinger,M.E. and Mattick,J.S. (2009) Long non-coding RNAs: insights into functions. *Nat. Rev. Genet.*, **10**, 155–159.
41. Schonrock,N., Harvey,R.P. and Mattick,J.S. (2012) Long noncoding RNAs in cardiac development and pathophysiology. *Circ. Res.*, **111**, 1349–1362.
42. Yu,W., Gius,D., Onyango,P., Muldoon-Jacobs,K., Karp,J., Feinberg,A.P. and Cui,H. (2008) Epigenetic silencing of tumour suppressor gene p15 by its antisense RNA. *Nature*, **451**, 202–206.
43. Bergmann,O., Bhardwaj,R.D., Bernard,S., Zdunek,S., Barnabe-Heider,F., Walsh,S., Zupicich,J., Alkass,K., Buchholz,B.A., Druid,H. *et al.* (2009) Evidence for cardiomyocyte renewal in humans. *Science*, **324**, 98–102.
44. Hsieh,P.C., Segers,V.F., Davis,M.E., MacGillivray,C., Gannon,J., Molkentin,J.D., Robbins,J. and Lee,R.T. (2007) Evidence from a genetic fate-mapping study that stem cells refresh adult mammalian cardiomyocytes after injury. *Nat. Med.*, **13**, 970–974.
45. Urbanek,K., Quaini,F., Tasca,G., Torella,D., Castaldo,C., Nadal-Ginard,B., Leri,A., Kajstura,J., Quaini,E. and Anversa,P. (2003) Intense myocyte formation from cardiac stem cells in human cardiac hypertrophy. *Proc. Natl Acad. Sci. USA*, **100**, 10440–10445.

4.2 Supplementary Data

Supplementary Figure Legends

Figure S1
Administration of TSA after TAC surgery attenuated the expression of hypertrophy associated gene expression in mice LV. *$p < 0.002$; **$p < 0.01$. n = 5

Figure S2
H3K9m3 histone enrichment at the intergenic bdP was examined from left ventricles of Sham, TAC and TSA by ChIP and assessed by qPCR.

Figure S3
Expression of *Ezh2* and *Hdac2* mRNA in Sham, TAC and TSA animals as determined by qRT-PCR.

Figure S4
RNA-ChIP using histone H3 antibody in left ventricles of control (Sham) animals show specific enrichment for *AS β-MHC* transcript in chromatin purified RNA samples.

Figure S5
shRNA-mediated silencing of Ezh2 enzyme is confirmed by immunoblot.
nt=non-target control, Ezh2KD=Ezh2 knockdown cells.

Figure S6
HDAC inhibition by TSA is associated with increased H3K9/14ac enrichment at the intergenic bdP in Ezh2-KD cells. *$p < 0.01$. n = 4

Figure S7
TSA stimulation in Ezh2-KD cells increased H3K4m3 methylation at the intergenic bdP.
*$p < 0.01$; **$p < 0.02$. n = 4

Figure S8
Loss of *AS β-MHC* transcript did not alter the chromatin binding of Ezh2 at the intergenic bdP.
*$p < 0.007$. n = 3

Figure S9
Enrichment of H3K27m3 marks at the intergenic bdP remains unaffected in *AS β-MHC* deficient cells.

Figure S10
The stable chromatin association of *pri-miR-208b* transcript in *AS β-MHC* deficient cells was reduced when stimulated with TSA

Figure S11
Nuclear snoRNA is nearly depleted in cytosolic fraction serving as control. *$p < 0.0007$. n = 3

Figure S12
18S rRNA expression is predominant to cytoplasmic fraction isolated from Sca1+ cells.
*$p < 0.0007$. n = 3

Figure S13
Immunoblotting for nuclear Brm, Mecp2 proteins and cytosolic Gapdh serves as controls for nuclear and cytosolic fractionation

Figure S14
Gene expression profiles of Sca1+ vascular progenitor cells compared to mouse neonatal ventricular cardiomyocytes (NVCM) after TSA treatment. Relative mRNA levels quantified by qRT-PCR.
*$p < 0.03$. n = 3

Oligonucleotide Sequences

Amplimer sets used for mRNA gene expression

Anp	ACAGCCAAGGAGGAAAAGGC	*GAPDH*	TGAAGCAGGCATCTGAGGG
	CCACAGTGGCAATGTGACCA		CGAAGGTGGAAGAGTGGGAG
Bnp	TCCAGAGCAATTCAAGATGCA	*18S rRNA*	TCGGAACTGAGGCCATGATT
	CTTTTGTGAGGCCTTGGTCC		CTTTCGCTCTGGTCCGTCTT
Serca2a	CCCCCTGGGAGAATATCTGG	*Med13*	ATCCATCAAGTGCCTGCTTC
	GATCTGGAAAATGAGCGGCA		GTGCGGACTGAGGATCAACT
EZH2	CTAATTGGTACTTACTACGATAACTTT	*Oct4*	CTCCCGAGGAGTCCCAGGACAT
	ACTCTAAACTCATACACCTGTCTACAT		GATGGTGGTCTGGCTGAACACCT
α-MHC	CCACCTGGGCAAGTCTAACAA	*Sca1*	TGCAGAAAGAGCTCAGGGACTGG
	TGTAGTCCACGGTGCCAGC		TCCATCAGGGTAGGGGCAGGT
β-MHC	GATGTTTTTGTGCCCGATGA	*Sox2*	AAGGAGAGAAGTTTGGAGCC
	ACCGTCTTGCCATTCTCCG		TCTGGCGGAGAATAGTTGG
Tgfb3	CCCAACCCCAGCTCCAAGCG	*Six*	TTAAGAACCGGAGGCAAAGA
	CCTCAACAGCCACTCGCGCA		GGGGGTGAGAACTCCTCTTC
Spp1	GCCTGTTTGGCATTGCCTCCTC		
	CACAGCATTCTGTGGCGCAAGG		
Sln	GAGGTGGAGAGACTGAGGTCCTTGG		
	GAAGCTCGGGGCACACAGCAG		
Nanog	CAAGGGTCTGCTACTGAGATGCTCTG		
	TTTTGTTTGGGACTGGTAGAAGAATCAG		

Amplimer sets used for ChIP

Primer A (-3.3 kb α-MHC)	CAAGAGAAAGCAGACAACAG
	CGGACTCACTCACTCTTTTT
Primer B (-2.7 kb α-MHC)	AGGGAGGATCACACTGGATG
	TGAGGCTCTACCACCAGTCC
Primer C (-2.2 kb α-MHC)	ATGGTCCTTCTCACCTGTGG
	GGTTTGCCCTCTTCTTCCTT
Primer D (-1.7 kb α-MHC)	GAGCCTCAAGTGACCTCCAG
	CTCCAAGGGACCTGATTCAA
Primer E (-1.2 kb α-MHC)	TCAGTCTGCAGAGCCCCTAT
	GGCTGAGGGAGAAAGGGTAT
Primer F (-0.8 kb α-MHC)	GCTGTGCAGCTGTTCAGTTC
	CAGGCCATCATCCAATCTCT
Primer G (-0.3 kb α-MHC)	TATTAAGCCTGGAAGAGAAG
	GCAGATAGAGGAGAGACAGG
Primer H (+0.7 kb α-MHC)	CAATCTTCCAGTGAGCCA CA
	CTGGACGGAGAGAGGAACAG
Antisense 3' end 1 (AS 3' end 1)	GCAACCACAATGGACTTTCC
	ACGATGGCGATGTTCTCTTT
Antisense 3' end 2 (AS 3' end 2)	GCATGCATTGGTTCAGAATG
	AGCCGCAGTAGGTTCTTCCT
Anp (+41 to +142)	GTGGGCAGAGACAGCAAACA
	AAGCCAAAAGGCCAAGACG
Bnp (-6 to +155)	AGCTCAGCCGGCAGGAAT
	CGTGTTCTCCCTTGTCTCGC

Supplementary Figures *S1-S8*

Figure S1

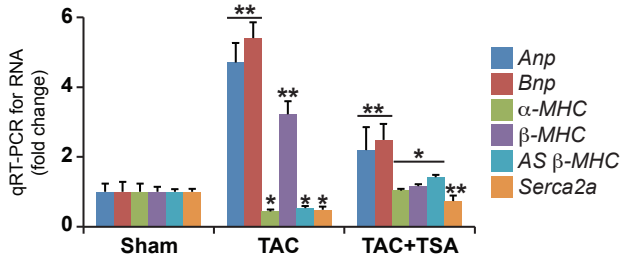

Figure S2

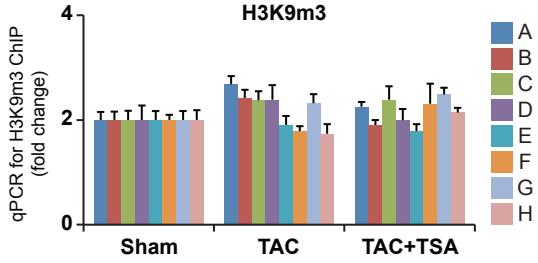

Figure S3

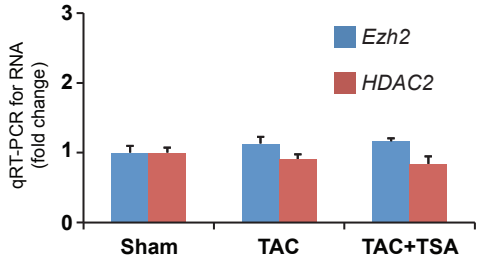

Figure S4

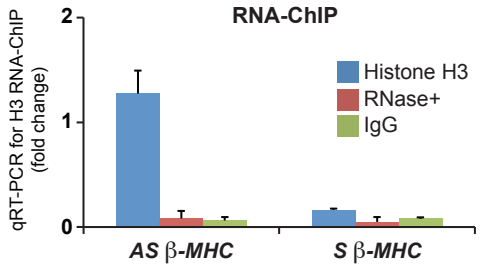

Figure S5

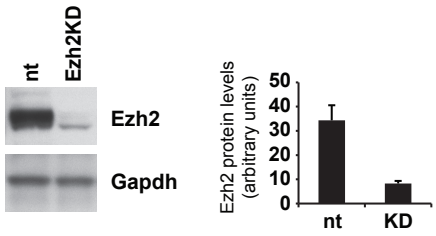

Figure S6

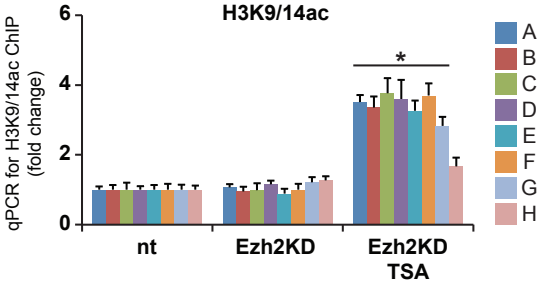

Figure S7

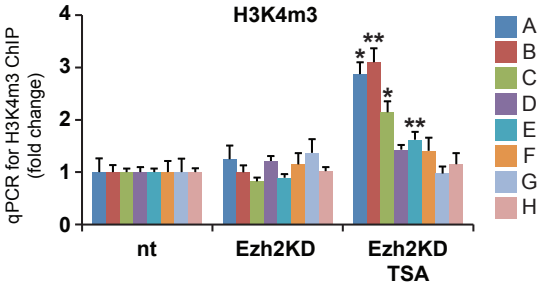

Figure S8

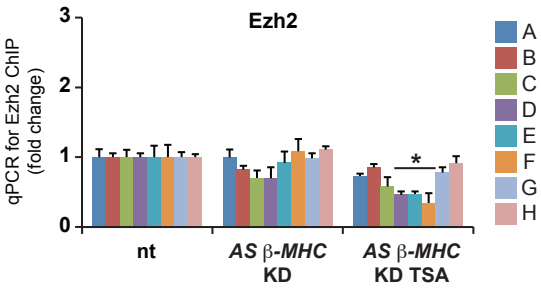

Supplementary Figures *S9-S14*

Figure S9

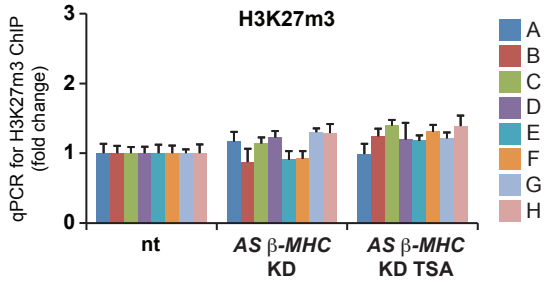

Figure S11

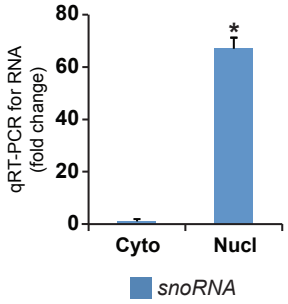

Figure S12

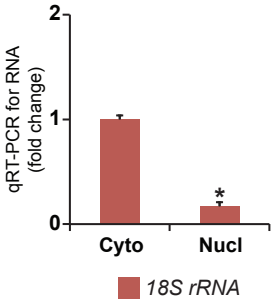

Figure S10

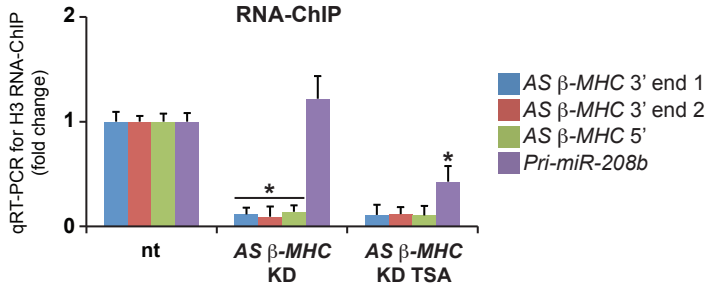

Figure S13

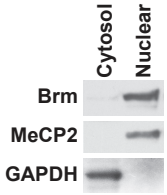

Figure S14

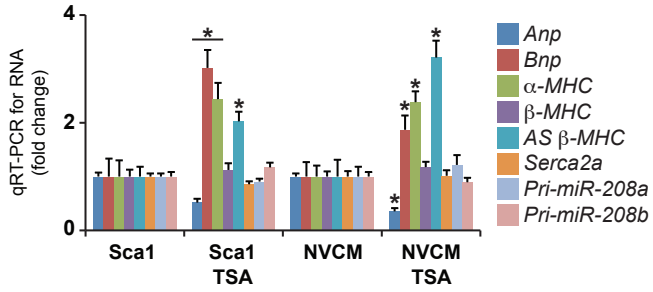

5. CONCLUSIONS AND FUTURE DIRECTIONS

The work presented in this thesis strengthens the current working hypothesis that the epigenetic modifications in terminally differentiated tissues such as the heart are crucial in determining the gene expression changes during pathological cardiac hypertrophy. The results showing chamber-specific (Chapter two) and gender-specific expression (Chapter three) of cardiac genes in the heart suggests that epigenetic regulation is essential in determining the level of expression of genes under physiological conditions in mouse heart ventricles. These observations initially established a strong base to further characterize epigenetic events in the pathological heart using TAC mouse as models of cardiac hypertrophy. Specifically, the experimental data discussed in Chapters three and four highlight the epigenetic regulation of key cardiac genes including the *MHC* expression. Importantly, the results presented in Chapter four highlights how the observed gene expression changes in the pathological heart could be mediated by combinatorial post-translational histone modifications and ncRNA interactions with chromatin.

Cardiac *MHC* genes show strong epigenetic mode of regulation as marked by changes associated with the intergenic bdP regulating the isoform-shift during cardiac hypertrophy. Research into the expression and regulation of *MHC* genes has been the focus over the last two decades. Although several observations have provided insights into the regulation of these genes under both physiological and pathological states, understanding the precise molecular events regulating the isoform-shift remains elusive. Additional complexity is apparent from recent reports suggesting a role for chromatin remodeling proteins and histone modifying proteins in regulating hypertrophy-associated gene expression including the prototypical *MHC* isoform shift. Indeed, emerging evidence highlight the functions of lncRNAs in pathological hypertrophy with recent descriptions of *AS β-MHC* transcript in regulating the *MHC* isoform shift during pathological states through mechanisms remain to be determined. Experimental results from RNA-ChIP procedures presented in this thesis identify *AS β-MHC* transcript to associate with chromatin. Results from *in vivo* as well as loss-of-function *in vitro* models are in accordance with interactions of *AS β-MHC* transcript and chromatin is associated with the expression

of *β-MHC* mRNA, and that *AS β-MHC* transcript functions through chromatin-level regulation.

MicroRNAs are pivotal modulators of cardiac development and function. Aberrant miRNA expression is associated with cardiac hypertrophy. Results presented in this thesis highlight an additional but previously uncharacterized function for the pri-miR-208b transcript in the mouse left ventricles. Primary microRNA transcripts are recognized and processed by miRNA-processing complexes and these mechanisms are initiated through recognition of stem-loop structures intrinsic to these long primary miRNA transcripts. The increased expression of pri-miR-208b in TAC hearts as well as the loss of pri-miR-208b in cell cultures support the transcriptional silencing functions for these transcripts through Ezh2-mediated H3K27me3 enrichment at gene promoters. Indeed, both the silencing of pri-miR-208b as well as Ezh2 induced the expression of similar sets of genes including the *MHC* isoform gene shift. These observations are consistent with the release of pri-miR-208b and Ezh2 from chromatin as well as H3K27me3 modifications at these genes. Thus, these findings add further complexity to the epigenetic mode of regulation in cardiac hypertrophy indicating functional roles for unprocessed primary microRNA transcripts modulating hypertrophic gene expression in the heart.

Small molecule therapies such as the administration of HDAC inhibitory compounds are considered potentially beneficial over traditional approaches that target outside-in signaling receptor molecules (Reviewed in Chapter One). HDAC inhibitors are known to be highly permeable through nuclear pores and can effectively alter the epigenetic profiles by modulating transcription factors. Although the administration of pan-inhibitors is generally effective in attenuating cardiac hypertrophy, it affects multiple cell types present within the myocardium causing off-target effects. These are considered as potential limitations for successful translation of HDAC inhibition from preclinical models to clinical therapy. Because HDACs are required for multiple cell types under physiological conditions, targeting specific class of HDACs that mediate pathological signaling in cardiomyocytes could potentially minimize off-target effects. Over recent years, distinct molecular pathways regulated by specific HDACs have

been identified and thought to improve the development of class-selective inhibitors to manipulate pathological signaling mediated by HDAC-dependent pathways (Reviewed in Chapter One). Results obtained from the current investigation highlight novel insights into HDAC functions especially in regulating the expression of ncRNAs such as the miR-208b, pri-miR-208b and the *AS β-MHC* transcript. These observations suggest that the cardioprotection conferred by HDAC inhibition in study models could also in part be attributed to regulatory mechanisms involving ncRNA interactions with chromatin.

Overall this project identified key epigenetic modifications associated with the expression of genes under physiological and pathological states of mouse heart ventricles. The study examined spatial maps of post-translational histone modifications and lncRNA expressions associated with the cardiac *MHC* gene locus. The results presented in this thesis provide invaluable knowledge toward identifying the molecular factors that regulate the transcriptional control of cardiac MHC genes. Both the identification of novel gene regulatory model mediated by primary microRNA-208b as an epigenetic substrate for modifications as well as the chromatin interactions of lncRNAs implicated in heart disease are promising avenues of investigation to improve our understanding of the pathological roles driven by these molecules in human heart function and disease.